

# Fluoride Removal from Contaminated Water by Limestone Reactor and Phosphate Rock Reactor

by  
Luning Fu

A thesis  
presented to the University of Waterloo  
in fulfillment of the  
thesis requirement for the degree of  
Master of Science  
in  
Earth Sciences

Waterloo, Ontario, Canada, 2014

©Luning Fu 2014

## **Author's Declaration**

I hereby declare that I am the sole author of this thesis. This is a true copy of the thesis, including any required final revisions, as accepted by my examiners.

I understand that my thesis may be made electronically available to the public.

## Abstract

Fluorosis, which results in mottling of teeth enamel, softening of bones, ossification of tendons and ligaments, and even neurologic damage, is endemic in many mid-latitude regions. It is caused by the long-term ingestion of high fluoride (F) drinking water, and the World Health Organization (WHO) recommends that drinking water have fluoride concentrations  $< 1.5$  mg/L. The most common technologies to remove fluoride from wastewaters are precipitation and sorption. The sorption methods are more effective in reducing fluoride concentration than precipitation methods. However, they typically require initial high setup costs and supervision. Therefore, the development of a simple, passive and inexpensive technology to reduce fluoride concentrations in waters to recommended drinking water limits is of significant benefit to communities affected by fluorosis world-wide. Three reactors were developed in this research and the fluoride removal efficiencies were evaluated.

The first reactor was composed of two columns of limestone granules and one column of calcium citrate powder. This reactor was developed based on a cost-effective reactor developed by Reardon and Wang, which is composed of two columns of limestone gravel. The reactor functions by adding carbon dioxide to inflowing water, which forces calcite ( $\text{CaCO}_3$ ) to dissolve and thus fluorite ( $\text{CaF}_2$ ) to precipitate in the first column. The exiting water then degasses by unsaturated flow through the second column of limestone gravel which results in a precipitation of the calcite that dissolved in the first column. In this study, a column containing quartz sand/calcium citrate mixture was introduced and connected between the original two columns. Citrate and additional calcium ions were brought into the solution through saturated flow. The feedwater then entered the second column of limestone gravel, where citrate promoted the incorporation of fluoride ions into calcite. This study examines the known role of citrate ion to induce fluoride ion to co-precipitate in calcite, and evaluates its effectiveness to improve the passive, two-column reactor of Reardon and Wang to attain drinking water quality fluoride concentrations.

The results of this study indicate that the limestone reactor designed in this study reduced fluoride concentration from up to 150 mg/L to below the maximum contaminant level (4 mg/L) at the residence time of 4 h. When the residence time was 24 h, fluoride concentration was reduced to below the drinking water standard (1.5 mg/L). This fluoride removal efficiency was higher than with the limestone reactor of Reardon and Wang (by a further reduction of 1.19 mg/L fluoride in total) yet still lower than the predicted efficiency. One important reason of the lower fluoride removal efficiency than with prediction is that the citrate ions suppressed the precipitation of calcite. In addition, a short residence time of the experiment decreased the removal efficiency of the limestone reactor and a longer residence time results in high removal efficiency. An improvement to this reactor was to inject a slurry containing  $\text{CaF}_2$  into the upper part of the first column, which further decreased fluoride concentration by 0.420 mg/L.

The second reactor was composed of two columns of dolomite granules and one column of calcium citrate powder. The results in the dolomite reactor experiments indicate that this reactor was only able to reduce the fluoride concentration to 4.30 mg/L at a residence time of 4 h. The three main reasons are the slow dissolution rate of dolomite, negative effect of magnesium on the precipitation of fluorite in column 1 and suppression effect of citrate on precipitation of calcite in column 2. However, the present of magnesium promoted more fluoride to co-precipitate in fluorite in column 2 than that in a limestone reactor.

Accurate determination of the fluoride concentration is critical in this research. Three commonly used fluoride determination techniques including SPADNS, IC and fluoride electrode methods were investigated on their sensitivities and interference from citrate. The results indicate that citrate has a significant interference on the SPADNS method, and the addition of a pH buffer does not eliminate the interference. In addition, citrate has a minor effect on the determination of fluoride using fluoride electrode and no effect on using IC method, since the peaks of the fluoride and citrate were well separated. However, the running

time is long for each sample with IC analysis, and the cost is much higher than with the fluoride electrode method. Consequently, fluoride electrode method was used throughout this research for determination of fluoride.

The third reactor was a single column of crushed phosphate rock from four sources: Carbonatite, Tennessee Brown, and two types of PSP with different particle sizes. Each of these materials was assessed as treatment options for fluoride. From mineralogical analysis, the results indicate that the major active mineral compositions among the four tested phosphate rocks are calcite, apatite and quartz. The results indicate that PSP rock, which contains the highest percentage of hydroxyapatite, is the best choice for fluoride remediation among the four. It can reduce fluoride concentration from 10 mg/L to 1.5 mg/L for up to 120 pore volumes. However, after 120 pore volumes the fluoride concentration continuously increased with adsorption sites becoming saturated over time. This outcome indicates a mechanism of adsorption rather than precipitation. The results from batch tests also provide evidence that adsorption contributed much more than precipitation for removal of fluoride.

Future work should be devoted to improvement of the removal efficiency of the limestone/dolomite reactor: one is to evaluate a single reactor incorporating both calcite and dolomite with a reasonable ratio of the two minerals, and the other is to consider and assess organic ligands other than citrate to more efficiently promote the incorporation of fluoride in calcite precipitates. In addition, future work should be done on improving the fluoride removal ability of the phosphate rocks. Investigation should be done on understanding the dissolution process of the calcite and apatite within the phosphate rocks in the columns, and methods should be developed to simulate the precipitation of fluorite in the columns of the reactor. Constant monitoring of the heavy metals in the effluent from the reactor is also recommended.

## **Acknowledgements**

The past three years of my graduate and research life in Waterloo is truly the most unique, precious and awarding time of mine. Along this way, there are so many people who deserve to be thanked for their friendship, help and support offered to me.

First and foremost, my deepest and sincerest gratitude goes to my supervisor Dr. Eric J. Reardon. It is his guidance, support, encouragement, patience and genuine expertise in the past three years that have made this study possible. What I appreciate the most of Dr. Reardon is his great patience and understanding to students and considerable insight into many aspects of this project and science in general. His enthusiasm and dedication to his work are really inspiring to me.

I extend my appreciation to my colleagues Colin Guthrie and Emily Taylor for their inspiring discussions and help with my study and research at university of waterloo. Thanks to our lab research assistance Emily Stephenson and Pan Hu for their help with my experiments.

Also, I would like to thank the honorable members of my thesis committee, Dr. Carol J. Ptacek and Dr. Will D. Robertson. They gave me many valuable suggestions which were helpful and very much appreciated.

The thesis is also dedicated to my parents and my boyfriend. Thanks to them all for their continuous and ever-caring support.

Last but not least, I would wish to acknowledge funding for this project provided by NSERC (Natural Sciences and Engineering Research Council of Canada).

## Table of Contents

Author's Declaration.....	ii
Abstract.....	iii
Acknowledgements.....	vi
Table of Contents.....	vii
List of Figures.....	ix
List of Tables.....	xi
Chapter 1 Introduction.....	1
1.1 Background.....	1
1.2 Thesis Objective.....	3
Chapter 2 Effect of Citrate on Fluoride Co-precipitation into Calcite and Its Application.....	4
2.1 Background.....	4
2.2 Experimental Methods.....	5
2.2.1 Materials.....	5
2.2.2 Designs and Operations of the Reactors.....	7
2.2.3 Sampling and Analysis.....	10
2.2.4 Modelling Program of the Reactors.....	10
2.3 Results and Discussion.....	12
2.3.1 Limestone Reactor.....	12
2.3.2 Dolomite Reactor.....	25
2.4 Conclusion.....	29
Chapter 3 Fluoride Determination Methods.....	31
3.1 Background.....	31
3.2 Experiment Methods.....	33
3.2.1 SPADNS Method.....	33
3.2.2 Fluoride Electrode Method.....	34
3.2.3 IC Method.....	36
3.3 Results and Discussion.....	37

3.3.1 SPADNS Method .....	37
3.3.2 Fluoride Electrode Method.....	46
3.3.3 IC Method.....	47
3.4 Conclusion.....	51
Chapter 4 Assessment of the Phosphate Rock as a Fluoride Treatment Option.....	53
4.1 Background .....	53
4.2 Experimental Methods .....	54
4.2.1 Mineralogical Analysis Procedure.....	54
4.2.2 Batch Test.....	55
4.2.3 Reactor Design and Operations .....	56
4.2.4 Sampling and Analysis .....	58
4.3 Results and Discussion.....	58
4.3.1 Mineralogical Analysis.....	58
4.3.2 Batch Test.....	61
4.3.3 Column Experiment.....	65
4.4 Conclusion.....	68
Chapter 5 Summary of Conclusions .....	70
Chapter 6 Recommendation for Future Work .....	72
Appendix A Reactor Apparatus .....	73
Appendix B Modelling Program of Phreeqc .....	77
Appendix C Results from the Limestone and Dolomite Reactors Experiments.....	80
Appendix D XRD Traces of Materials and Precipitates formed in column experiments.....	82
Appendix E Preparation of Samples for Fluoride Determination Experiments .....	84
Appendix F Physical Appearances of the Phosphate Rocks.....	88
Appendix G XRD and FT-IR Traces of the Phosphate Rocks .....	89
Appendix H XRD Traces Comparisons of the Phosphate Rock Before and After Batch Test (a) and (b).....	95
Bibliography .....	100

## List of Figures

Figure 2-1 Schematic of the limestone reactor: The feedwater is bubbled with 97 kPa CO <sub>2</sub> (g) before flowing through column 1 containing limestone via saturated flow, column 3 containing calcium citrate via saturated flow and column 2 containing limestone via unsaturated flow continuously .....	7
Figure 2-2 Schematic of the dolomite reactor: The feedwater is bubbled with 97 kPa CO <sub>2</sub> (g) before flowing through column 1 containing dolomite via saturated flow, column 3 containing calcium citrate via saturated flow and column 2 containing both dolomite and limestone via unsaturated flow continuously .....	9
Figure 2-3 F concentrations in the effluents vs. residence times of when a simulated 10 mg/L F wastewater flows through the limestone reactor after a passage of 10 pore volumes at each residence time .....	18
Figure 2-4 F concentrations in the effluent vs. F concentrations in the influent after a passage of 10 pore volumes each when various concentrations of simulated F wastewater flows through the limestone reactor at a residence time of 4 h.....	20
Figure 2-5 F concentrations vs. distances along column 1 after a passage of 60 pore volumes when a simulated 10 mg/L F wastewater flows through at a residence time of 4 h.....	21
Figure 2-6 F concentrations in the effluents vs. column pore volumes when a simulated 10 mg/L F wastewater flows through the limestone reactor at a residence time of 4 h.....	22
Figure 2-7 F concentrations vs. distance along the column with and without injection of a slurry after a passage of 20 pore volumes when a 10 mg/L NaF feedwater flows through at a residence time of 4 h.....	24
Figure 2-8 F concentrations in the effluent from each column vs. pore volumes when a 10 mg/L NaF feedwater flows through the dolomite reactor at a residence time of 4 h.....	28
Figure 3-1 Standard curves when UV length ranged from 550 nm to 600 nm with an increment of 10 nm each time .....	38
Figure 3-2 Standard curves at a range of citrate concentrations.....	40

Figure 3-3 Absorbances of standard fluoride samples and fluoride samples with citrate when 200 $\mu$ L pH buffer was added (UV length was at 590 nm).....	43
Figure 3-4 Absorbances of standard fluoride samples and fluoride samples with citrate when 1000 $\mu$ L pH buffer was added (UV length was at 590 nm) .....	43
Figure 3-5 Measured absorbances of fluoride standards at 1st hour (a), 2nd hour (b) and 3rd hour (c) after the spectrometer started.....	45
Figure 3-6 Standard peaks of common anions in an IC curve.....	50
Figure 4-1 Schematic of the phosphate rock reactor: Feedwater is equilibrated with CO <sub>2</sub> (g) and flows through four columns of phosphate rocks via saturated flow .....	56
Figure 4-2 F concentrations vs. pore volumes in treatment when a 10 mg/L NaF feedwater flows through the phosphate rock reactor at a residence time of 4 h .....	66

## List of Tables

Table 2-1 Measured and predicted (bracket values) results a passage of 100 pore volumes when a 10 mg/L NaF feedwater flows through the limestone reactor .....	13
Table 2-2 Comparison of the results from limestone reactor and the reactor designed by Reardon and Wang (in bracket) after a passage of 100 pore volumes when a 10 mg/L NaF feedwater flows through the limestone reactor .....	16
Table 2-3 Measured and predicted (in bracket) results after a passage of 100 pore volumes when a 10 mg/L NaF feedwater flows through the dolomite reactor at a residence time of 4 h.....	25
Table 2-4 Comparison of the results from the dolomite reactor and the limestone reactor (in bracket) after a passage of 100 pore volumes when 10 mg/L NaF feedwater flows through the reactors at a residence time of 4 h.....	27
Table 3-1 Predicted pH values of fluoride samples when a range of citrate concentrations were presented.....	42
Table 3-2 Interference from citrate on determination of F standard using fluoride electrode .....	46
Table 3-3 QA/QC report of the determination of fluoride by fluoride electrode .....	47
Table 3-4 Concentrations of the gradient eluent in IC method .....	48
Table 3-5 Standard peaks of common anions in an IC curve .....	49
Table 3-6 QA/AC report of the determination of fluoride by IC .....	51
Table 4-1 Phosphate rocks used in this research .....	54
Table 4-2 Materials in each column of the reactor.....	57
Table 4-3 Summary of X-ray and FT-IR results of the four types of phosphate rocks.....	59
Table 4-4 Calculation of percentage of CaCO <sub>3</sub> in phosphate rocks .....	60
Table 4-5 Calculation of percentage of fluorapatite in phosphate rocks.....	60
Table 4-6 Calculation of percentage of hydroxyapatite in phosphate rocks .....	60
Table 4-7 Summary of the composition of each phosphate rock .....	61

Table 4-8 Comparison of the fluoride and calcium concentrations after batch test (a) and (b) .....	63
Table 4-9 Comparison of the phosphate concentrations (in mg/L P) after batch test (a) and (b).....	63
Table 4-10 Comparison of pH change in batch test (a) and (b) .....	64
Table 4-11 Major cations in the effluents from columns when a 10 mg/L NaF feedwater flows through the limestone reactor at a residence time of 4 h after a passage of 100 pore volumes .....	67

# Chapter 1

## Introduction

### 1.1 Background

Fluoride (F) is an essential element for humans and drinking water is the primary source of fluoride intake. Small concentrations of fluoride help prevent tooth decay by making the tooth more resistant to acid attack (Featherstone, 1999). However, long-term ingestion of high fluoride drinking water causes fluorosis. This chronic disease is typically developed in many mid-latitude regions of the world when the fluoride concentration of drinking water is  $> 5$  to  $10$  mg/L (Handa, 1975; Maheshwari, 2006). Depending on the fluoride concentration level ingested, fluorosis results in mottling of teeth enamel, softening of bones, ossification of tendons and ligaments, and even neurologic damage (Dissanayake, 1991; Reardon & Wang, 2000).

The World Health Organization (WHO) recommends that surface and groundwater used as drinking water have fluoride concentrations  $< 1.5$  mg/L (Geneva, 2006; Hespanhol & Prost, 1994). Most natural waters have fluoride concentrations below  $2$  mg/L. However, under certain hydrogeochemical conditions (granitic terrains, areas with hydrothermal activity, areas of high rates of groundwater evapotranspiration, or where low pH waters are generated) fluoride concentration can be ten times higher (Ayoob & Gupta, 2006; Edmunds & Smedley, 2013). In addition to natural sources of fluoride, certain industries can produce wastewaters with thousands of mg/L fluoride. These sources include the manufacture of semiconductors, coal power plants, the ceramic industry, and fertilizer production (Dissanayake, 1991; Shen et al., 2003).

Precipitation and sorption are the two most commonly used techniques for the remediation of fluoride (Maheshwari, 2006; Mohapatra et al., 2009). The application of lime (CaO) with subsequent precipitation of fluorite (CaF<sub>2</sub>) is the dominant technique to reduce high fluoride wastewaters to  $< 5$  mg/L (the approximate solubility of a fresh fluorite precipitate). The theoretical lower limit is actually  $2$  mg/L for a water saturated with respect to both fluorite and portlandite (Ca(OH)<sub>2</sub>) (Nordstrom & Jenne, 1977). However, this lower limit is rarely attained in

reality. To achieve further reductions of fluoride in wastewater or to treat naturally-high fluoride water for municipal use and drinking water, the standard treatment world-wide involves flow through ion sorption or exchange columns. These ion retention methods are more effective in reducing fluoride concentration than precipitation methods, because they can reduce fluoride to below 1.0 mg/L. Activated alumina (Sujana et al., 1998; Tripathy et al., 2006) is a commonly-used sorbent but many other materials have been tested, including fly ash (Chaturverdi et al., 1990), silica gel (Wasay et al., 1996), bone charcoal (Bhargava, 1992), carbon nanotubes (Li, 2003), and some low-cost geomaterials, including soils (Wang et al., 2003; Wang & Reardon, 2001), volcanic ash (Srimurali et al., 1998) and zeolites (Onyango, 2004) and macrophyte biomass (Miretzky et al., 2008). Sorption methods typically require initial high setup costs and ongoing management, which includes monitoring concentration levels, periodic regeneration of the sorbent. A reliable, passive treatment technology to attain the WHO recommended drinking water limit of 1.5 mg/L has the potential to be more cost-effective.

Reardon and Wang (2000) remediated fluoride by developing a passive reactor composed of two columns of limestone gravel. The reactor works by adding carbon dioxide to inflowing water, which forces calcite ( $\text{CaCO}_3$ ) to dissolve, and thus, fluorite ( $\text{CaF}_2$ ) to precipitate in the first column. The effluent water then degasses by unsaturated flow through the second column of limestone gravel and this process results in precipitation of calcite that dissolved in the first column. In operation, the reactor attains the predicted reduction to  $< 5$  mg/L (solubility of freshly-precipitated fluorite) in the first column but no further reductions occur in the second column. Consequently, the technology was applicable only as an initial treatment of high fluoride wastewaters, not as a treatment to produce drinking-water quality fluoride concentrations.

Okumura et al. (1983) discovered the effect of citrate ion to induce fluoride to co-precipitate in calcite. This study, therefore, evaluated the impact of this process to potentially improve the passive, two-column reactor technology of Reardon and Wang to attain drinking water quality fluoride concentrations. The addition of citrate ion is considered being feasible because citric

acid is universally accepted as a safe food ingredient additive (Pizzocaro et al., 1993; Pokorný, 1991). The development of a simple, inexpensive, and passive technology to reduce fluoride concentrations in waters to recommended drinking water limits is an important contribution to wastewater treatment technology, and of significant benefit to communities affected by fluorosis world-wide. Okumura et al. (1983) also indicated that the presence of magnesium ion promoted more fluoride to co-precipitate in calcite. Therefore, a dolomite reactor was also constructed and its efficiency in remediation of fluoride was evaluated.

Moreover, phosphate rock, a material containing calcite and apatite, has a potential to remediate fluoride contaminated water by both precipitation and adsorption. Fluoride can be precipitated as fluorite, and previous studies found that different forms of apatite can absorb fluoride and reduces fluoride concentration to below 1 mg/L (Murutu et al., 2010; Gao et al., 2009; Tomar et al., 2013). Therefore, in this research, the effectiveness of the phosphate rock is also assessed.

## **1.2 Thesis Objective**

This research aims to develop a fluoride removal method, which needs less maintenance but can achieve higher removal efficiencies at a lower cost than conventional treatment methods.

The objectives were studied by:

- Examining the known role of citrate ion to induce fluoride to co-precipitate in calcite and its impact to improve the passive, two-column reactor technology described by Reardon and Wang to attain drinking water quality fluoride concentrations;

- Determining the interferences of citrate on analytical determination of fluoride.

Investigating three methods of fluoride analysis to determine the most sensitive technique with the least interference;

- Examining removal of fluoride by cost-effective Phosphate rocks through precipitation and sorption.

## Chapter 2

# Effect of Citrate on Fluoride Co-precipitation into Calcite and Its Application

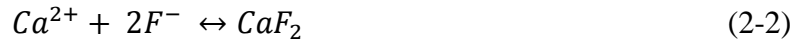
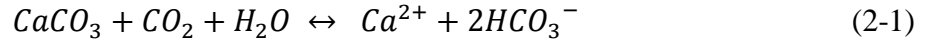
### 2.1 Background

Fluoride contamination is a serious problem in some mid-latitude regions since ingestion of excess fluoride through drinking contaminant water typically cause fluorosis. Reardon and Wang (2000) developed a reactor composed of two columns of limestone gravel to reduce fluoride concentrations in simulated groundwater. The reactor works by adding carbon dioxide to inflowing water, which promotes dissolution of calcite ( $\text{CaCO}_3$ ) and thus precipitation of fluorite ( $\text{CaF}_2$ ) in the first column. The exiting water then degasses by unsaturated flow through the second column of limestone gravel. This process results in a precipitation of the calcite that dissolved in the first column. In operation, the reactor attains the predicted reduction to  $< 5$  mg/L fluoride (solubility of freshly-precipitated fluorite) in the first column, but no further reductions occur in the second column. In other words, no substantive substitution of fluoride ion for carbonate ion occurred in the lattice of the precipitating calcite in the second column. Consequently, the technology is only applicable as an initial treatment of high fluoride wastewaters, not as a treatment to produce drinking-water quality fluoride concentrations.

Citrate ions, however, has a potential to be used to improve the reactor designed by Reardon and Wang by decreasing fluoride in the second column. Okumura et al. (1983) evaluated several organic ligands and found that citrate ions can promote the co-precipitation of fluoride into calcite. In their research, when the citrate concentration in the parent solution reaches 0.5 mmol/L, it can promote 1 g of fluoride to co-precipitate in 1 kg  $\text{CaCO}_3$ . In addition, with an increasing concentration of magnesium in the parent solution, fluoride co-precipitated in calcite/Mg-calcite increased up to 2 g per 1 kg calcite.

Therefore, in this study, a third column containing calcium citrate was added in between the original two columns in the reactor of Reardon and Wang. Citrate and additional calcium ion was

brought into the solution from the dissolution of calcium citrate, and thus, the citrate was supposed to promote the incorporation of fluoride ions into calcite (Okumura et al., 1983). The potential reaction occurred in the reactor is as indicated by equation 2-1, 2-2 and 2-3.



This study then evaluates the ability of citrate ion to induce fluoride ion to co-precipitate in calcite, and to evaluate its impact to improve the passive, two-column reactor of Reardon and Wang to attain drinking water quality fluoride concentrations. The addition of citrate ion is considered to be feasible since citric acid is universally accepted as a safe food ingredient additive (Pizzocaro et al., 1993; Pokorný, 1991). In addition, since magnesium ions also affect the ability for citrate to promote fluoride co-precipitation (Okumura et al., 1983), a similar reactor was designed with dolomite. Experiments were conducted to evaluate the co-effect of magnesium and citrate ions on fluoride removal.

This reactor has a potential to be used for treatment of high fluoride wastewater. Application of this treatment technology is inexpensive because of the materials (crushed limestone or dolomite and carbon dioxide), and it is also simple because column regeneration is not required. The development of this passive technology to reduce fluoride concentrations in waters to recommended drinking water limits is an important contribution to wastewater treatment technology, and of significant benefit to communities affected by fluorosis world-wide.

## 2.2 Experimental Methods

### 2.2.1 Materials

White-marble gravel obtained commercially from a local landscaping vendor was the source of calcium carbonate used for the limestone reactor. "Marble" is defined as a metamorphosed limestone. The metamorphism process causes variable recrystallization of the original carbonate

mineral grains (most commonly limestone). As a result, marble is more resistant to dissolution by acid than limestone. The occurrence of limestone, however, is more widely distributed in the world than marble, and more easily obtained as a treatment material. Therefore, the term “limestone reactor” was used in this thesis even though the material used was marble. The marble was crushed and sieved, and then particles with a grain size between 1.4 mm and 2.0 mm were used for columns 1 and 2. Results of x-ray diffraction (XRD) analyses revealed only peaks for calcite, indicating >95% purity (Appendix C). Ottawa Quartz sand (size between 0.85 mm to 1.4 mm, also obtained from a local landscaping vendor) and calcium citrate tetrahydrate powder (supplied by Alfa Aesar, 96%) were used to fill the plastic column 3 (made from a 120 mL syringe) between the two plexiglas columns (columns 1 and 2).

Grey dolomite (size between 0.85 mm to 1.4 mm) attained commercially from a local landscaping vendor was used to fill the column 1. Results of the XRD analyses revealed only peaks for dolomite indicating >95% purity (Appendix C). The same Ottawa quartz sand and calcium citrate tetrahydrate powder were used to fill a plastic column 3 (made from a 120 mL syringe). A mix of the white-marble gravel and dolomite (size between 0.85 mm to 1.4 mm) was used to fill column 2 of the reactor.

Two types of feedwaters were used: a sodium fluoride (NaF) solution with 10 mg/L fluoride, and a high-fluoride simulated wastewater. The high-fluoride simulated wastewater was made by combining one part laboratory tap water with 4 parts deionized water, and NaF powder (supplied by Fisher Scientific, > 99%) was added to keep the fluoride concentration at 10 mg/L. This kind of dilution achieved a low calcium concentration so that the initial feedwater was not supersaturated with respect to fluorite.

## 2.2.2 Designs and Operations of the Reactors

### 2.2.2.1 Limestone Design and Operations

The limestone reactor was created based on the design of Reardon and Wang (2000). The two original limestone plexiglas columns (column 1 and column 2) were 49 cm in length by 5 cm in diameter, and a third column was made of a 60 mL syringe (Figure 2-1).

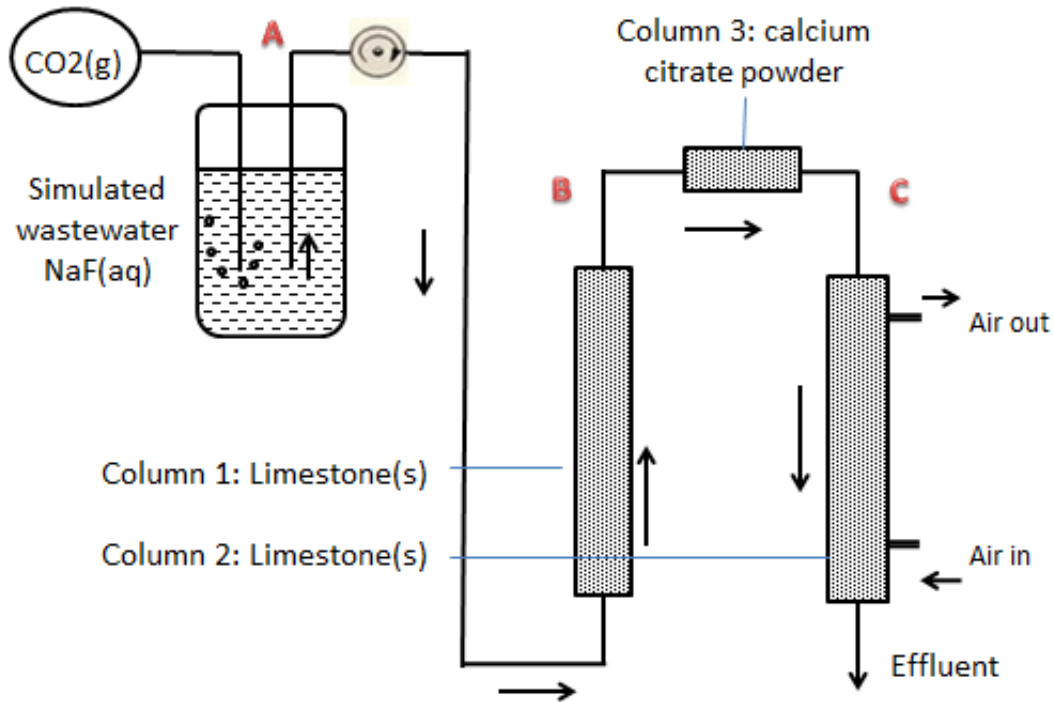


**Figure 2-1 Schematic of the limestone reactor: The feedwater is bubbled with 97 kPa  $\text{CO}_2$  (g) before flowing through column 1 containing limestone via saturated flow, column 3 containing calcium citrate via saturated flow and column 2 containing limestone via unsaturated flow continuously**

A 20 L glass carboy was used to store feedwater. Before the system started to flow, the carboy was connected to a tank of carbon dioxide at 97 kPa pressure by an immersion bubbler, and the  $\text{CO}_2$  (g) was bubbled into the feedwater until equilibrium was reached. The equilibrium can be identified by measuring the pH of the feedwater. The pH was predicted to fall to approximately

3.9, and carbonic acid concentration increased. The air-entry tube was connected to a source of  $\text{CO}_2$  (g) so that when feedwater was displaced to the reactor columns, the remaining solution maintained saturation with respect to  $\text{CO}_2$  (g). Then, the feedwater entered the bottom of the first column via saturated flow. This column contained 943 g of limestone, and the total pore volume was 206 mL. Sampling ports, which were pre-installed with rubber septa, were located at 1, 4, 9, 14, 19, 29, and 39 cm from the entry of column 1. Water exiting column 1 entered column 3, which contained a mixture of 176 g of Ottawa Quartz sand and 35 g of calcium citrate tetrahydrate. Column 3 was a plastic column, and it was 10 cm in length by 3.8 cm in diameter. The pore volume of this column is 30.7 mL, and thus, the residence time of the water in this column was 0.6 h when the residence time of column 1 was 4 h. This is a sufficient time to achieve saturation with the calcium citrate, and citrate is supposed to be brought into the solution from the dissolution of calcium citrate tetrahydrate and promote the incorporation of fluoride ions into calcite (Okumura et al., 1983). Then, water exiting column 3 entered the top of column 2 via unsaturated flow by pumping air through this column continuously. Column 2 contained 950 g of limestone and was the same size as column 1. In this column calcite is supposed to become supersaturated and the water is supposed to return to its initial composition in the process, because degassing of the water removed dissolved carbon dioxide across the water and air interface. During operation of the reactor, the feedwater was delivered to the reactor columns at a constant flow rate via a pump (model 7553-80, supplied by Masterflex). By adjusting the flow rate, a diverse range of residence times of column 1 was achieved. Then, the numbers of pore volumes were calculated by dividing the operating time of the reactor by the residence time of column 1.

### **2.2.2.2 Dolomite Design and Operations**

The dolomite reactor has the same structure as the limestone other than the size of the columns and the materials in columns 1 and 2 (Figure 2-2).

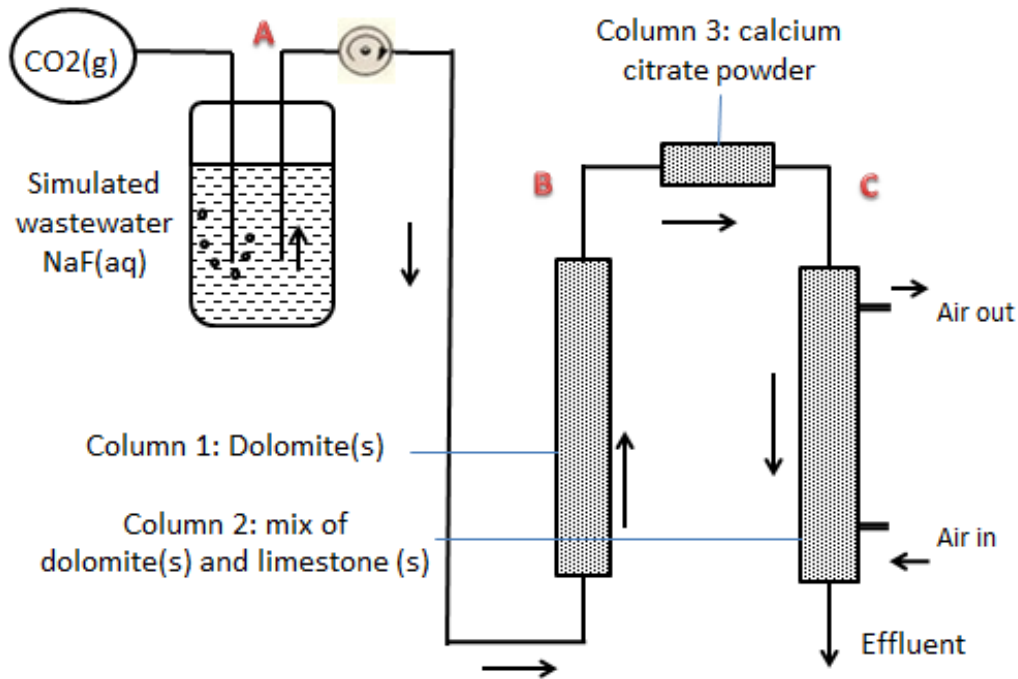


**Figure 2-2 Schematic of the dolomite reactor: The feedwater is bubbled with 97 kPa  $\text{CO}_2$  (g) before flowing through column 1 containing dolomite via saturated flow, column 3 containing calcium citrate via saturated flow and column 2 containing both dolomite and limestone via unsaturated flow continuously**

Two Plexiglas columns (i.e., column 1 and column 2) were 28.5 cm in length by 2.5 cm in diameter, and column 3 of this dolomite reactor was the same as the column 3 in the limestone reactor. Column 1 was filled with 172.5 g of dolomite and the pore volume was 76.72 mL, and column 2 was filled with a mix of 82.3 g limestone and 94.3 g of dolomite. The feedwater was delivered to the reactor columns with a constant flow rate of 19.18 mL/h via the same pump (model 7553-80, supplied by Masterflex) and thus, resulted in a residence time of 4 h in column 1. Other residence times were also applied by adjusting the flow rate.

### **2.2.3 Sampling and Analysis**

Column effluent samples were regularly collected from columns 1, 3 and 2 of both limestone and dolomite reactors using syringes. Samples were filtered through Whatman 0.45 micron cellulose acetate filters and analyzed for pH and calcium, fluoride and citrate concentrations. Measurement of the pH was performed potentiometrically with an accumet pH meter and an Orion combination pH electrode (both supplied by Fisher Scientific). Calcium, magnesium and other major cations were analyzed by a Thermo Scientific Inductively Coupled Optical Spectrophotometry (ICP). Fluoride was analyzed using an accumet ion meter (supplied by Fisher Scientific) and a fluoride double junction ions selective fluoride electrode (supplied by Oakton). Details of fluoride electrode method are discussed in chapter 3. Citrate was analyzed using a Thermo Scientific Ion Chromatography (IC). Analytical reproducibility of duplicate samples was better than  $\pm 5\%$ . Periodically, profile sampling was undertaken using the sampling ports along the length of column 1. These samples were analyzed for pH and calcium, fluoride and citrate concentrations.

Suspended material in solution samples collected from the lower sampling ports of both column 1 and column 2 were analyzed by X-ray diffraction spectrometer. The spectrometer (XRG 3000, supplied by INEL) ran at a Cu and Ka radiation at a wave length of 0.154 nm for 20 min per sample.

### **2.2.4 Modelling Program of the Reactors**

#### **2.2.4.1 Modelling for the Limestone Reactor**

A chemical equilibria program—PHREEQC was used to predict the composition changes when a 10 mg/L fluoride feedwater flows through reactors. The model program is demonstrated in Appendix B. In the program for limestone reactor, “SOLUTION 1” simulated the composition of the stockwater. “EQUILIBRIUM PHASES 1” modelled the change when the stockwater was equilibrated with 97.6 kPa CO<sub>2</sub> (g) in average, and then, “EQUILIBRIUM PHASES 2” simulated the process in column 1 when the flow entered from the bottom of column 1 and equilibrated with calcite. Next, “EQUILIBRIUM PHASES 3” modelled the composition change

of the feedwater when it passed through column 3 equilibrating with calcium-citrate. Finally, “EQUILIBRIUM PHASES 4” simulated the process when the flow passed through column 3, where it became equilibrated with atmospheric pressure and calcite become super-saturated and precipitated. This process was modeled by assuming an open system in equilibrium with a  $10^{-1.4}$  kPa  $p\text{CO}_2$ , which represent an average  $\text{CO}_2$  partial pressure of the laboratory air.

However, PHREEQC alone cannot accurately predict the fluoride concentration in the effluent because it does not include the amount of fluoride co-precipitated in calcite in column 2. The accurate prediction should be calculated based on PHREEQC results and results from research conducted by Okumura et al. (1983). PHREEQC predicted that the citrate concentration in the effluent from column 3 was 1.74 mmol/L, and Okumura et al. (1983) stated that this amount of citrate should promote at least 1 g of fluoride to co-precipitate in 1 kg calcite. According to the predicted results, the calcium concentration difference between effluent and influent from column 2 was 7.95 mmol/L, and this calcium loss was caused by 795 mg/L calcite precipitation. Therefore, if 1 L of feedwater passed through column 2, 795 mg calcite should precipitate in column 2. With the sufficient citrate, 0.795 mg of fluoride can co-precipitate in the 795 mg calcite. Consequently, fluoride concentration should be reduced by 0.795 mg/L. As a result the fluoride concentration in the effluent should be 1.25 mg/L by prediction, which attains the drinking water standard by WHO.

#### **2.2.4.2 Modelling for the Dolomite Reactor**

The PHREEQC program for the dolomite reactor was the same as that for limestone reactor except that dolomite was simulated to be dissolved in “EQUILIBRIUM PHASES 2” rather than calcite. In addition, PHREEQC predicted that the citrate concentrations in the effluents from column 3 and column 2 in the dolomite reactor were both 3.16 mmol/L, and Okumura et al. (1983) stated that this citrate should promote at least 2 g of fluoride to co-precipitate in 1 kg calcite. Prediction results indicate that the calcium concentration difference between effluent and influent from column 2 was 10.9 mmol/L. Similarly as prediction procedure in 2.2.5.1, 2.18 mg of fluoride should co-precipitate into calcite if 1 L of feedwater passed through column 2. Therefore, fluoride concentration should be reduced by 2.18 mg/L. In conclusion, the fluoride

concentration in the effluent should be 1.29 mg/L by prediction, which attains the drinking water standard by WHO.

## **2.3 Results and Discussion**

### **2.3.1 Limestone Reactor**

#### **2.3.1.1 Removal Efficiency and Comparison with Predicted Results and the Results of the Reactor Described by Reardon and Wang**

In reactor operation of this research, the residence times were designed to be 4 h and 20 h, respectively, by adjusting the flow rates. At each residence time, at least 100 pore volumes of stockwater were passed through the reactor. Then, the results of chemical analysis are shown in Table 2-1, and those results are compared to the prediction results. Table 2-1 (a) demonstrates the comparison when the residence time of limestone reactor was 4 h; while Table 2-1 (b) shows the comparison when the residence time was 20 h.

**Table 2-1 Measured and predicted (bracket values) results a passage of 100 pore volumes when a 10 mg/L NaF feedwater flows through the limestone reactor**

a) When residence time of limestone reactor at the time of sampling was 4 h

	1) Initial water	2) Port A Equilibrium with CO <sub>2</sub>	3) Port B column 1 effluent	4) Port C column 3 effluent	5) Effluent column 2 effluent
pH	(7.12)	(4.03) 3.98	(6.12) 6.63	(6.11) 6.56	(8.07) 7.34
F (mg/L)	(10.0) 10.0	(10.0) 10.0	(2.05) 4.18	(2.05) 4.18	(1.25) 3.41
Na (mmol/L)	(0.526)	(0.526)	(0.526) 0.638	(0.526) 0.660	(0.526) 0.680
Ca (mmol/L)			(8.23) 10.2	(10.8) 13.8	(2.85) 5.92
Citrate (mmol/L)				(1.75) 1.02	(1.74) 0.980

b) When residence time of limestone reactor at the time of sampling was 20 h

	1) Initial water	2) Port A Equilibrium with CO <sub>2</sub>	3) Port B column 1 effluent	4) Port C column 3 effluent	5) Effluent column 2 effluent
pH	(7.12)	(4.03) 4.97	(6.12) 6.71	(6.11) 6.66	(8.07) 7.74
F (mg/L)	(10.0) 10.0	(10.0) 10.0	(2.05) 1.81	(2.05) 1.82	(1.25) 1.65
Na (mmol/L)	(0.526)	(0.526)	(0.526) 0.748	(0.526) 0.776	(0.526) 0.761
Ca (mmol/L)			(8.24) 7.13	(10.8) 7.79	(2.85) 4.83
Citrate (mmol/L)				(1.75) 0.930	(1.74) 1.05

As demonstrated in Table 2-1, the removal efficiency of the reactor was not optimal as the predicted on the whole. Although the measured values showed close correspondence to the predicted values, fluoride concentration in the effluent from each column was higher than predicted.

When the residence time was 4 h after a passage of 100 pore volumes, the fluoride concentration measured in the effluent was 3.41 mg/L, and this concentration was much higher than the predicted value (1.25 mg/L). The introduction of column 3 increased citrate concentrations but only promoted 0.77 mg/L fluoride to co-precipitate in column 2. In addition, measured fluoride concentrations in the effluents from column 1 and column 3 were also higher than the predicted values.

When the residence time was 20 h after a passage of 100 pore volumes, the measured results were closer to predicted results than when the residence time is 4h. The biggest difference of the measured and predicted results was the calcium concentration in the influent and effluent from column 2. The results indicate that the measured calcium loss in the column 2 was much less than the predicted loss. This also means that less calcite precipitated in column 2 than by predicted. The fluoride concentrations in the effluent that were predicted and measured were 1.25 mg/L and 1.65 mg/L, respectively. The measured result was higher than the World Health Organization (WHO) recommended drinking water fluoride concentrations (1.5 mg/L).

Two reasons resulted in the lower removal efficiency than predicted. First of all, Okumura et al. (1983) pointed out that the presence of a small amount of citrate significantly decreases the rate of calcite formation and favors the formation of magnesian calcite. Therefore, citrate, which was brought into the flow from column 3, suppressed the precipitation of calcite in column 2. Consequently, less calcite precipitated in column 2, and fluoride co-precipitation decreased. The evidence is also shown in Table 2-2. The calcium reduction that occurred in column 2 in the reactor of Reardon and Wang was larger than what occurred in reactor of this research (Table 2-2). Another factor is the residence time. The results indicate that when the residence time was 4 h,

the fluoride removal efficiency was much lower than that when the residence time is 20 h. the results indicate that the longer the residence time is, the higher the removal efficiency (closer to predicated results). More discussion is included in section 2.3.1.2.

The results of limestone reactor in this research were also compared to the results from the research by Reardon and Wang (Table 2-2).

**Table 2-2 Comparison of the results from limestone reactor and the reactor designed by Reardon and Wang (in bracket) after a passage of 100 pore volumes when a 10 mg/L NaF feedwater flows through the limestone reactor**

a) When residence time of both reactors at the time of sampling was 4 h

	1) Port A Equilibrium with CO <sub>2</sub>	2) Port B column 1 effluent	3) Port C column 3 effluent	4) Effluent column 2 effluent
pH	(4.35) 4.19	(6.86) 6.63	(-) 6.56	(8.35) 7.34
F (mg/L)	(10.0) 10.0	(3.93) 4.18	(-) 4.18	(4.01) 3.41
Na (mmol/L)	(0.541)	(0.524) 0.638	(-) 0.660	(0.533) 0.680
Ca (mmol/L)	(0.260)	(11.5) 10.1	(-) 13.8	(0.810) 5.92
Citrate (mmol/L)			(-) 0.921	(-) 0.842

b) When residence time of both reactors at the time of sampling was 20 h

	1) At Port A Equilibrium with CO <sub>2</sub>	2) At Port B column 1 effluent	3) At Port C column 3 effluent	4) Effluent column effluent
pH	(4.97) 4.23	(6.53) 6.71	(-) 6.66	(8.42) 7.74
F (mg/L)	(10.0) 10.0	(1.77) 1.81	(-) 1.82	(1.75) 1.65
Na (mmol/L)	(0.790)	(0.820) 0.748	(-) 0.776	(0.890) 0.761
Ca (mmol/L)	(0.550)	(8.07) 7.13	(-) 7.98	(0.580) 4.83
Citrate (mmol/L)			(-) 0.932	(-) 1.05

When the residence time was 4 h, the fluoride concentration measured in the effluent was 3.41 mg/L, and it was lower than that from the reactor of Reardon and Wang (4.01 mg/L). This result indicates that the limestone reactor in this research performed better than the reactor of Reardon and Wang by a fluoride deduction of 0.60 mg/L. The results from Table 2-2 also indicate that calcium reduction in column 2 in this research was less than that in the reactor of Reardon and Wang. By calculation, 10.6 mmol/L calcium was reduced in column 2 of the reactor of Reardon and Wang, while only 7.87 mmol/L calcium was reduced in the limestone reactor. This result indicates that less calcite was precipitated in the limestone reactor than in the reactor of Reardon and Wang, and thus, the amount of fluoride co-precipitated in calcite in column 2 of the limestone reactor was not as much as predicted. In addition, calcium concentration in the effluent of the limestone reactor (5.92 mmol/L) was higher than that of the reactor of Reardon and Wang (0.810 mmol/L).

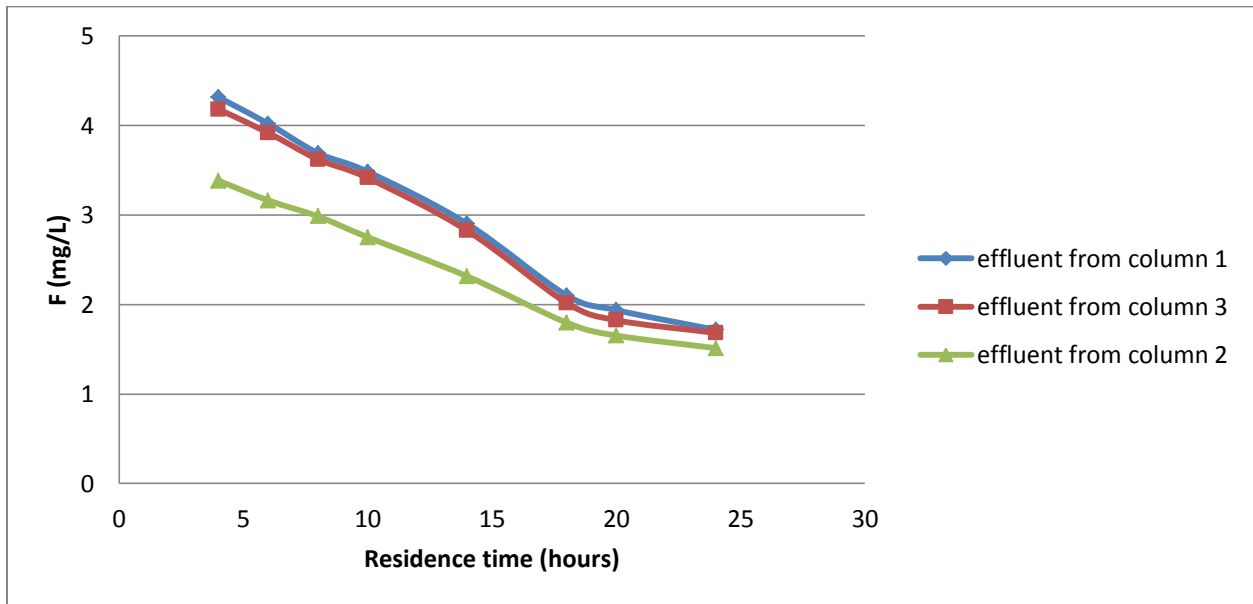
When the residence time was 20 h, the fluoride concentration in the effluent from the limestone reactor (1.65 mg/L) was still lower than of the reactor of Reardon and Wang (1.75 mg/L). In addition, the calcium deducted in column 2 in the limestone reactor was 3.14 mmol/L, and it was less than that of the reactor of Reardon and Wang (7.49 mmol/L). Moreover, the calcium concentration in the effluent was still as high as 4.83 mmol/L, and it was not significant lower than that when the residence time was 4 h (5.92 mmol/L). This result indicates that longer residence time did not significantly enhance the precipitation of calcite in column 2 of the limestone reactor.

In conclusion, the results from Table 2-1 and Table 2-2 show fluoride concentrations were further reduced in the limestone reactors than the reactor of Reardon and Wang by 0.6 mg/L, which achieved the goal of this research. However, the improvement was not optimistic as predicted. The fluoride concentrations should be reduced to 1.25 mg/L by prediction. In this limestone reactor, even when the residence time is 20 h, the fluoride concentration was 1.65 mg/L; while when the residence time is 4 h, the fluoride concentration was 3.41 mg/L. The reason for this was: inhibition effect of citrate on calcite formation. More research is needed to

improve the efficiency of this reactor, and preliminary experiment for improvement is discussed in section 2.3.1.6.

### 2.3.1.2 Effect of Residence Time

To investigate the influence of residence time on fluoride removal efficiency, the residence time were designed to increase from 4 h to 20 h by adjusting the flow rate when a 10 mg/L fluoride simulated groundwater was flowing through the reactor. At each residence time, at least 10 pore volumes of stockwater were passed through the reactor, and effluent samples were collected from each column. The fluoride concentrations in the effluent from each column were measured and recorded (Appendix C and Figure 2-3). The results show that when residence time decreased from 24 h to 4 h, the concentration of fluoride increased from 1.72 mg/L to 4.31 mg/L in column 1, from 1.49 mg/L to 3.38 mg/L in column 2, and from 1.68 mg/L to 4.18 mg/L in column 3.



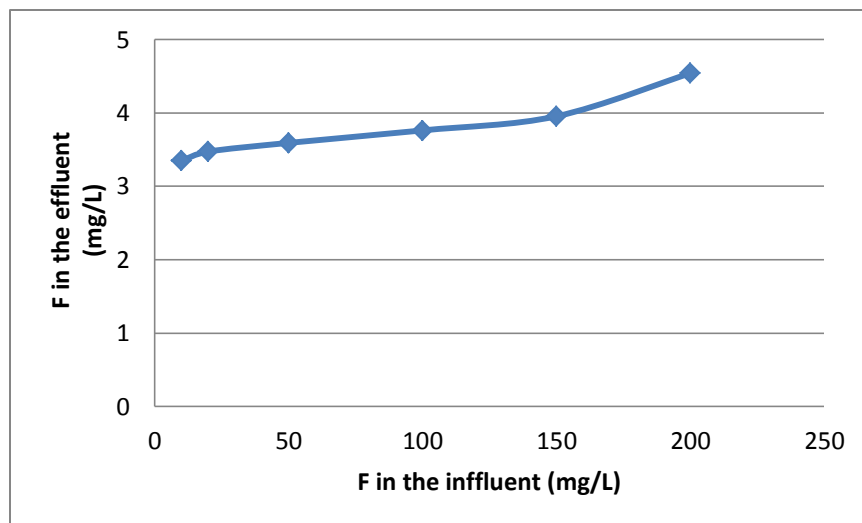
**Figure 2-3 F concentrations in the effluents vs. residence times of when a simulated 10 mg/L F wastewater flows through the limestone reactor after a passage of 10 pore volumes at each residence time**

Figure 2-3 illustrates the fluoride concentrations in the effluent from each column decreased with the increase of residence time. With the increase of residence time, the reduction of fluoride in column 2 also decreased. Because longer residence times resulted in a lower concentration in the feedwater entering into column 2, fluoride co-precipitated into calcite decreased. The results also indicate that, with the increase of residence time, the fluoride concentration decreased, and the decreasing rate of the fluoride concentration decreased.

Overall, the fluoride removal efficiency increased with the increase of the residence time. The reason for this effect was caused by the precipitation rate. The longer residence time resulted in a larger amount of fluorite precipitation in column 1. 24 h is an acceptable residence time for domestic treatment. In a typical household in North America, 300 L water is consumed a day. Of this approximately 5% is used in the kitchen for drinking and cooking. Therefore, the reactor should be able to remediate 15 L water per day. Column 1 of the reactor designed in this research has a porosity of 21.4%. Then, the volume of the column 1 of the reactor should be 70 L, which is a reasonable size for a household. However, improvement should still be proposed to increase the removal efficiency at a relatively low residence time (4h), which is more practical and more efficient.

### **2.3.1.3 Maximum Level of Fluoride Treatable Capacity**

Maximum level of treatable fluoride was examined in the research. Wide concentration ranges of fluoride simulated groundwater (concentrations ranged from 10 mg/L to 200 mg/L) were prepared as the stockwater (influent) for the experiment. The residence time was designed to be 4 h throughout the experiment. Samples were collected from each column after a passage of 10 pore volumes for each influent. The results of this experiment are shown in Appendix C and Figure 2-4.



**Figure 2-4 F concentrations in the effluent vs. F concentrations in the influent after a passage of 10 pore volumes each when various concentrations of simulated F wastewater flows through the limestone reactor at a residence time of 4 h**

The fluoride concentrations in the effluents increased with the increase of fluoride concentrations in the influents. When the fluoride concentrations in the influent were below 150 mg/L, the fluoride concentrations in the effluent were below the maximum contaminant level (4 mg/L). Therefore, the reactor has good potential to be used for high fluoride wastewater treatment. Although the concentrations do not meet the drinking water standard, it can be applied as a pre-treatment option in combination with ion exchange techniques.

#### **2.3.1.4 Characterization of Precipitation**

The 10 mg/L fluoride simulated groundwater was prepared as the stockwater and the residence time were designed to be 4 h. After a passage of 60 pore volumes, samples along column 1 of the reactor were collected and analyzed. The results are shown in Figure 2-5.

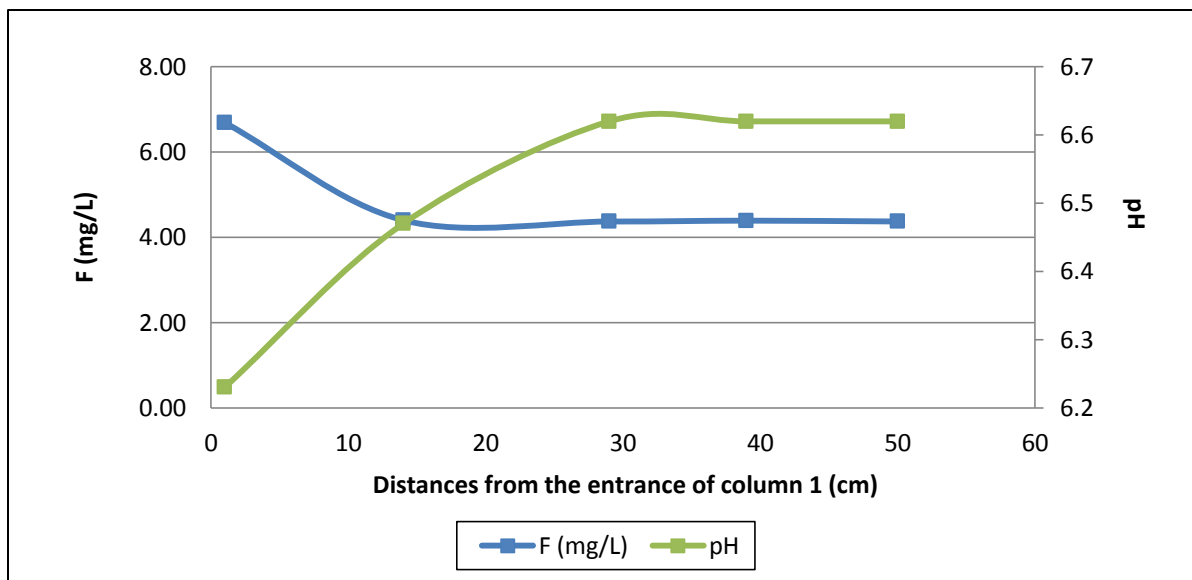


**Figure 2-5 F concentrations vs. distances along column 1 after a passage of 60 pore volumes when a simulated 10 mg/L F wastewater flows through at a residence time of 4 h**

Most of the fluoride reduction occurred in the first 10 cm of the reactor. White-yellow precipitation, assumed to be fluorite, was observed to at the bottom of column 1 of the reactor. While in the upper parts of the column 1, the yellow precipitation was rarely seen. Therefore, both of these two observations indicate that most of the fluorite precipitated at the influent end of column 1. According to Reardon and Wang (2000), this fluorite precipitation provided nuclei site for fluoride ion to crystallize on and the overall fluoride removal rate improved. This finding is described as “column conditioning” by Reardon and Wang, and the reactor after the process is described as “conditioned” reactor. Samples of the yellow precipitates in the first column were collected and examined using X-ray diffraction (Appendix D). The results revealed the presence of fluorite.

The formation of precipitates was also observed in column 2. When inflow from column 3 entered into column 2 through unsaturated flow and became equilibrated with atmosphere air,

calcite precipitated in column 2. White and fine calcite precipitation was observed on the top of column 2.

### 2.3.1.5 Long Term Behavior of the Reactor

For a “conditioned” reactor (as discussed in 2.3.1.4), investigation was made on the long term behavior of the reactor. A 10 mg/L fluoride simulated groundwater was prepared as the stockwater for the experiment. The residence time were designed to be 4 h. The fluoride concentrates as the running of the reactor are shown in Figure 2-6.

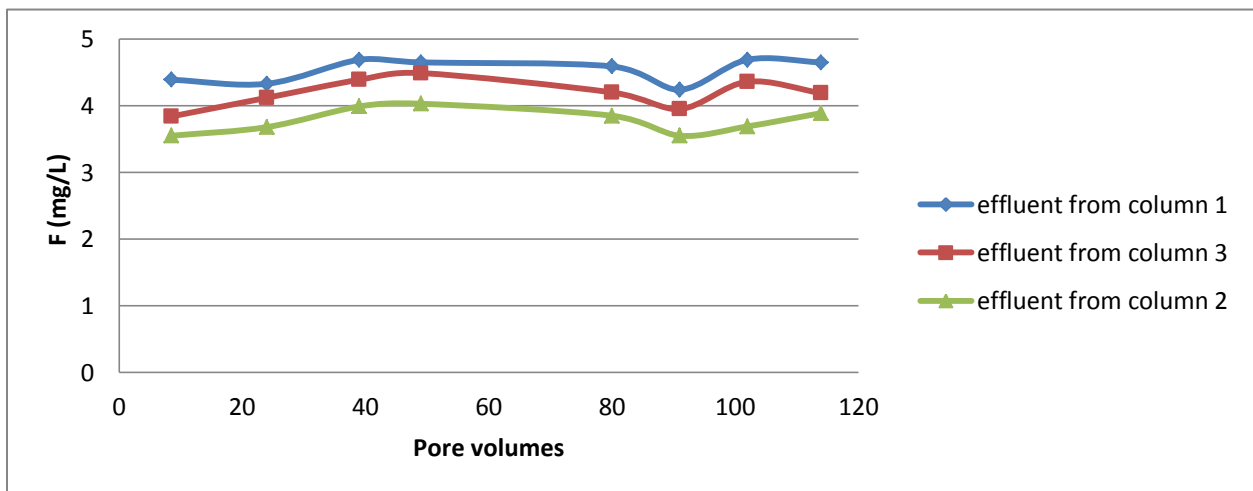


**Figure 2-6 F concentrations in the effluents vs. column pore volumes when a simulated 10 mg/L F wastewater flows through the limestone reactor at a residence time of 4 h**

The column performed well until a passage of 120 pore volumes. In addition, experiments results indicate that after running for 6 months, concentrations of fluoride remained constant. No obvious problem occurred in the long-term operations including clogging of the column and treatment capacity of the column.

### **2.3.1.6 Preliminary Experiment to Improve Removal Efficiency**

Previous research indicated that the limestone reactor designed in this research can successfully reduce fluoride concentration from up to 150 mg/L to below the maximum contaminant level (4 mg/L), at the residence time of 4 h. However, more research is required to improve the limestone reactor to attain higher fluoride removal efficiency (reducing fluoride concentration to below the drinking water standard – 1.5 mg/L).

As discussed in 2.3.1.4, in column 1 of the reactor, most of the fluorite precipitated at the influent end of column 1, and this fluorite precipitation provided nuclei site for fluoride ion to crystallize and the overall fluoride removal rate improved (Reardon & Wang, 2000). However, in the last 40 cm of the column 1, the process of precipitation of fluorite is minimal because the nucleation sites for fluoride ions to crystallize on were insufficient. Therefore, 20 mL slurry containing a few grams of fine-grained, reagent-grade  $\text{CaF}_2$  was injected into the column through the last three septa port to condition the column. After a passage of 20 pore volumes (the residence time was designed to be 4 h), samples were then collected at each port when a 10 mg/L fluoride simulated groundwater passed through the reactor. Fluoride concentrations of the samples are shown in Appendix C and Figure 2-7.

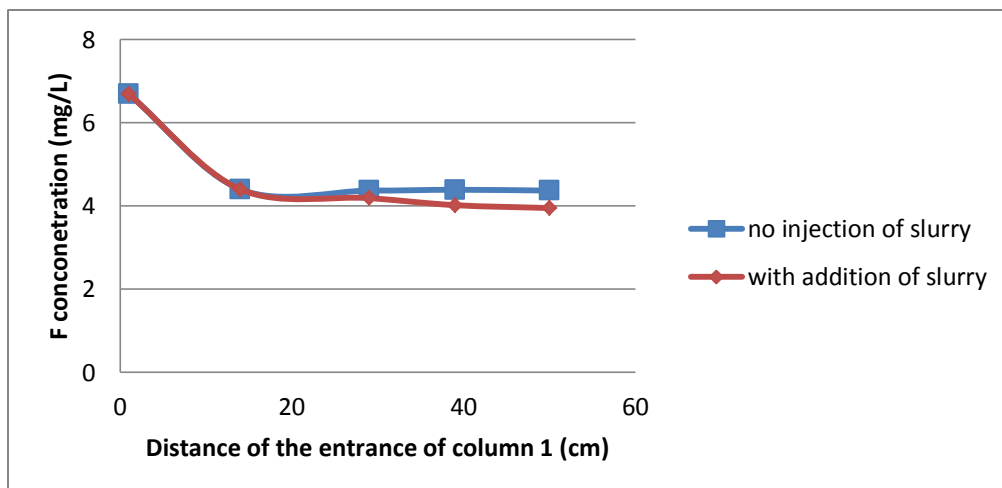


**Figure 2-7 F concentrations vs. distance along the column with and without injection of a slurry after a passage of 20 pore volumes when a 10 mg/L NaF feedwater flows through at a residence time of 4 h**

A further 0.420 mg/L reduction occurred in the last 40 cm of column 1 with an injection of slurry containing a few grams of fine-grained, reagent-grade  $\text{CaF}_2$ . Therefore, an addition of nucleation sites (fluorite precipitation) in the later parts of the reactor promoted the precipitation of fluorite and improved the fluoride removal efficiency. However, no further reduction was observed. The main reason was likely that the residence time was not sufficient for fluoride to fully precipitate as fluorite. Another possible reason may be due to the pH. Since pH values remained stable at 6.62 after 30 cm from the entrance, no more calcite can be dissolved. Consequently, no more calcium was introduced to the flow to promote precipitation of fluorite.

As discussed in 2.3.1.1, citrate greatly decreased the rate of calcite formation in column 2. This was a reason why fluoride concentration cannot be reduced to predicted level. Okumura et al. (1983) stated that presence of magnesium promotes fluoride to co-precipitate. Therefore, use of magnesium has a great potential to increase fluoride removal efficiency of the reactor. Magnesium can be introduced to the flow by replacing limestone with dolomite in column 1. More investigation is discussed in section 2.3.2.

### 2.3.2 Dolomite Reactor

The reactor operations and sampling processes were the same as described for the limestone reactor. A 10 mg/L NaF solution was prepared as the stockwater for the dolomite reactor. The stockwater was pumped and directed through the reactor, and samples were collected from each column. The residence time was designed to be 4 h by adjusting the flow rate. Samples from each column of the reactor were collected and analyzed. The results of this reactor were compared to the predicted results and the results of the limestone reactor discussed in section 2.3.1. Table 2-3 shows the comparison of the results of the prediction and the measurement.

**Table 2-3 Measured and predicted (in bracket) results after a passage of 100 pore volumes when a 10 mg/L NaF feedwater flows through the dolomite reactor at a residence time of 4 h**

	1) Initial water	2) Port A Equilibrium with CO <sub>2</sub>	3) Port B column 1 effluent	4) Port C column 3 effluent	5) Effluent column 2 effluent
pH	(7.12)	(4.03)	(6.22) 7.63	(6.21) 7.10	(8.09) 8.43
F (mg/L)	(10.0)	(10.0) 10.0	(3.48) 6.51	(3.48) 6.43	(1.30) 4.30
Na (mmol/L)	(0.526)	(0.526) 0.602	(0.526) 0.604	(0.526) 0.621	(0.526) 0.639
Ca (mmol/L)			(5.99) 4.22	(12.3) 8.57	(1.42) 4.74
Mg (mmol/L)			(4.99) 3.24	(5.06) 3.51	(2.17) 3.34
Citrate (mmol/L)				(3.16) 1.78	(3.16) 1.92

As demonstrated in Table 2-3, the fluoride concentrations in the effluent from each column were still higher than the predict concentrations. In column 1, the fluoride concentration was reduced

from 10.0 mg/L to 6.51 mg/L, while predicted fluoride concentration was 3.48 mg/L. Then, the introduction of column 3 brought a 1.78 mmol/L citrate into the flow. In total, this reactor reduced fluoride concentration to 4.30 mg/L.

The removal efficiency of the reactor was not optimal as the predicted on the whole. The reason for the difference may be due to the short residence time. As similarly as discussed in 2.3.1.1, 4 h was not sufficient for fluorite to fully precipitate in column 1, and thus, the fluoride concentration had not been reduced to optimal values. Then, the introduction of column 3 brought sufficient citrate, and it was predicted to promote 2.18 mg/L fluoride to co-precipitate in column 2 (the results from discussion in section 2.2.5). The reduced fluoride in column 2 was very close to the predicted (2.13 mg/L). Overall, the fluoride concentration in the effluent from the reactor was much higher than the predicted value of 1.29 mg/L. The results also indicate that dissolution of dolomite in column 1 brought 3.24 mmol/L magnesium into solution. This magnesium concentration remained stable when the feedwater flowed through the reactor, and the presence of this magnesium ion likely promoted fluoride removal in column 2.

The results from the dolomite reactor were also compared to the results from the limestone reactor in section 2.3.1, and the differences are illustrated in Table 2-4.

**Table 2-4 Comparison of the results from the dolomite reactor and the limestone reactor (in bracket) after a passage of 100 pore volumes when 10 mg/L NaF feedwater flows through the reactors at a residence time of 4 h**

	1) At Port A Equilibrium with CO <sub>2</sub>	2) At Port B column 1 effluent	3) At Port C column 3 effluent	4) Effluent column 2 effluent
pH	(3.98) 3.99	(6.21) 7.63	(6.21) 7.1	(8.09) 8.43
F (mg/L)	(10.0) 10.0	(4.18) 6.51	(4.18) 6.43	(3.41) 4.30
Na (mmol/L)		(0.638) 0.604	(0.660) 0.621	(0.680) 0.639
Ca (mmol/L)		(10.1) 4.22	(13.7) 8.57	(5.92) 4.74
Mg (mmol/L)		3.24	3.51	3.34
Citrate (mmol/L)			(1.02) 1.78	(0.980) 1.92

Overall, the limestone reactor had higher removal efficiency than the dolomite reactor. At the same residence time (4 h), the limestone reactor reduced fluoride concentration from 10 mg/L to 3.41 mg/L, while the dolomite reactor lowered the fluoride concentration to 4.30 mg/L. This concentration is higher than the maximum contaminant level (4 mg/L).

Separately, column 1 of the limestone performed better than column 1 of the dolomite reactor. Because dolomite was used in the column 1 rather than limestone, when it got dissolved, less calcium was produced in the column, and thus fluorite precipitation in the first column decreased and less fluoride was removed from the water. Moreover, previous research indicated that under the same conditions (salinity, pH, and pCO<sub>2</sub>), the dissolution rate of dolomite is lower than the dissolution rate of calcite in a rotating disk system (Pokrovsky et al., 2005; Lund et al., 1973; Lund et al., 1975). Under the same residence time (4 h) in the experiment, less dolomite was

dissolved than calcite, and thus, less calcium ion was produced. Therefore, a column containing both dolomite and calcite with a reasonable ratio of the two minerals should be developed to achieve improved removal efficiency.

Although fluoride removal in column 1 of the dolomite was less than removed from column 1 of the limestone reactor, fluoride removal in column 2 of the dolomite reactor (2.13 mg/L) was higher than that reduced in column 2 of the limestone reactor (0.770 mg/L). This result indicates that the presence of magnesium further reduced the fluoride concentration in column 2 of the reactor. The reason may be due to that magnesium promoted calcite precipitation and also promoted fluoride co-precipitation in calcite.

The long term behaviour of the dolomite reactor is demonstrated in Appendix C and Figure 2-8.

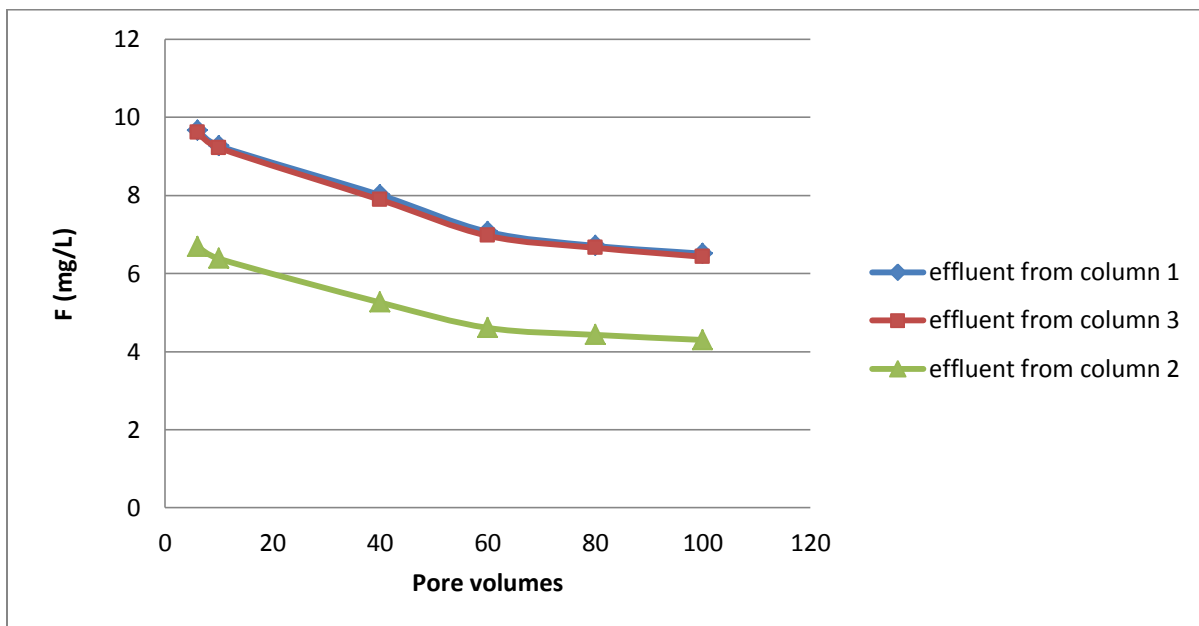


**Figure 2-8 F concentrations in the effluent from each column vs. pore volumes when a 10 mg/L NaF feedwater flows through the dolomite reactor at a residence time of 4 h**

The results from Figure 2-8 indicate that fluoride removal efficiency of the reactor increased with time. Fluoride concentration in the effluent from each column decreased with the operating time of the reactor, and became stable after a passage of approximately 80 pore volumes. The fluoride precipitated in column 1 continued to increase with time. The reason is similar as discussed for the limestone reactor and the reactor of Reardon and Wang (accumulated fluorite precipitation provide more nucleation sites for fluoride ion to crystallize). The fluoride removed in column 3 remained stable, and this amount of fluoride removed in column 2 decreased, because lower concentrations of fluoride in column 2 resulted in less fluoride to co-precipitate in calcite formed in column 2.

## 2.4 Conclusion

This study indicates that the modified limestone reactor reduced fluoride concentration from up to 150 mg/L to below the maximum contaminant level (4 mg/L), at a residence time of 4 h. When the residence time was 24 h, fluoride concentrations were maintained at concentrations below the drinking water standard (1.5 mg/L).

The observed fluoride removal efficiency of the limestone reactor was lower than the predicted efficiency. One important reason is that citrate suppressed the precipitation of calcite. The short residence time of the experiment also decreased the removal efficiency of the limestone reactor. When residence time decreased from 24 h to 4 h, the concentration of fluoride increased from 1.82 mg/L to 4.18 mg/L in the effluent from column 3 and increased from 1.65 mg/L to 1.82 mg/L in the effluent from column 2. An improvement for the reactor was to inject a slurry containing  $\text{CaF}_2$  into the upper part of the first column, and this further decreased fluoride concentration by 0.420 mg/L. Although the removal efficiency of the limestone reactor is not optimal as predicted, it is higher than the removal efficiency of the reactor designed by Reardon and Wang by a further reduction of 1.19 mg/L F in total at a residence time of 4 h.

The dolomite reactor was not efficient as the limestone reactor. The reasons are the slow dissolution rate of dolomite, negative effect of magnesium on the precipitation of fluorite in column 1 and suppression effect of citrate on precipitation of calcite in column 2. However, the

presence of magnesium promoted more fluoride to co-precipitate in fluorite in column 2 than in column 2 of the limestone reactor.

Further study should be devoted to improving the fluoride removal efficiency of these two reactors. A single reactor incorporating both calcite and dolomite should also be evaluated. Another avenue for research is to explore the possibility of organic ligands other than citrate to more efficiently promote the incorporation of fluoride in calcite. Further investigation on the dissolution and precipitation processes in the dolomite reactor should also be considered.

## Chapter 3

### Fluoride Determination Methods

#### 3.1 Background

Chapter 2 concludes that citrate can promote fluoride co-precipitation into calcite. However, interference from citrate on determination of fluoride is unknown, and few studies have been conducted on this topic. Accurate determination of fluoride concentration is fundamental in this research; therefore, in this chapter, interference from citrate on various fluoride determination methods is studied, and the most accurate, convenient, and cost-effective method is determined.

Currently, three methods have been widely used for the determination of fluoride. The colorimetric methods and fluoride electrode are the most satisfactory and cost-effective. In addition, ion chromatography has also been used for accurate determination (Eaton et al., 1995; Crosby et al., 1968).

A commonly used colorimetric method utilizes sodium 2-(parasulfophenylazo)-1, 8-dihydroxy-3, 6-naphthanlene disulfonate (SPANDS). This SPADNS method is based on the reaction between fluoride and a zirconium-dye lake. Fluoride dissociates a portion of the dye lake into a colorless complex anion ( $ZrF_6^{2-}$ ). As a result, the color produced becomes gradually lighter with the increase of fluoride (Eaton et al., 1995; Sukanya et al., 2005). Since the linear analytical range is from 0 to 1.40 mg/L fluoride, this range of samples was tested in this study, and a linear curve developed from standards was used for determining the fluoride concentration. In addition, spectrophotometer was used to determine the color photometrically. When the fluoride concentrations extend to 3.5 mg/L, a nonlinear calibration can be used for determination. Because no studies have been conducted on the effect of citrate on this fluoride determination method, and accurate determination of fluoride is fundamental to fluoride removal studies, this research is of significant importance.

The fluoride electrode used in this research was an ion-selective sensor. Previous research

indicated that this method yields good results and it is extremely useful in routine analyses (Harwood, 1969; Fuchs et al., 1975). The core composition of the fluoride electrode is the laser-type doped lanthanum fluoride crystal, which is a semiconductor that contacts the sample solution at one face and an internal reference solution at the other. A potential is established by fluoride solutions of different concentrations across the crystal, and thus the fluoride concentration in solution can be determined. (Stahr & Clardy, 1973; Eaton et al., 1995) in previous research, interference from citrate on this fluoride determination method was not observed, and citrate was added to eliminate interferences from other ions, including aluminum (Kauranen, 1977) and as an ionic strength adjustment buffer (Frant & Ross, 1968). This research further evaluates the sensitivity of this method when comparing to the other two methods.

Ion chromatography (IC) has become the standard and the most prevalent method of analysis for low-molecular-weight inorganic and organic anions in many types of environmental samples including river water, groundwater and wastewater (Krzyszowska et al., 1996; Michalski, 2006). The low-capacity anion-exchange column is commonly used for separation for detecting ions in this technique, and it is efficient for a large number of samples for analysis (Small et al., 1975; Gjerde & Fritz, 1979). IC was initially developed to analyze inorganic anions including fluoride, chloride and sulfate. However, with the development of this technique, it has expanded to analyze a variety of mono-, di- and trivalent inorganic and organic anions (including citrate). Gradient elution or coupled separation systems with specialty columns are widely applied to enlarge the peak capacity (Jones et al., 1989).

This chapter investigates citrate interference on determination of fluoride by the three methods. Fluoride standard samples with citrate and without citrate were prepared and analyzed, respectively. Then the results of the two sets of samples were compared to determine the interferences. In addition, for SPADNS method, the effect of the citrate concentration, effect of pH, and effect of UV length were studied. A preliminary experiment was conducted to eliminate the citrate interference on fluoride determination using the SPADNS method.

## **3.2 Experiment Methods**

### **3.2.1 SPADNS Method**

#### **3.2.1.1 Apparatus and Reagents**

A 10 mmol/L sodium citrate stock solution was prepared by dissolving 372.3 g of sodium citrate solution (99%, supplied by Alfa Aesar) in 1 L DI water. Solutions including SPADNS, zirconyl-acid, acid zirconyl-SPADNS and sodium fluoride stock solution were prepared according to the standard SPADNS method 4500F- D described by Eaton et al. (1995). The SPADNS solution and zirconyl-acid were supplied by Aldrich Chem., and sodium fluoride powder was supplied by Fisher Scientific. To make a pH buffer, 1.43 mL acetic acid (99.7%, supplied by Sigma Aldrich) and 2.0714 g sodium acetate (99%, supplied by Sigma Aldrich) were diluted with distilled water to 250 mL. The pH of this sodium acetate pH buffer is 4.68. All reagents used in this study were of ACS grade quality. A Pharmacia Lkb Novaspec ii spectrophotometer was used in the experiment, and the absorbances were measured when the UV lengths were at 550 nm, 560 nm, 570 nm, 580 nm and 590 nm.

#### **3.2.1.2 Sample Preparation**

The description of the prepared samples was illustrated in Appendix E. To evaluate the effect of citrate on the determination of fluoride, a batch of 20 mL fluoride samples with a range of citrate concentrations and without citrate was prepared from a sodium fluoride stock solution and sodium citrate stock solution (Table E-1).

To examine the co-effect of the pH and citrate, three batches of samples were prepared (Table E-2 and Table E-3). Batch 1 contained fluoride samples with various concentration of citrate and sodium acetate buffer. The buffer generated a stable pH of 4.68 for all samples. Stabilization of the pH was aimed to eliminate the influence of pH when investigating the effect of citrate alone. In addition, to evaluate the effect of volume of the pH buffer on the determination of fluoride, batch 2 and batch 3 samples were prepared (Table E-3). Each sample was 20 mL.

### 3.2.1.3 Analysis Procedure

The analysis procedure was divided into two steps. Firstly, a calibration curve was prepared. A set of 20 mL standards samples was prepared and 4 mL acid zirconyl-SPADNS reagent was added into each sample. Color was left to develop for 1 min before putting samples into the spectrometer chamber for measurements. The absorbances were measured at a particular UV length and then, calibration curve was drawn up. Secondly, 4 mL acid zirconyl-SPADNS reagent was added into each fluoride sample (20 mL each), and color was also left to develop for 1 min. Absorbances were then measured and the concentrations of the fluoride samples were read off of the calibration curve or calculated by equations 3-1. Absorbance errors were determined using equations 3-2. Fluoride concentration errors were determined using equations 3-3.

$$\text{Fluoride concentrations (mg/L)} = (A_0 - A_x) / (A_0 - A_1)$$

Where  $A_0$  = absorbance of the prepared 0 mg F/L standard

$A_1$  = absorbance of a prepared 1 mg F/L standard

$A_x$  = absorbance of the prepared sample (3-1)

$$\text{Absorbance error} = (A_x - A_s) / A_s$$

Where  $A_s$  = absorbance of the prepared standard

$A_x$  = absorbance of the prepared sample (3-2)

$$\text{Fluoride concentration error} = (F_x - F_s) / F_s$$

Where  $F_s$  = Fluoride concentration of the prepared standard

$F_x$  = Fluoride concentration of the prepared sample (3-3)

## 3.2.2 Fluoride Electrode Method

### 3.2.2.1 Apparatus and Reagents

The apparatus used in this experiment included an accumet ion meter (supplied by Fisher Scientific), a fluoride double junction ions selective fluoride electrode (supplied by Oakton), and a Corning magnetic stirrer with TFE-coated stirring bar. A 100 mg/L fluoride stock solution was

prepared by dissolving 221.0 mg anhydrous sodium fluoride powder (supplied by Fisher Scientific) in distilled water and diluting to 1 L and a 10 mmol/L sodium citrate stock solution was prepared by dissolving 372.3 g of sodium citrate (supplied by Alfa Aesar, 99%) in 1 L DI water.

Because the fluoride electrode measures the ion activity of fluoride in solution rather than concentration, a buffer was added to minimize the difference. This buffer can provide a nearly uniform ionic strength background and decompose complexes (Nicholson and Duff, 1981). Therefore, the electrode can provide a good representation of concentration. This buffer was prepared by placing approximately 500 mL distilled water in a 1 L beaker before adding 57 mL glacial acetic acid (Fisher Scientific, reagent grade), 58 g NaCl (Fisher Scientific, >99.5%), and 4.0 g of 1,2 cyclohexane diamine tetra acetic acid (supplied by VWR) in the same beaker. Then, this beaker was placed in a cool water bath, and 6 N NaOH (about 125 mL) (prepared from NaOH pellets, > 97%, supplied by Fisher Scientific) was slowly added while stirring until the pH reached between 5.3 and 5.5.

### **3.2.2.2 Sample Preparation**

Two batches of 20 mL fluoride standards with and without citrate were prepared according to Table E-4 in Appendix E from sodium fluoride stock solution and sodium citrate stock solution.

### **3.2.2.3 Analysis Procedure**

An electrode slope check was accomplished before analysis. Firstly, 50 mL distilled water and 50 mL of the fluoride buffer was added in a 150 mL plastic beaker, the beaker was then placed on the magnetic stirrer and stirred at a constant rate. Secondly, 1 mL of 0.1 mol/L standard was added into the beaker by a pipet. When the reading stabilized, the millivolt reading was recorded. Thirdly, another 10 mL of the same 0.1 mol/L standard was added into the beaker. The millivolt reading was recorded when the reading stabilized. Afterwards, the difference between the two readings was determined. The electrode operates correctly if the mV potential has changed by 57

$\pm 2$  mv when the temperature is stable at 25 °C. If not, these four steps were repeated until the requirements are met.

After finishing the slope check, 1 mg/L and 10 mg/L standard samples were used for calibration. Then, fluoride electrode was dipped into each sample after adding fluoride buffer for measurement. The fluoride concentration errors were determined using equation 3-4.

$$\text{Absorbance error} = (F_x - F_s) / F_s$$

Where  $F_s$  = fluoride concentration of the prepared standard

$$F_x = \text{measured fluoride concentration of the prepared sample} \quad (3-4)$$

### **3.2.3 IC Method**

#### **3.2.3.1 Apparatus and Reagents**

ICS5000-Cap-Anion-Citrate was used as the method. The apparatus used in this research included an Ion Chromatograph (IC) --Dionex ICS 5000, a Dionex AS20 Column, a conductivity detector and an auto sampler (all supplied by Thermo Scientific).

The eluent used was KOH (Dionex EGC III KOH, ACS grade), and it passed through the columns at a flow rate of 0.01 mL/min with a concentration gradient. Moreover, the eluent was stored under helium to exclude oxygen and carbon dioxide to prevent carbonate formation. Inorganic anion standards of fluoride, chloride, nitrite, bromide, nitrate, phosphate and sulfate were supplied by Thermo Scientific, the citrate standard was purchased from Inorganic Ventures.

#### **3.2.3.2 Analysis Procedure**

Working standards at four different concentration concentrations were prepared by diluting the standard stock with deionized water. Calibrations were performed at startup and the end. In addition, on-going precision recovery (OPR) standard was analyzed after every 10 samples. Three Calibration blanks were run for every batch of analysis and sample matrix spike was run for every 10 samples.

### **3.3 Results and Discussion**

#### **3.3.1 SPADNS Method**

##### **3.3.1.1 Effect of UV length**

Standard methods for the examination of water and wastewater indicate that a UV length range from 550 nm to 600 nm of a spectrometer is applicable to determine the concentration of fluoride (Eaton et al., 1995). To determine the most accurate UV length of the spectrometer, standard curves at UV lengths of 550 nm, 560 nm, 570 nm, 580 nm, 590 nm and 600 nm were prepared (Figure 3-1).

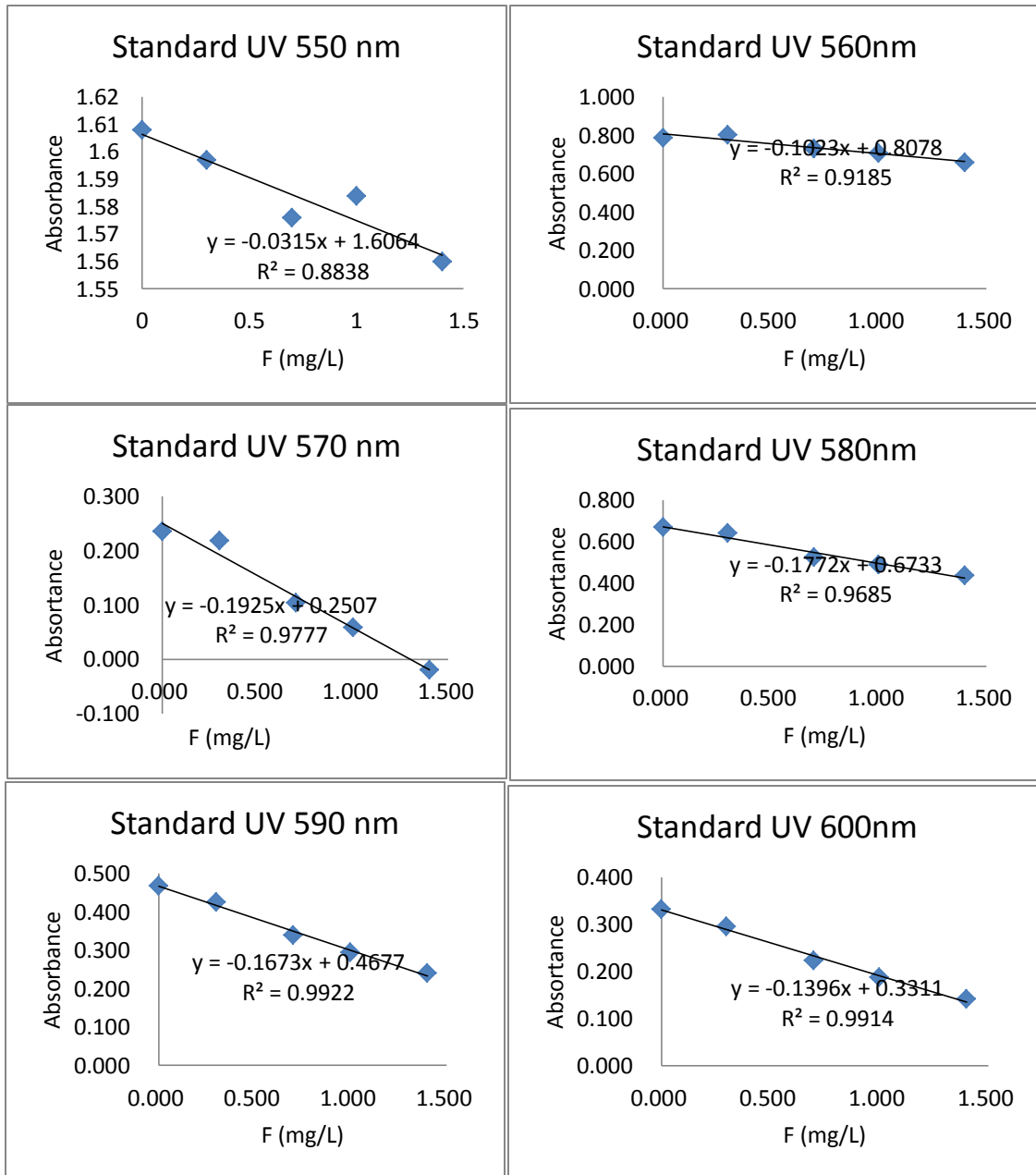


**Figure 3-1 Standard curves when UV length ranged from 550 nm to 600 nm with an increment of 10 nm each time**

The results of the standard samples reveal a linear relationship between the concentrations of fluoride and the absorbance. The larger the UV lengths, more relevant the data (higher R<sup>2</sup> values)

are, which means higher sensitivity of the methods. As shown in Figure 3-1, when the UV lengths were at 590 nm and 600 nm, the  $R^2$  values were both 0.99. They were the highest observed for the wave lengths evaluated. Therefore, these two UV lengths can be considered in this research. 590 nm was finally chosen as the UV length for this experiment.

### **3.3.1.2 Effect of Citrate Ions**

Standard curves were prepared with a range of concentrations of citrate. Sample preparation procedure is presented in Table 3-1 in section 3.1.1.2, and the results of the sample analysis are shown in Figure 3-2. UV length was set at 590 nm for this experiment.

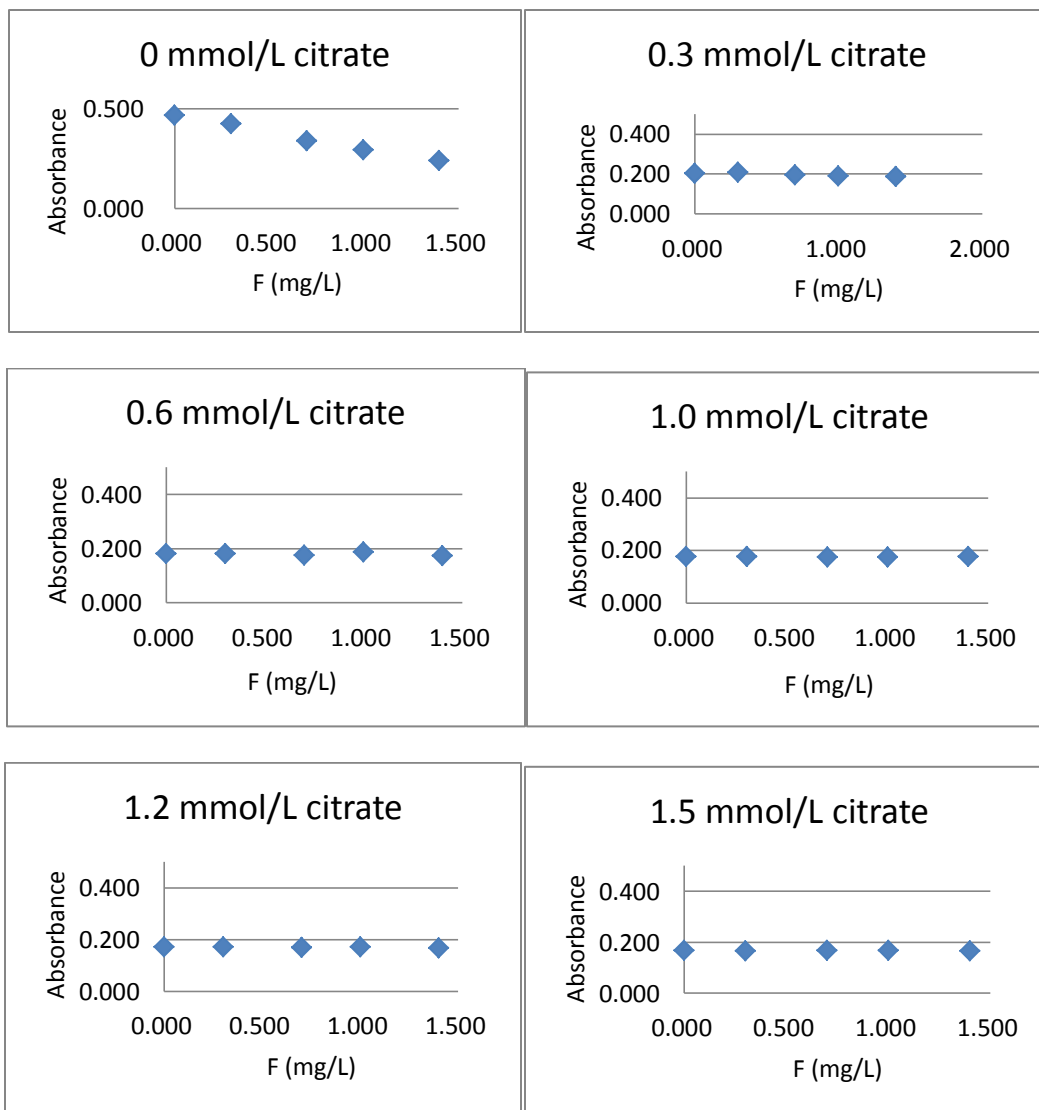


**Figure 3-2 Standard curves at a range of citrate concentrations**

Overall, the citrate interference from citrate was significant. The presence of citrate concentration greatly lowered the absorbance. Moreover, the concentrations of fluoride and the absorbances no longer demonstrated a linear relationship. The results indicate that, regardless of the concentrations of fluoride, with presence of citrate, the absorbances of all the fluoride samples dropped to around 0.2. When the citrate concentration of the samples was 0.3 mmol/L, absorbances of standard samples fluctuated around 0.2 with increased concentrations of fluoride.

The results were similar when the citrate concentrations increased from 0.3 mmol/L to 1.5 mmol/L. Therefore, presence of citrate made the standard curve impossible to be used to accurately determine the fluoride concentration. The interference from citrate was significant in determining the fluoride using this SPADNS method.

### **3.3.1.3 Effect of pH**

Tamas et al. (2011) indicated that the absorbance of the SPADNS reagent changed greatly with the increase of pH. For instance, when pH increased from 4 to 12, the absorbance of SPADNS reagent decreased from 1.13 to 0.80 approximately. In addition, Rizk et al. (1994) indicated that the absorbance changed with the change of pH when measuring the concentrations of aluminum ions and copper ions by SPADNS method. As stated in section 3.3.1.2, the interference of citrate was significant in determining the fluoride by this SPADNS method. The interference may be due to the observation that the addition of citrate ion influenced the pH value of the samples, and thus affected the absorbance value. This section then investigates if the interference from citrate can be eliminated by the stabilization of pH.

Because the ionic strengths of samples (especially when the citrate concentration was 0 mg/L) were very low, the measurement of pH of the samples by pH electrodes is inaccurate. Therefore, PHREEQC was used to model the pH value of the samples. The samples included standard fluoride samples (without presence of citrate) and fluoride samples with citrate from 0.1 mmol/L to 1.0 mmol/L. The result is demonstrated in Table 3-1.

**Table 3-1 Predicted pH values of fluoride samples when a range of citrate concentrations were presented**

When [F] = 0.3 mg/L		When [F] = 1.0 mg/L		When [F] = 1.4 mg/L	
Citrate (mmol/L)	pH	Citrate (mmol/L)	pH	Citrate (mmol/L)	pH
0.0 (standard)	7.00	0.0 (standard)	7.01	0.0(standard)	7.02
0.1	7.88	0.1	7.88	0.1	7.88
0.3	7.96	0.3	7.96	0.3	7.96
0.5	8.00	0.5	8.00	0.5	8.00
1.0	8.04	1.0	8.04	1.0	8.04

The pH values of the standard samples (when citrate is not present) stayed at approximately 7 (varied from 7.00 to 7.02), which meant that fluoride concentrations do not to have much effect on the pHs. However, pHs changed greatly when citrate was added into the samples. When 0.1 mmol/L citrate was added into a 0.3 mg/L fluoride solution, pH changed from 7.00 to 7.88, and the pH values of this 0.3 mg/L fluoride samples changed from 7.88 to 8.05 when citrate was increased from 0.3 mmol/L to 1.0 mmol/L. The change of pH values should have a great effect on absorbances of these samples.

Research was conducted to determine whether interference from citrate on the absorbance of the samples was a result of changes of the pH values. A pH buffer was used to eliminate the change of pH values caused by addition of citrate into samples. This experiment was aimed to investigate if the interference cause by the citrate can be eliminated by stabilizing the pH. Figure 3-3 shows the results when 0.2 mL pH buffers were added to standard samples and samples with 1 mmol/L citrate, and Figure 3-4 indicates the same results when 1 mL of buffer were added into the samples.

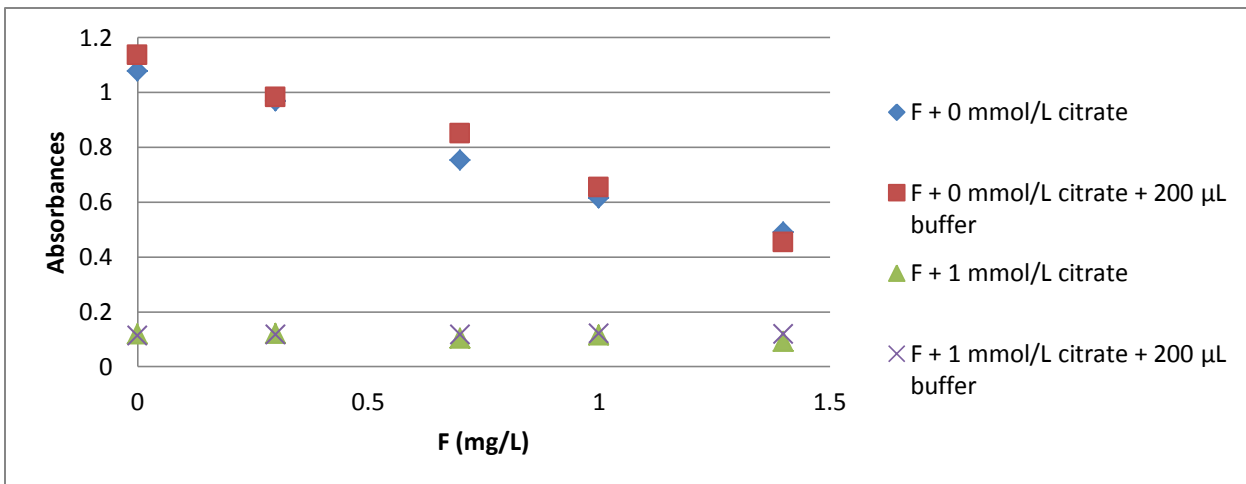


**Figure 3-3 Absorbances of standard fluoride samples and fluoride samples with citrate when 200 µL pH buffer was added (UV length was at 590 nm)**

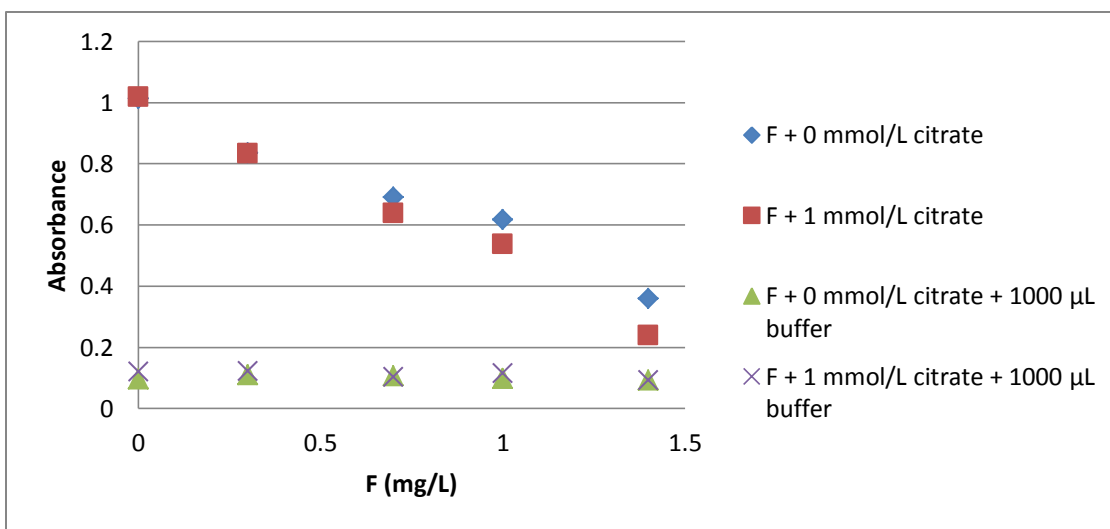


**Figure 3-4 Absorbances of standard fluoride samples and fluoride samples with citrate when 1000 µL pH buffer was added (UV length was at 590 nm)**

An addition of buffer did not influence the results of absorbance. For both standard samples and samples with 1 mmol/L citrate, the addition of pH buffer did not change the absorbance. This means that the addition of a pH buffer did not eliminate the interference from citrate. Moreover,

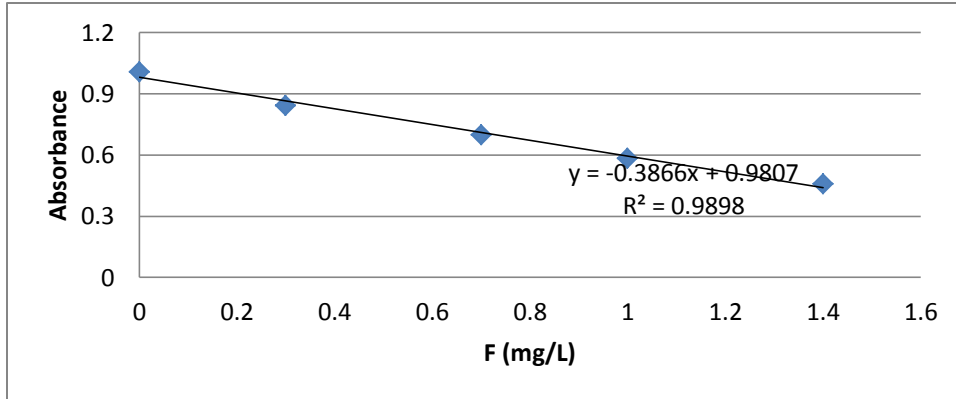
as shown in Figure 3-4, even when a larger volume of buffer was added (1 mL), the absorbances were not influenced. In conclusion, presence of citrate significantly influenced the absorbances of the samples, and the addition of pH buffer cannot eliminate the interference. The citrate made the SPADNS method inappropriate for the determination of fluoride.

#### **3.3.1.4 Effect of Temperature**

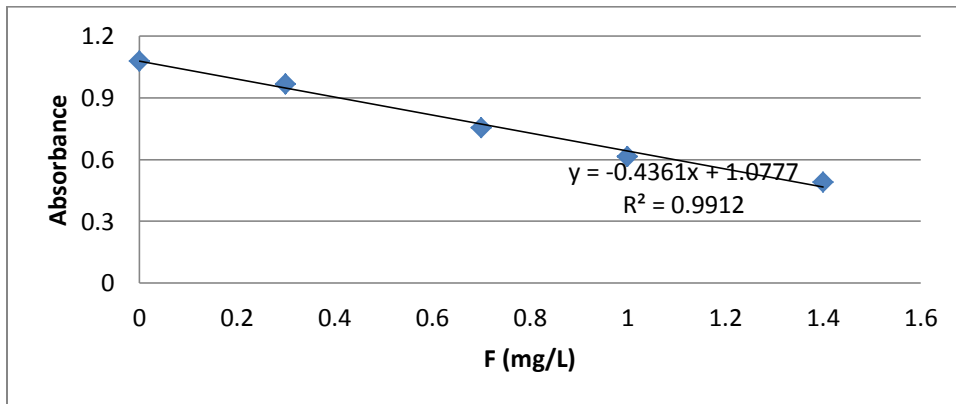
Another factor that affected the absorbances is the temperature of the spectrophotometer. With the running of the spectrophotometer, the temperature of the equipment increased. Two different readings were obtained for the same sample when measurements were taken immediately after starting the spectrophotometer and after three hours running. Any difference in readings was due to the temperature change in the sample chamber during the measurements. The variation of environmental temperature caused the reading value of the absorbance to decrease with running of the equipment.

Experience of analysis by the spectrometer indicated that, during the first hour of the running after the equipment started, temperature of the equipment and sample chamber increased significantly. However, during the second hour, the temperature of the equipment changed slightly. After 2 h running, temperature of the equipment went very high. The temperature rise was not suitable for accurate determination of the absorbances.

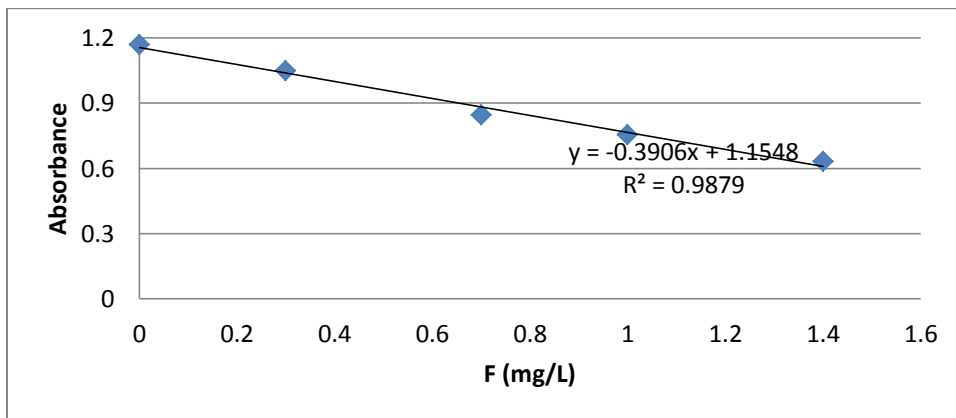
An experiment was conducted to investigate the effect of temperature on the determination of absorbances. Three sets of standard fluoride samples (concentrations ranged from 0 mg/L to 1.4 mg/L) were prepared. Then the absorbance of each set was measured at different times, and the standard curve was prepared for each set of samples. The results are demonstrated in Figure 3-5.



(a) Measurement at 1st hour



(b) Measurement at 2nd hour



(c) Measurement at 3rd hour

**Figure 3-5 Measured absorbances of fluoride standards at 1<sup>st</sup> hour (a), 2<sup>nd</sup> hour (b) and 3<sup>rd</sup> hour (c) after the spectrometer started**

When the measurements were made at 2<sup>nd</sup> h, the R<sup>2</sup> of the standard curve was the highest. This means that the measurements made at 2<sup>nd</sup> h was the most sensitive among the three time sections. This conclusion is in agreement with experience of analysis using the spectrometer. Therefore, through the experiment, the spectrometer was pre-heated for 1 hour each time before measurement, and all the measurement were taken within the 2<sup>nd</sup> h after the spectrometer started each time. Then the spectrometer was shut down and allowed to cool for 2 h and then restarted to take new measurements.

### 3.3.2 Fluoride Electrode Method

Two set of samples were prepared for this experiment according to Table E-4. Fluoride electrode was then used for the measurement and the results are demonstrated in Table 3-2.

**Table 3-2 Interference from citrate on determination of F standard using fluoride electrode**

Standard F solution			Standard F solution with presence of 1 mmol/L citrate		
F standard (mg/L)	Measured F value (mg/L)	Error (%)	F standard with 1 mmol/L citrate (mg/L)	Measured F value (mg/L)	Error (%)
0	0.000	--	0	0.004	--
0.3	0.304	1.33	0.3	0.303	1.00
0.7	0.688	1.71	0.7	0.698	0.286
1.0	0.991	0.900	1.0	1.00	0.200
1.4	1.44	2.85	1.4	1.43	2.14

As illustrated in Table 3-2, citrate has a very minor effect on the determination of fluoride using this fluoride electrode method. When no citrate was presented, the errors were from 0.900% to

2.86%. However, when citrate was presented, the errors ranged from 0.200% to 2.14% and were even lower than when no citrate was presented. QA/QC report is shown in Table 3-3.

**Table 3-3 QA/QC report of the determination of fluoride by fluoride electrode**

<b>Instrument Performance Check (IPC)</b>	<b>Fluoride (mg/L)</b>
Measured 1	2.02
Measured 2	2.03
Measured 3	1.98
Average	2.01
Standard concentration (mg/L)	2.00
Recovery (%)	100.5
<b>Method Detection Limit (n=7)</b>	0.02

The QA/QC report shows that the recovery of the method was 100.5%, which indicates a high stability and accuracy. The method detection limit was calculated to be 0.02 mg/L.

### **3.3.3 IC Method**

Although ion chromatograph (IC) has been commonly used for determination of fluoride, and the precision and accuracy is satisfactory, problems occur when doing simultaneous analysis of fluoride and citrate using ion chromatographic method. Because citrate is very strongly retained, a very strong eluent must be used in most situations. However, strong eluents generally sacrifice the ability to analyze for the early-eluting fluoride (Smith & MacQuarrie, 1988; Wildman et al., 1991). Moreover, if an eluent that works for fluoride was chosen, a peak for the strongly retained citrate may not be observed for a long time.

Two methods were used to solve the problem. One is to use the ion exclusion chromatograph with direct conductivity detection rather than commonly-used ion exchange chromatograph (Wildman et al., 1991). This ion exclusive chromatograph method has been successfully applied

to detect citrate and fluoride within 11 min by using a 6.1005.200 Metrosep Organic Acids column and a 0.5 mmol/L H<sub>2</sub>SO<sub>4</sub> solution as the eluent at Metrohm. The peak for citrate appears at 7.7 min and peak for fluoride appears at 11 min. The interval between their peaks using this ion exclusion chromatograph method is much smaller than ion exchanged chromatograph, which can make the analysis more cost-effective. However due to equipment restrictions, this method was not applied in this research. Also, the cost of this method is much higher than SPADNS and the fluoride electrode method.

Gradient eluent is another strategy when doing the simultaneous determination of fluoride and citrate (Jones & Jandik, 1991; Rocklin et al., 1987). Gradient elution is accomplished by changing from a weak to a strong eluent during the run. In the ion exchange method, it is achieved by either a concentration gradient of the displacing ion, or by a composition gradient, which means to change from a weakly retained eluent ion to a more strongly retained ion. However, problems are associated with changing the eluent during the run. Severe baseline shifts and contaminants in the eluents can make the application of the gradient elution difficult (Rocklin et al., 1987). Unless steps are taken to minimize baseline shift, composition gradient elution cannot be successfully employed (Jandik et al., 1990). Therefore, in this research concentration gradient was used, and the change of the concentration during an experiment is shown in Table 3-4.

**Table 3-4 Concentrations of the gradient eluent in IC method**

Running time (min)	Concentrations of the eluent (KOH) (mmol/L)
0	5
5	5
15	30
30	55
35	5

Based on previous experience, fluoride is weakly retained while citrate is strongly retained. The peak for fluoride is supposed to occur within the first 10 min when the concentration of eluent was 5 mM. Therefore, as shown in Table 3-8, the eluent concentration was set at 5 mM within the first 15 min, and then the concentration increased to 30 mM for 15 min. After that, the concentration was increased to 55 mM to allow any other peaks to occur. The results of the run are indicated in Table 3-5 and Figure 3-6.

**Table 3-5 Standard peaks of common anions in an IC curve**

No.	Ret.Time (min)	Peak Name	Height ( $\mu$ S)	Area ( $\mu$ S*min)	Rel.Area (%)	Amount (mg/L)
1	5.98	F	6.499	1.385	8.57	1.989
2	10.12	Cl	4.007	1.175	7.27	2.989
3	12.38	NO <sub>2</sub>	9.963	2.699	16.72	9.840
4	14.13	Br	7.597	1.677	10.38	9.421
5	15.04	NO <sub>3</sub>	9.564	2.203	13.64	10.022
6	16.59	SO <sub>4</sub>	23.515	4.461	27.63	14.899
7	20.03	HPO <sub>4</sub>	8.759	1.981	12.27	14.847
8	22.16	Citrate	2.336	0.568	3.52	4.801

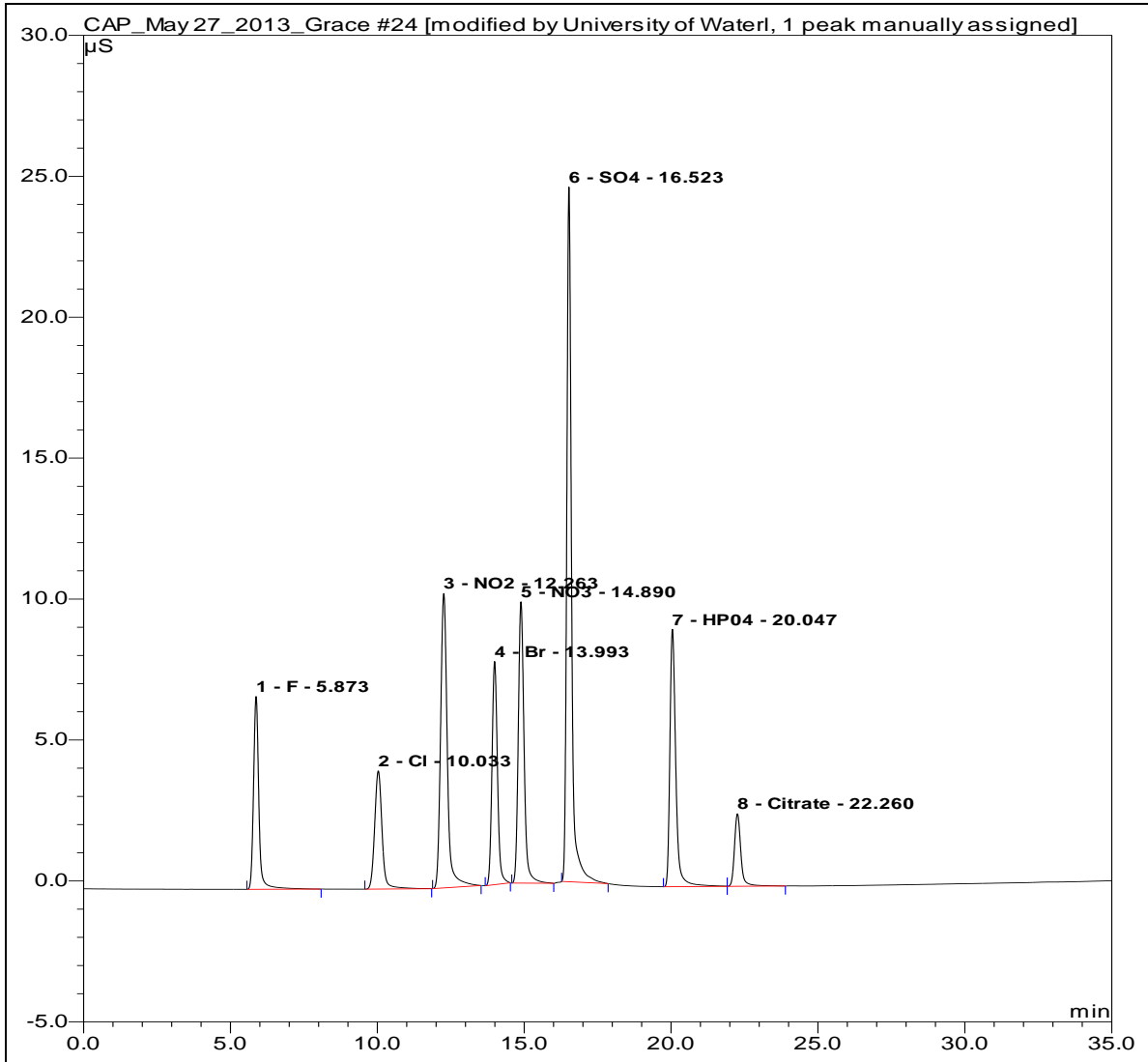


**Figure 3-6 Standard peaks of common anions in an IC curve**

As shown in Figure 3-6, the peak of citrate occurred at 22.16 min approximately, while the fluoride peaks occurred at 5.98 min. The peaks of fluoride and citrate were well separated, and the citrate does not have any interference on fluoride. However, this method is still not cost-effective, because the running time of the IC should be at least 25 min to allow both peaks to appear on the graph. Future research should be done on improving this method when doing simultaneous analysis of fluoride and citrate.

A QA/QC report was performed, and the results are shown in Table 3-6.

**Table 3-6 QA/AC report of the determination of fluoride by IC**

<b>Instrument Performance Check (IPC)</b>	<b>Fluoride (mg/L)</b>
Measured 1	2.0042
Measured 2	2.0133
Measured 3	1.9888
Average	2.0021
Standard concentration (mg/L)	2.0000
Recovery (%)	100.10
<b>Method Detection Limit (n=7)</b>	0.004

The QA/AC report indicates that the recovery of the method was 100.1%, which indicates a high stability and accuracy. The method detection limit was 0.004 mg/L. This method is more accurate than fluoride electrode method according to the QA/QC report. However, since this method is more time and cost consuming than the fluoride electrode method, fluoride electrode method was used in this research. It is the quickest and most economic method among the three methods, and its errors are very low. The IC method was used for the determination of citrate in this research.

### **3.4 Conclusion**

The citrate has a significant interference on determination of fluoride using the SPADNS method. Overall, results indicate that the higher the citrate concentration, the lower the absorbance. The presence of citrate significantly interfered with the standard curve and made it impossible to be used for fluoride determination. Addition of a pH buffer did not eliminate the interference. Therefore, pH is not the main reason of this interference, and a possible reason for the interference is due to the molecular interaction and combination between citrate and the dye, which significantly influenced the absorbance once citrate was present. In addition, the method is also very sensitive to the change of temperature.

Citrate has a minor effect on the determination using fluoride electrode. In addition, citrate had no effect on the IC method, because the peaks for the two were well separated. However, the running time is high for each sample when doing IC analysis and the cost is much higher than the fluoride electrode method. Therefore, fluoride electrode was used for this research.

Future work should be done on investigating other possible reasons for interference from citrate on the SPADNS method in order to improve the method. Also, methods using IC to achieve a short residence time but still allow the separation of citrate and fluoride peaks should be studied. Ion exclusion chromatography and more effective gradient eluent ion techniques should be studied for simultaneous determination of fluoride and citrate.

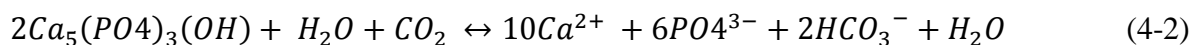
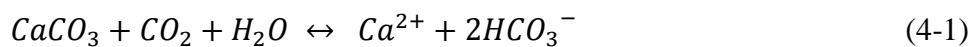
## Chapter 4

### Assessment of the Phosphate Rock as a Fluoride Treatment Option

#### 4.1 Background

Phosphate rock is a general term that refers to rock with high concentrations of phosphate minerals. Phosphate rocks occurring in the primary environment include fluor-apatite ( $\text{Ca}_{10}(\text{PO}_4)_6\text{F}_2$ ), hydroxy-apatite ( $\text{Ca}_{10}(\text{PO}_4)_6(\text{OH})_2$ ), carbonate-hydroxy-apatites ( $\text{Ca}_{10}(\text{PO}_4)_6(\text{CO}_3)_2(\text{OH})_2$ ) and calcite ( $\text{CaCO}_3$ ). They have been used in water treatment for contaminants including lead, zinc, and cadmium (Cao et al., 1995; Basta et al., 2001). However, it has never been applied for removal of fluoride from water.

Phosphate rock is a potential material for fluoride treatment because of its effective components - apatite and calcite. Apatites in different forms including synthetic nano-hydroxyapatite (n-Hap), biogenic apatite, treated biogenic apatite and geogenic apatite have been used for fluoride removal (Tomar et al., 2013). Previous research (Murutu et al., 2010; Gao et al., 2009; Tomar et al., 2013; Bhatnagar et al., 2011) indicate that apatite can remove fluoride from contaminated water by adsorption to less than 1 mg/L. In addition, calcite in phosphate rock can also precipitate fluoride as fluorite as discussed in chapter 2. Potential mechanisms for fluoride removal are shown as equation 4-1, 4-2, 4-3 and 4-4.



Due to the extensive availability of the phosphate rock, the price for the treatment should be low. Phosphate rock is deposited in layers that cover thousands of square miles. Large deposits of phosphate rock are found in Canada, Russia, and South Africa. In the United States, phosphate rock is found in Florida, North Carolina, Utah and Idaho. Resource from Florida and North Carolina accounts for approximately 85% of phosphate rock production in the U.S. (Van-

(Kauwenbergh et al., 2010; Cook & Shergold, 1990). The development of an inexpensive and simple phosphate rock reactor would be of significant benefit to fluoride treatment technology. This study examined the efficiencies of four phosphate rocks from ON, Canada and Florida, USA in removing fluoride from contaminated water, and the mechanism is also discussed in this chapter.

## 4.2 Experimental Methods

### 4.2.1 Mineralogical Analysis Procedure

Four kinds of materials were used in this research, the names and the particle sizes, origins of the material are shown in Table 4-1 and the physical appearances of the materials are illustrate in Appendix E.

**Table 4-1 Phosphate rocks used in this research**

Material	Particle size of the material (mm)	Origins	Supplier
Carbonatite	0.1 - 0.5	ON, Canada	Boreal
Tennessee Brown	0.006 - 0.008	ON, Canada	Agrominerals Inc.
PSP rock (Fine)	< 0.2	Florida, USA	Potash Corp.
PSP rock (Coarse)	0.2 - 0.8	Florida, USA	

X-ray diffraction (XRD) spectroscopy and Fourier transform infrared (FT-IR) spectroscopy were used to determine the mineral composition of the materials. The X-ray spectrometer (XRG 3000, supplied by INEL) ran at a Cu and Ka radiation at a wave length of 0.154 nm for 20 min per sample. The FT-IR spectrometry (Tensor 27, supplied by Bruker) was conducted at a wavelength from 400 to 4000  $\text{cm}^{-1}$ .

However, X-ray and FT-IR techniques cannot reveal the percentage of each mineral in the phosphate rock. Therefore, more investigation was conducted to determine the percentage of the major minerals. Each material was dissolved by concentrated hydrochloric acid (37%, supplied by Sigma Aldrich), and then cations and anions analysis of the diluted solution were conducted. Specifically, 0.5 g of each material was placed in vials and sealed using rubber septa. Then, a glass syringe with 5 mL concentrated HCl was injected into the vials. Gas emerged at once, and the pressure pushed the syringe. The gas column was then read from the scale. The process is illustrated in Appendix C. The  $\text{CO}_2$  (g) was the major gas produced in the process and  $\text{CaCO}_3$  is the main source of the gas. Therefore, the mass of  $\text{CaCO}_3$  from the phosphate rock was calculated. Next, the solutions left in the vials were diluted to 20 mL and filtered using Whatman 0.45 micron cellulose acetate filters. The fluoride and phosphorus concentrations in those liquid samples were then analyzed. The results were used to infer the approximate mineral percentages of each phosphate rock.

#### **4.2.2 Batch Test**

Preliminary experiments were conducted to investigate the efficiencies of the four kinds of phosphate rocks to remove fluoride. The experiments included two batches: Batch (a) and Batch (b). The fluoride removal efficiencies of the two experiments were compared.

For batch (a), a set of four 250 mL bottles was filled with 30 g of the four kinds of materials and 200 mL 10 mg/L sodium fluoride solution, respectively. These bottles were placed in a water bath at a temperature of 25 °C and rotated at a speed of 15 rpm for 24 h. Then 50 mL of the solution was sampled and about 2 g wet solid sample were collected. The water sample was filtered using Whatman 0.45 micron cellulose acetate filters before analysis. The concentrations of orthophosphate were measured via the ascorbic acid method described by Eaton et al. (1995), fluoride concentrations were measured by a fluoride electrode and the cations were measured by a Thermo Scientific Inductively Coupled Optical Spectrophotometry (ICP); the wet solid samples were put into a fume hood for drying before the X-ray diffraction analysis. The same procedure was conducted again after 48 h and 72 h.

For batch (b), another same set of four 250 mL bottles were filled with 30 g of the four rock samples and 200 mL 10 mg/L sodium fluoride solution, respectively. However, the samples were first equilibrated with 97 kPa CO<sub>2</sub> (g) before being put into the water bath at the same temperature and rotation speed as batch (a) for 24 h.

### 4.2.3 Reactor Design and Operations

A column experiment was conducted to evaluate the potential of the phosphate rock to be used as a fluoride removal material. The design of the reactor is as illustrated in Figure 4-1.

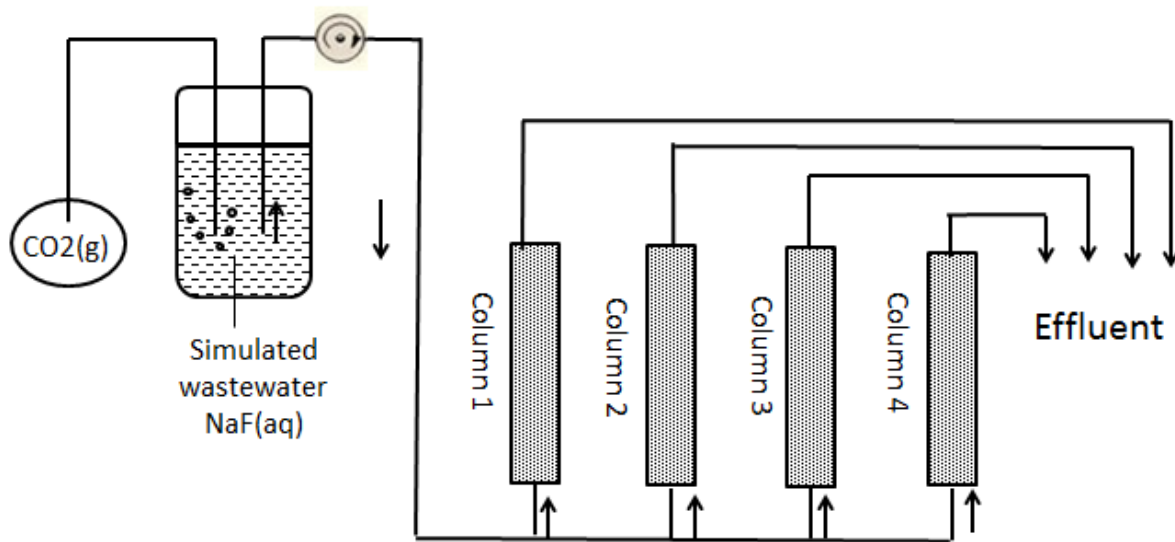


**Figure 4-1 Schematic of the phosphate rock reactor: Feedwater is equilibrated with CO<sub>2</sub> (g) and flows through four columns of phosphate rocks via saturated flow**

Four columns each with a diameter of 2.5 cm and a length of 31 cm were assembled and each was filled with a type of phosphate rock with Ottawa silica sand (size between 0.85 mm to 1.4 mm, obtained from a local landscaping vendor) (Table 4-2). DI water entered the bottom of each column via saturated flow, and the effluent from each column was collected for analysis.

**Table 4-2 Materials in each column of the reactor**

	Material	Mass of the material (g)	Percentage of materials in columns (%)	Particle size of the material (mm)	Pore volume (mL)
Column 1	Carbonatite (with silica sand)	132	62.3	0.1 - 0.5	25.8
Column 2	Tennessee Brown (with silica sand)	84.2	45.3	0.006 - 0.008	35.8
Column 3	PSP rock (Fine with silica sand)	142	67.1	0.2 - 0.8	19.6
Column 4	PSP rock (Coarse)	142	84.2	0.8 - 2	72.4

The feedwater to this phosphate rock reactor was a 10 mg/L sodium fluoride solution, and a 20 L glass carboy was used to store feedwater. Before the system started to flow, the carboy was connected to a tank of carbon dioxide at 97 kPa pressure by an immersion bubbler, and the CO<sub>2</sub> (g) was bubbled into the feedwater until equilibrium was reached. The equilibrium can be determined by measuring the pH of the feedwater, which should fall to around 3.9. The air-entry tube was connected to a source of CO<sub>2</sub> (g) so when feedwater was displaced to the reactor columns, the remaining solution maintained saturation with respect to CO<sub>2</sub> (g). During operation of the reactor, the feedwater was delivered to the reactor columns with a constant flow rate via a peristaltic pump. The flow rate corresponds to a residence time of 4 h in each column. Other residence times were also applied by adjusting the flow rates.

#### **4.2.4 Sampling and Analysis**

Effluent samples were regularly collected from the four columns using syringes. Samples from dissolution experiment were collected and stored. Those samples were filtered through Whatman 0.45 micron cellulose acetate filters, and then were analyzed for pH, fluoride (F), phosphorus (P) and major cations including calcium, magnesium and sodium. Calcium concentrations of samples from the batch tests were analyzed by EDTA titrimetric method (Eaton et al., 1995), calcium, magnesium and other major cations of all other samples were analyzed by a Thermo Scientific Inductively Coupled Optical Spectrophotometry (ICP). Measurement of the pH was performed potentiometrically with an accumet pH meter and an Orion combination pH electrode (both supplied by Fisher Scientific). Fluoride was analyzed using an accumet ion meter (supplied by Fisher Scientific) and a fluoride double junction ions selective fluoride electrode (supplied by Oakton). Then, phosphorus was analyzed by ascorbic acid method. The principle of this method is based on the reaction between ammonium molybdate and potassium antimonyl tartrate in an acid medium. In the process, orthophosphate forms a heteropoly acid—phosphomolybdic acid. This acid is then reduced to intensely colored molybdenum blue by ascorbic acid (Eaton et al., 1995). The higher the concentrations are, the deeper the colors. The detection limit of this method is 0.01 mg/L, anions or cations within the materials do not interfere with the determination. Analytical reproducibility of duplicate samples was  $\pm 5\%$ .

### **4.3 Results and Discussion**

#### **4.3.1 Mineralogical Analysis**

X-ray spectroscopy and FT-IR spectrometer were applied to determine the compositions of the four phosphate rock samples. The results of the X-ray were analyzed by a program “Visual XRD”, and the results of the FT-IR were analyzed by comparing peaks from analysis and known minerals. The results of the X-ray analyses are included in Appendix D, and the results of the FT-IR results are indicated in Appendix E. A summary of the results are shown in Table 4-3.

**Table 4-3 Summary of X-ray and FT-IR results of the four types of phosphate rocks**

	X-ray results	FT-IR results
Carbonatite	calcite, hillebrandite, and quartz	calcite, quartz and vivianite
Tennessee Brown	carbonate-hydroxylapatite, carbonate-fluorapatite and quartz	calcite, quartz, hydroxyapatite, and dolomite
PSP rock	Calcite, dolomite, quartz and carbonate-apatite	calcite and hydroxyapatite

The X-ray and FT-IR results from Table 4-3 indicate that the major active mineral compositions among the phosphate rocks are calcite, apatite and quartz.

Then, each phosphate rock was dissolved by concentrated hydrochloric acid (HCl). CO<sub>2</sub> (g) was evolve immediately, and the volume of the CO<sub>2</sub> (g) was measured. The major source of the CO<sub>2</sub> (g) comes from calcite, and thus the mass and percentage of calcite was calculated. The calculations and the results are tabulated in Table 4-4. Fluoride concentration in each acid solution was determined by fluoride electrode, and assuming the fluoride mainly comes from fluorapatite, then the mass and percentage of fluorapatite was determined. The calculations and the results are demonstrated in Table 4-5. The phosphorus concentration in each solution was determined by ascorbic acid method. The major source of this phosphorus is apatite including hydroxyapatite and fluorapatite. As shown in Table 4-5, the mass of fluorapatite is known, and then the mass of phosphorus in hydroxyapatite can be calculated. This mass of phosphorus in hydroxyapatite is the total mass of phosphorus minus by the mass of phosphorus in fluorapatite. With the knowledge of the mass of phosphorus in hydroxyapatite, the mass of hydroxyapatite was calculated and the results are indicated in Table 4-6. A summary of the calculated compositions of the three phosphate rocks is shown in Table 4-7.

**Table 4-4 Calculation of percentage of CaCO<sub>3</sub> in phosphate rocks**

Material	CO <sub>2</sub> Volume (mL)	CO <sub>2</sub> (mmol)	CaCO <sub>3</sub> mass (mg)	Material mass (g)	Mass Percentage (%)
Carbonatite	17.5	0.728	72.7	0.202	36.1
Tennessee Brown	7.50	0.312	31.1	0.483	6.45
PSP rock	16.0	0.666	66.5	0.520	12.7

**Table 4-5 Calculation of percentage of fluorapatite in phosphate rocks**

Material	F concentration (mg/L)	F (mg) mass	F (mmol) in fluorapatite (mmol)	Fluorapatite (mg)	Material mass (g)	Mass Percentage (%)
Carbonatite	0.121	0.001	3.18*E-5	0.016	0.495	0.003
Tennessee Brown	11.4	0.057	0.003	1.50	0.503	0.300
PSP rock	56.1	0.281	0.015	7.41	0.495	1.49

**Table 4-6 Calculation of percentage of hydroxyapatite in phosphate rocks**

Material	P concentration (mg/L)	P (mg) mass	P (mmol) in apatite	P (mmol) in hydroxylapatite	Hydroxylapatite (mg)	Material mass (g)	Mass Percentage (%)
Carbonatite	0.105	0.021	0.001	9.55*E-5	0.292	0.495	0.059
Tennessee Brown	2.67	0.535	0.017	0.009	4.14	0.503	0.825
PSP rock	9.85	1.97	0.064	0.044	9.70	0.495	1.95

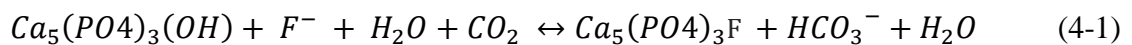
**Table 4-7 Summary of the composition of each phosphate rock**

Material	Major composition
Carbonatite	36.127% calcite 0.059% hydroxylapatite quartz
Tennessee Brown	6.455% calcite 0.825% hydroxylapatite quartz
PSP rock	12.799 % calcite 1.959% hydroxylapatite quartz

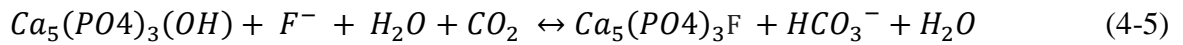
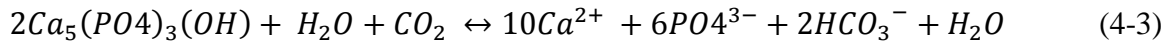
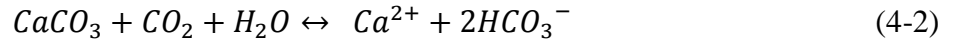
The analysis results of indicate that the PSP rock has the highest portion of hydroxylapatite. Spanish River carbonatite has the least portion of hydroxylapatite, while it contains the highest percentage of calcite.

#### **4.3.2 Batch Test**

Weighed amounts of the four phosphate rock samples were placed into four bottles of 10 mg/L sodium fluoride solutions. According to previous research (Murutu et al, 2010; Gao et al, 2009; Tomar et al, 2013), different forms of apatite removes fluoride from contaminated water by adsorption. Burner (2005) also found evidence that fluoride can also be absorbed by calcite. Therefore, in this process, fluoride in the solution was supposed to be absorbed by apatite and calcite from the phosphate rocks. This major fluoride removal mechanism is as indicated by equation 4-1.



In batch (b), samples were bubbled with 97 kPa CO<sub>2</sub> (g) before being placed in the water bath. The effect of CO<sub>2</sub> equilibration was to decrease pH and increased the carbonic acid concentration. This carbonated solution was then in contact with phosphate rocks, and thus calcite and apatite dissolved. Fluorite was supposed to become supersaturated and precipitate in this process, and thus, fluoride was supposed to be removed by precipitation and adsorption. This fluoride removal mechanism is as indicated by equation 4-2, 4-3, 4-4, 4-5.



Solid samples before batch test, after batch tests (a) and after (b) were collected and analyzed by XRD. These analyses aimed to explain the mechanism of the process, and the results are included in Appendix H. If adsorption occurred in the batch test (a) and (b), the amount of fluorapatite should have increased after batch test (a) and (b) compared to the amount before batch tests, and if precipitation occurred in the process of batch (b) test, fluorite should have been observed in the solid after batch (b) test. The XRD results (shown in Appendix H) indicate that the intensities of the peaks for fluorapatite increased after batch tests, and no peaks of fluorite were observed after batch tests (b). These XRD results indicate that adsorption occurred in both batch tests (a) and (b), but precipitation was not observed in batch tests (b). However, since XRD analyses can reveal the mineral whose composition percentage is only larger than 5%, these XRD results do not indicate there is no precipitation of fluorite in batch test (b) and they indicate that precipitation was not the major mechanism that occurred in batch test (b). In addition, analyses of the material by techniques including FT-IR, X-ray photoelectron (XPS) spectroscopy are needed for future study to determine if there is a less than 5% fluorite precipitate in batch test (b). Overall, XRD results indicate that no more than 5% fluorite was formed in the batch test (b), and adsorption was the major contribution for fluoride removal rather than precipitation of fluorite.

Liquid samples after batch tests (a) and (b) were also collected and analyzed. The fluoride and calcium results are demonstrated in Table 4-8, the phosphorus results are shown in Table 4-9, while the change of pH before and after the batch tests are indicated in Table 4-10.

**Table 4-8 Comparison of the fluoride and calcium concentrations after batch test (a) and (b)**

	Batch (a)		Batch (b)	
	Fluoride concentration (mg/L)	Ca concentration (mg/L)	Fluoride concentration (mg/L)	Ca concentration (mg/L)
Carbonatite	1.49	39.5	1.07	156
Tennessee Brown	4.24	20.4	4.08	93.36
PSP rock (Fine)	1.12	95.5	0.730	279
PSP rock (Coarse)	1.24	73.4	0.746	236

**Table 4-9 Comparison of the phosphate concentrations (in mg/L P) after batch test (a) and (b)**

	Batch (a)	Batch (b)
Carbonatite	< 0.02	< 0.02
Tennessee Brown	0.223	0.382
PSP rock (Fine)	0.081	0.121
PSP rock (Coarse)	0.107	0.169

**Table 4-10 Comparison of pH change in batch test (a) and (b)**

	Batch (a)		Batch (b)	
	pH of fluoride samples	pH after 24h of rotation	pH after bubbled with CO <sub>2</sub>	pH after 24h of rotation
Carbonatite	7.12	7.73	5.23	6.52
Tennessee Brown	7.11	7.56	5.44	6.82
PSP rock (Fine)	7.12	7.80	5.27	6.31
PSP rock (Coarse)	7.12	7.82	5.30	6.47

Entry “Batch (a)” of the Table 4-8, Table 4-9 and Table 4-10 show the changes of fluoride concentrations after the samples were rotated in water bath for 24 h. Entry “Batch (b)” of the Table 4-8 show the same changes when the samples were bubbled with 97 kPa CO<sub>2</sub> (g) before being placed in the water bath. The results from Table 4-8 shows the fluoride removal efficiencies of the two batch was similar, with or without CO<sub>2</sub> (g) equilibration. In batch (a), due to adsorption by material 1, material 3 and material 4, fluoride concentrations were reduced to below drinking level standard (<1.5 mg/L). As a result, hydroxyl ion was replaced and released to the solution, and this process caused the increase in pH (Table 4-10). Use of material 3 was the most efficient for removal of fluoride, because material 3 had the highest apatite level and the smallest particle size (biggest surface area). The application of material 2 reduced fluoride concentration to 4.24 mg/L. This concentration was much higher than the drinking level standard. The reason was due to the low percentage of apatite and calcite in this material. Inefficient apatite and calcite cannot provide enough adsorption sites for fluoride. In batch test (b), fluoride removal efficiencies of the four materials were better than that in batch (a). Material 1, material 3

and material 4 reduced fluoride concentrations to below 1.5 mg/L. Material 3 demonstrated the highest removal efficiency, and reduced fluoride concentration to 0.73 mg/L. Similarly, the application of material 2 reduced fluoride concentration to only 4.08 mg/L. The pH values increased as a result of dissolution of calcite and apatite. Calcium concentrations ranged from 93.36 mg/L to 279.81 mg/L, and are much higher than in batch test (a). The phosphorus concentrations of the sample from batch test (b) were also slightly higher than samples from batch test (a). These increases were a result of dissolution of calcite and apatite by carbonated fluoride samples.

A possible reason to explain why precipitation did not contribute significantly to fluoride removal in batch teste (b) is that phosphate ion inhibited dissolution of calcite. Griffin and Jurinak (1973) stated that phosphate can be adsorbed onto calcite. Then Berner and Morse (1974) observed that adsorption of the phosphate by calcite inhibited calcite dissolution by blocking surface site. In addition, Svensson and Dreybrodt (1992) stated that electrostatic attraction between phosphate and calcium ions inhibited dissolution of calcite. These findings agree with the results in this research. Calcium concentration after the batch test (b) was low due to insufficient dissolution of calcite, and the amount of fluoride that precipitated as fluorite was lower than 5% fluorite.

### **4.3.3 Column Experiment**

Column effluent samples were regularly collected from the four columns of the reactor using syringes. After filtrations, these samples were analyzed. The fluoride concentrations are indicated in Figure 4-2.

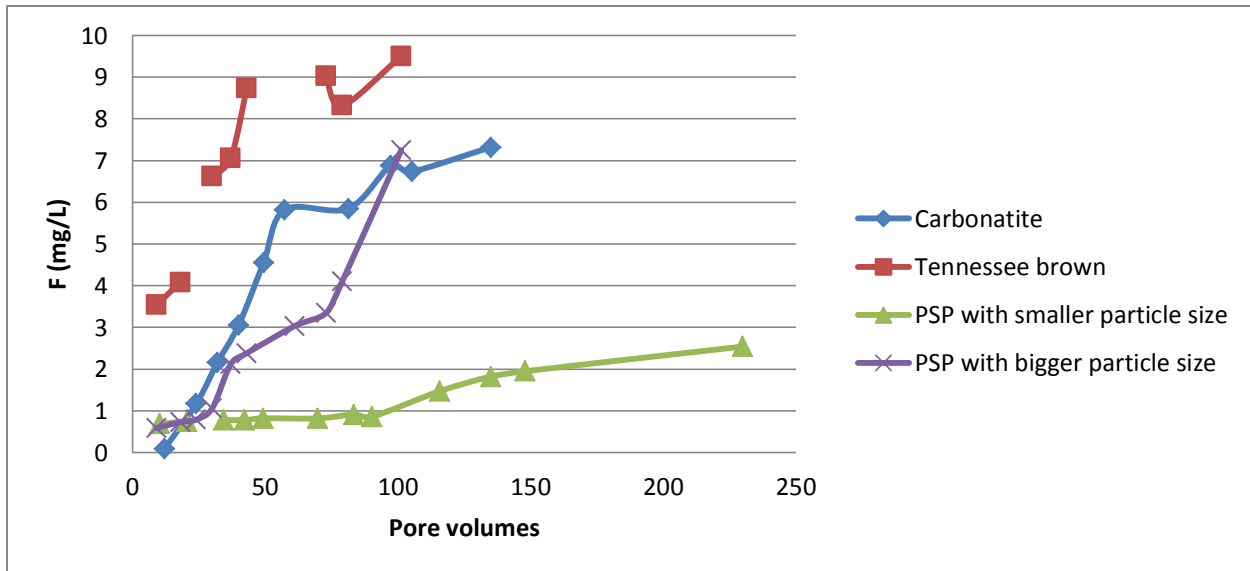


**Figure 4-2 F concentrations vs. pore volumes in treatment when a 10 mg/L NaF feedwater flows through the phosphate rock reactor at a residence time of 4 h**

PSP rock (in Column 3) is a potential material for fluoride remediation. This material reduced fluoride concentration from 10 mg/L to 1.5 mg/L until a passage of 120 pore volumes (equals to 3.92 L). However, after that, the fluoride concentration continuously increased. This curve pattern indicates that the mechanism was adsorption rather than precipitation. If precipitation had been the major mechanism for removal of fluoride, the calcite in phosphate rock should have continually dissolved while the reactor ran. Then, fluorite should have continued precipitating and fluoride concentration in the effluent should stay stable. The finding of this mechanism is in accordance with the results of the batch tests. Precipitation could have occurred in the process, but it had a minor effect on removal of fluoride.

Materials in column 3 and column 4 are of the same composition, except that material in Column 3 has a smaller particle size. In column 4, fluoride concentration was higher than 1.5 mg/L after a passage of about 30 pore volumes (equals to 2.17 L). This result indicates that material with small particle sizes has a high fluoride removal capacity. The reason may due to the fact that

material with smaller particle sizes has larger surface area and higher density of adsorption sites for fluoride than materials with larger particle sizes.

After a passage of 100 pore volumes, samples from the four columns were collected, filtered and analyzed. ICP results of the cations are shown in Table 4-11. The phosphate rocks are known to contain heavy metals, and the analyses aimed to determine whether the phosphate rocks leached heavy metals and thus contaminated the water. Concentrations of the potential contaminant cations were analyzed and were compared to maximum allowable drinking water concentrations.

**Table 4-11 Major cations in the effluents from columns when a 10 mg/L NaF feedwater flows through the limestone reactor at a residence time of 4 h after a passage of 100 pore volumes**

	Cr (µg/L)	Mn (µg/L)	Ni (µg/L)	As (µg/L)	Cd (µg/L)	Cu (µg/L)	Ca (mg/L)
Carbonatite	0.591	43.2	4.02	4.88	2.07	3.11	196
Tennessee Brown	0.897	485	12.2	10.3	5.07	83.3	93.3
PSP rock (Fine)	0.477	20.6	23.9	6.15	3.07	353	172
PSP rock (Coarse)	4.01	2.90	10.5	3.74	0.587	153	309

According to the standards by EPA, the Maximum Contaminant Level (MCL) of arsenic (As) is 0.01 mg/L, that of cadmium (Cd) is 0.005 mg/L, and level of the copper (Cu) is 1.3 mg/L. As shown in Table 4-11, only arsenic and cadmium concentrations in the effluent from column 2 exceeded the MCL level by 3% and 1.56%, and other heavy metals did not exceed the MCL level in the effluents from the other columns. Therefore, material 2 is not an ideal choice for

removal of fluoride. In addition, this research did not constantly monitor heavy metals in the effluents, but the monitoring should be recommended in future research.

The results also show that calcium concentrations in the effluents from the phosphate rock reactors were lower than calcium in the effluent from column 1 of the limestone reactor (chapter 2) due to insufficient dissolution of calcite. This is a reason why the amount of fluoride that precipitated as fluorite was low and precipitation was not a major mechanism for removal of fluoride.

#### **4.4 Conclusion**

The results of the mineralogical analyses indicate that the major active mineral compositions among the four types of phosphate rocks are calcite, apatite and quartz. PSP rock has the highest portion of hydroxylapatite. Spanish River carbonatite has the least portion of hydroxylapatite, while it contains the highest percentage of calcite.

These four types of phosphate rocks were assessed on their ability to remove fluoride from contaminant water. PSP rock, which contains the highest percentage of hydroxyapatite and with small particle size, is the best choice for fluoride remediation among the four. It can reduce fluoride concentration from 10 mg/L to 1.5 mg/L until a passage of 120 pore volumes. However, after 120 pore volumes the fluoride concentration continuously increased. This indicates a mechanism of adsorption rather than precipitation, with adsorption sites becoming saturated over time. The results from batch tests also provide evidence that adsorption contributes much more than precipitation for removal of fluoride. In addition, the results show that material with a smaller particle size performed better in removal of fluoride than material with larger particle sizes, because small particle size resulted in a large surface area and more adsorption sites for fluoride. The precipitation of fluorite was not observed in this process, and one of the reasons is phosphate ion inhibition effect on calcite dissolution.

Future work should be done on improving the fluoride removal ability of the phosphate rocks. Investigation should be done on understanding the dissolution process of the calcite and apatite within the phosphate rocks in the columns, and methods should be developed to simulate the precipitation of fluorite in the columns of the reactor. Therefore, fluoride removal efficiency of the phosphate rock reactor can be increased by precipitation, and the long-term performance of the reactor can be improved. Constant monitoring of the heavy metal contents in the effluents is also suggested.

## Chapter 5

### Summary of Conclusions

The limestone reactor designed in this research reduced fluoride concentration from up to 150 mg/L to below maximum contaminant level (4 mg/L), at the residence time of 4 h. When the residence time was 24 h, fluoride concentration can be reduced to below the drinking water standard (1.5 mg/L). The fluoride removal efficiency was higher than observed in the reactor designed by Reardon and Wang. However, measured fluoride concentrations in the effluent were still higher than the predicted values. One reason is that citrate suppressed the precipitation of calcite. The short residence time of the experiment also decreased the removal efficacy of the limestone reactor. The results indicate that a long residence time enhanced precipitation of fluorite in column 1 and calcite in column 2, and increased the removal efficiency of the reactor. An improvement to this reactor was to inject a slurry containing  $\text{CaF}_2$  into the upper part of column 1, and this amendment further reduced fluoride concentration by 0.42 mg/L. The dolomite reactor reduced fluoride concentration to 4.30 mg/L and was not as efficient as the limestone reactor. The three main reasons are the slow dissolution rate of dolomite, negative effect of magnesium on the precipitation of fluorite in column 1 and suppression effect of citrate on precipitation of calcite in column 2. However, the presence of magnesium promoted more fluoride to co-precipitate in fluorite in column 2 than of the limestone reactor.

Mineralogical analyses results for the four phosphate rocks indicate that the major active mineral compositions are calcite, apatite and quartz. PSP rock that contains the highest percentage of hydroxyapatite with a small particle size is the best choice for fluoride remediation among the four. It can reduce fluoride concentration from 10 mg/L to 1.5 mg/L until a passage of 120 pore volumes. However, after 120 pore volumes, the fluoride concentration continuously increased. This indicates a mechanism of adsorption rather than precipitation. Outcomes from batch tests also provide evidence that adsorption contributes much more than precipitation for removal of fluoride.

Of the three fluoride analytical techniques, fluoride electrode method was selected as the most suitable method for this research. This study indicates that citrate has a significant interference on the SPADNS method, and the addition of a pH buffer does not successfully eliminate the interference. Citrate has a negligible effect on the determination using fluoride electrode; and it had no effect on the IC method, since the peaks for the two were well separated. However, the running time of the IC methods is long for each sample, and the cost is much higher than the fluoride electrode method. Therefore, fluoride electrode was used throughout this study.

## **Chapter 6**

### **Recommendation for Future Work**

Further study should be devoted to improve fluoride removal efficiency of the limestone/dolomite reactors. A single reactor incorporating both calcite and dolomite should also be evaluated. Another avenue for research is to consider the possibility of organic ligands other than citrate to more efficiently promote the incorporation of fluoride into calcite precipitates. Further investigation on the dissolution and precipitation processes in the dolomite reactor should also be done.

Future work should also be done on improving the fluoride removal ability of the phosphate rocks. Investigation should be done on understanding the dissolution process of the calcite and apatite within the phosphate rocks in the columns, and methods should be developed to simulate the precipitation of fluorite in the columns of the reactor. Thus, fluoride removal efficiency of the phosphate rock reactor can be increased, and the long-term performance of the reactor can be improved. Constant monitoring of the heavy metals in the effluent from the reactor is also recommended.

Reasons for interference effect from citrate on the SPADNS methods for fluoride analysis should be further investigated. Methods using IC to reduce the column residence time but still allow the separation of citrate and fluoride peaks should also be studied. Ion exclusion chromatography and more effective gradient eluent techniques should be applied for simultaneous determination of fluoride and citrate.

## Appendix A

### Reactor Apparatus

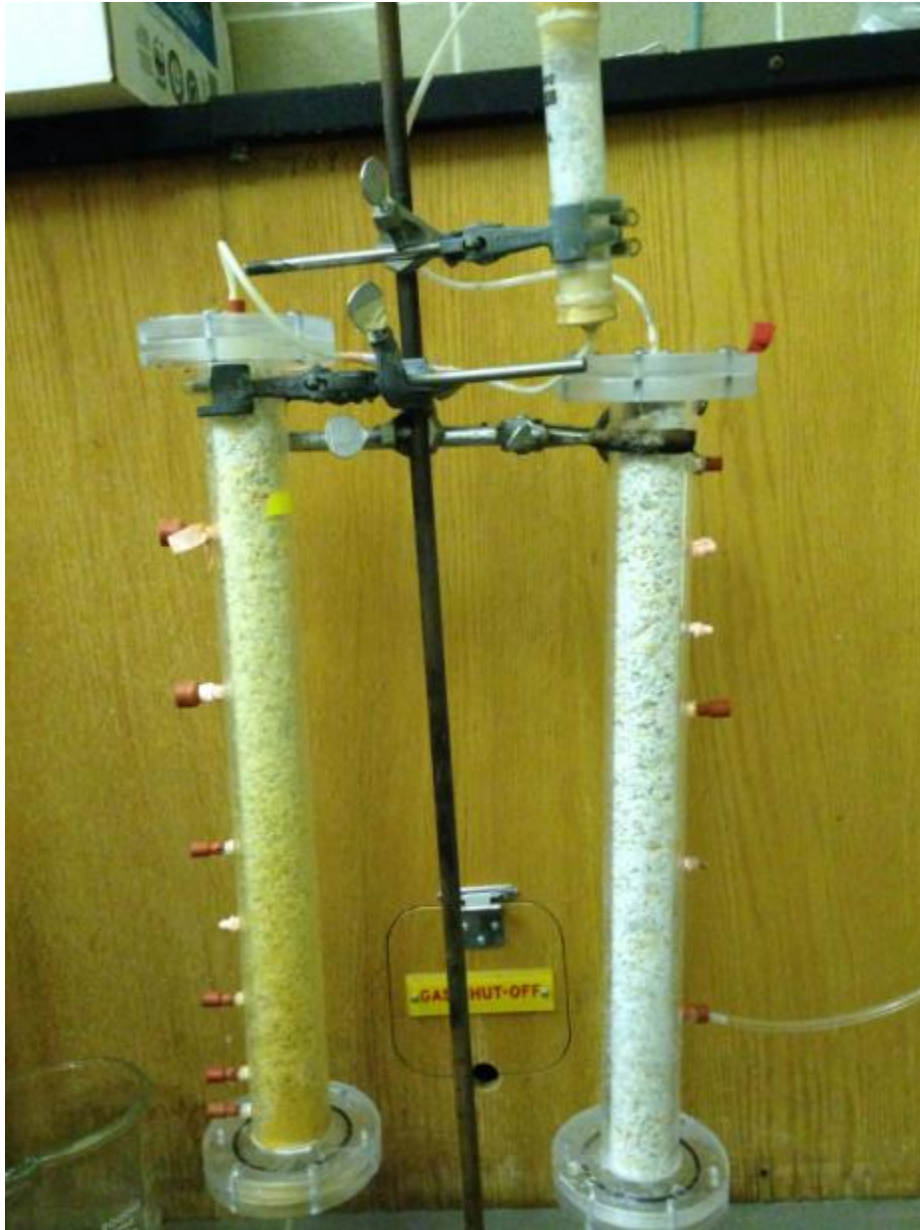


Figure A-1 The limestone reactor



Figure A-2 The dolomite reactor



Figure A-3 The phosphate rock reactor



Figure A-4 Acidolysis of the phosphate rocks and the exsolution of  $\text{CO}_2$  (g)

## Appendix B

### Modelling Program of Phreeqc

#### Program of the limestone reactor

```
SOLUTION 1
  temp      25
  pH        7 charge
  pe        4
  redox     pe
  units     mmol/kgw
  density   1
  F         0.526
  Na        0.526
  -water    1 # kg

EQUILIBRIUM_PHASES 1
  CO2 (g)   -0.032 10

SAVE solution 1
END

USE solution 1

EQUILIBRIUM_PHASES 2
  Calcite   0 10
  Fluorite  0 10

SAVE solution 2
END

USE solution 2

EQUILIBRIUM_PHASES 3
  Ca-Citrate4H2O 0 10

SAVE solution 3
```

END

USE solution 3

EQUILIBRIUM\_PHASES 4

CO2(g) -3.40 10

Calcite 0 10

Fluorite 0 10

END

### Program of the dolomite reactor

SOLUTION 1

temp 25

pH 7 charge

pe 4

redox pe

units mmol/kgw

density 1

F 0.526

Na 0.526

-water 1 # kg

EQUILIBRIUM\_PHASES 1

CO2(g) -0.032 10

SAVE solution 1

END

USE solution 1

EQUILIBRIUM\_PHASES 2

Fluorite 0 10

Dolomite 0 10

SAVE solution 2

END

USE solution 2

EQUILIBRIUM\_PHASES 3

Ca-Citrate4H2O 0 10

SAVE solution 3

END

USE solution 3

EQUILIBRIUM\_PHASES 4

CO2(g) -3.40 10

Calcite 0 10

Fluorite 0 10

Dolomite 0 10

END

## Appendix C

### Results from the Limestone and Dolomite Reactors Experiments

Table C-1 F concentrations vs. residence times from the columns in the limestone reactor

Residence times (hours)	F concentration (mg/L) in the effluent from column 1	F concentration (mg/L) in the effluent from column 3	F concentration (mg/L) in the effluent from column 2
4	4.31	4.18	3.38
6	4.02	3.92	3.16
8	3.69	3.62	2.98
10	3.48	3.41	2.75
14	2.90	2.83	2.31
18	2.10	2.02	1.80
20	1.94	1.82	1.65
24	1.72	1.68	1.49

Table C-2 F concentrations in the influent vs. F concentrations in the effluent

F concentration in the influent (mg/L)	F concentration in the effluent (mg/L)
10.1	3.35
20.0	3.47
50.1	3.59
100	3.76
150	3.95
200	4.54

Table C-3 F concentrations vs. distances along the column when with and without injection of a slurry

Distance from entrance of column 1 (cm)	F concentration (mg/L) without injection of slurry	F concentration (mg/L) with injection of slurry
1	6.69	6.69
14	4.40	4.40
29	4.37	4.19
39	4.39	4.02
50 (exit of column 1)	4.37	3.95

Table C-4 F concentration vs. pore volumes in the effluent from each column

Pore volume	F concentration (mg/L) in the effluent from column 1	F concentration (mg/L) in the effluent from column 3	F concentration (mg/L) in the effluent from column 2
6	9.67	9.61	6.69
10	9.27	9.22	6.38
40	8.01	7.89	5.26
60	7.07	6.97	4.61
80	6.71	6.66	4.43
100	6.51	6.43	4.3

# Appendix D

## XRD Traces of Materials and Precipitates formed in column experiments

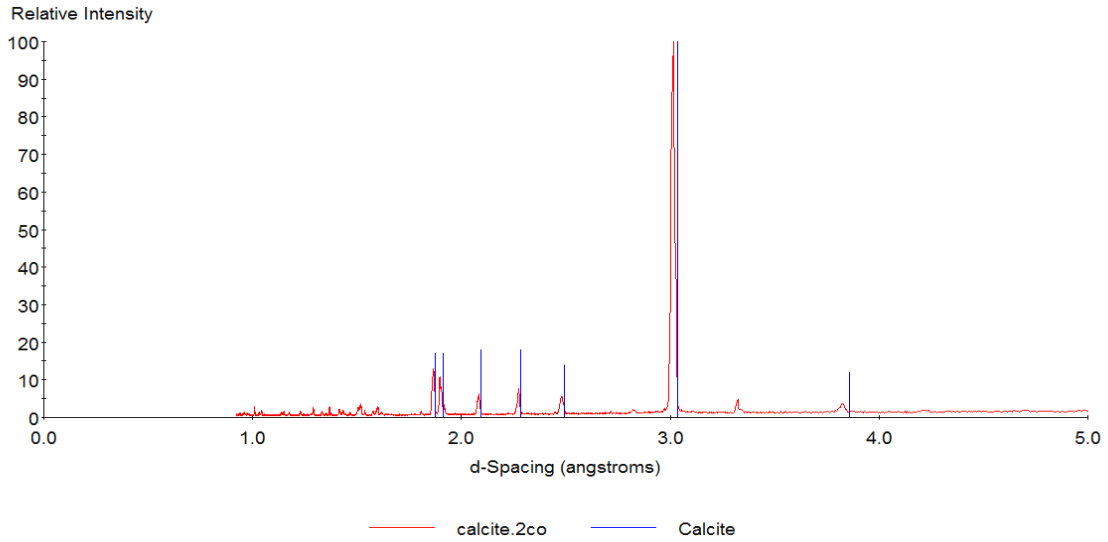


Figure D-1 XRD traces of the limestone

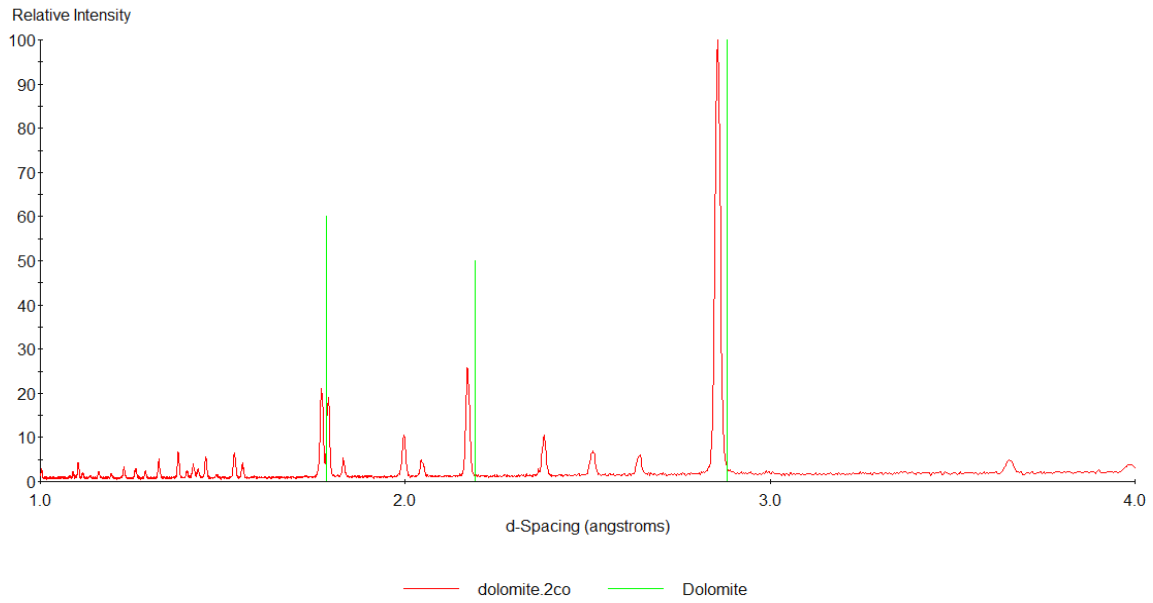


Figure D-2 XRD traces of the dolomite

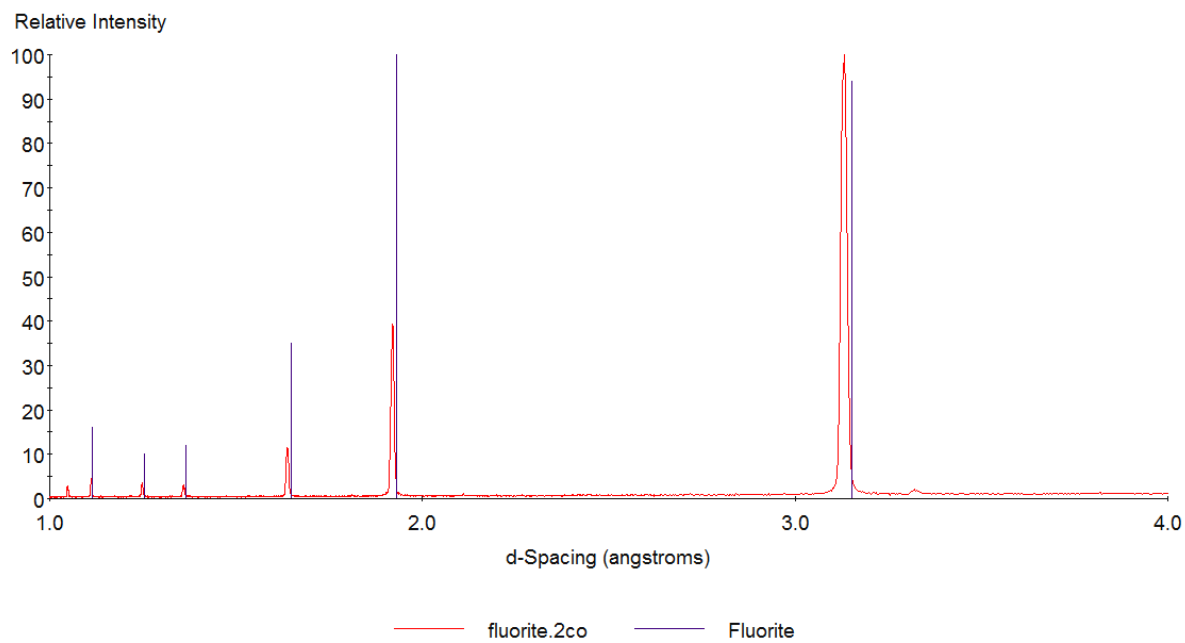


Figure D-3 XRD traces of the precipitates column 1 of the limestone reactor

## Appendix E

### Preparation of Samples for Fluoride Determination Experiments

Table E-1 Prepared Samples for investigating the effect of citrate on SPADNS method

Set	Fluoride (mg/L)	Citrate (mmol/L)	Set	Fluoride (mg/L)	Citrate (mmol/L)
Standard	0	0	1.0 mmol/L Citrate	0	1.0
	0.3	0		0.3	1.0
	0.7	0		0.7	1.0
	1.0	0		1.0	1.0
	1.4	0		1.4	1.0
0.3 mmol/L Citrate	0	0.3	1.2 mmol/L Citrate	0	1.2
	0.3	0.3		0.3	1.2
	0.7	0.3		0.7	1.2
	1.0	0.3		1.0	1.2
	1.4	0.3		1.4	1.2
0.6 mmol/L Citrate	0	0.6	1.5 mmol/L Citrate	0	1.5
	0.3	0.6		0.3	1.5
	0.7	0.6		0.7	1.5
	1.0	0.6		1.0	1.5
	1.4	0.6		1.4	1.5

Table E-2 Prepared samples for investigating citrate and pH effect on SPADNS method (Batch 1)

Set	Fluoride (in mg/L)	Citrate (in mmol/L)	Sodium acetate pH buffer added ( $\mu$ L)
1	0	0	0
	0.3	0	0
	0.7	0	0
	1.0	0	0
	1.4	0	0
2	0	1.0	0
	0.3	1.0	0
	0.7	1.0	0
	1.0	1.0	0
	1.4	1.0	0
3	0	0	200
	0.3	0	200
	0.7	0	200
	1.0	0	200
	1.4	0	200
4	0	1.0	200
	0.3	1.0	200
	0.7	1.0	200
	1.0	1.0	200
	1.4	1.0	200

Table E-3 Prepared samples for investigating citrate and pH effect on SPADNS method (Batch 2 and batch 3)

Batch 2

Essentially the same as batch 1 except that the volume of the pH buffer added was 1000  $\mu\text{L}$  (rather than 200  $\mu\text{L}$ )

Batch 3

Fluoride (in mg/L)	Citrate (in mmol/L)	Sodium acetate pH buffer added ( $\mu\text{L}$ )
0	0	0
0	1.0	0
0	1.0	200
0	1.0	500
0	1.0	1000
0	1.0	3000
0	1.0	5000

Table E-4 Prepared Samples for fluoride electrode method

Set	Fluoride (mg/L)	Citrate (mmol/L)
Standard	0	0
	0.3	0
	0.7	0
	1.0	0
	1.4	0
1 mmol/L citrate	0	1.0
	0.3	1.0
	0.7	1.0
	1.0	1.0
	1.4	1.0

## Appendix F

### Physical Appearances of the Phosphate Rocks

Table F-1 Physical appearance of the phosphate rocks

Material	Physical Appearances
Carbonatite	
Tennessee Brown	
PSP rock (Fine)	
PSP rock (Coarse)	

# Appendix G

## XRD and FT-IR Traces of the Phosphate Rocks

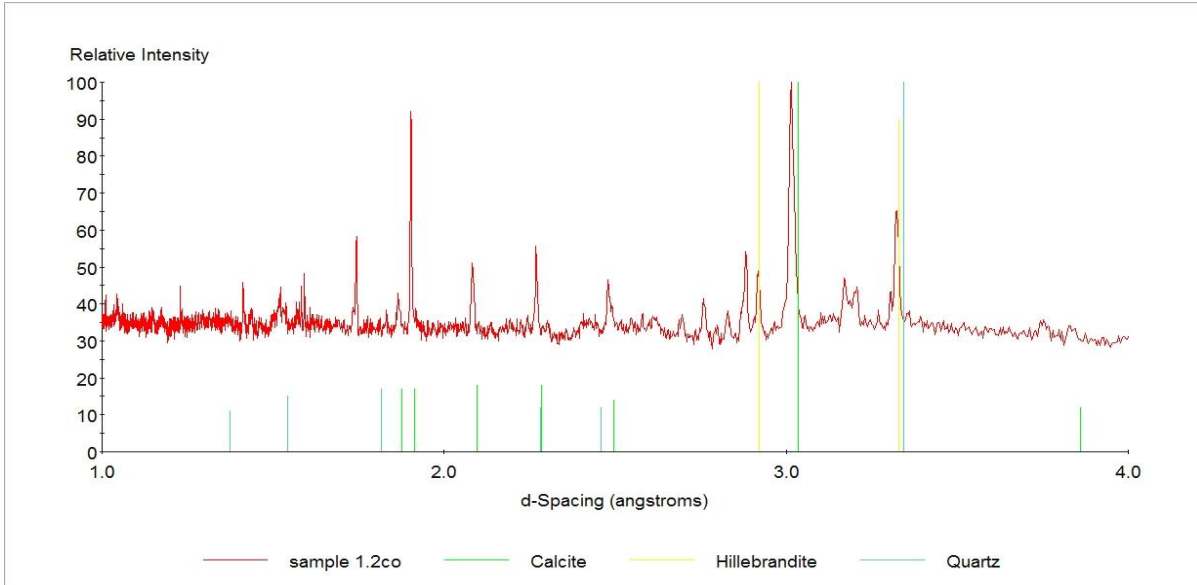


Figure G-1 XRD traces of Carbonatite

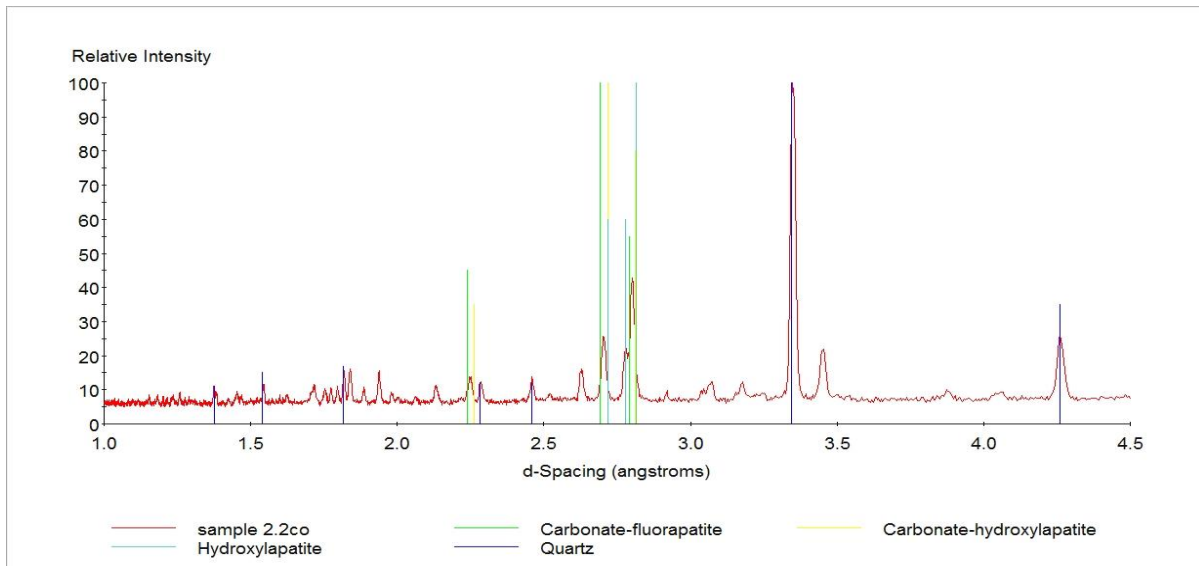


Figure G-2 XRD traces of Tennessee Brown

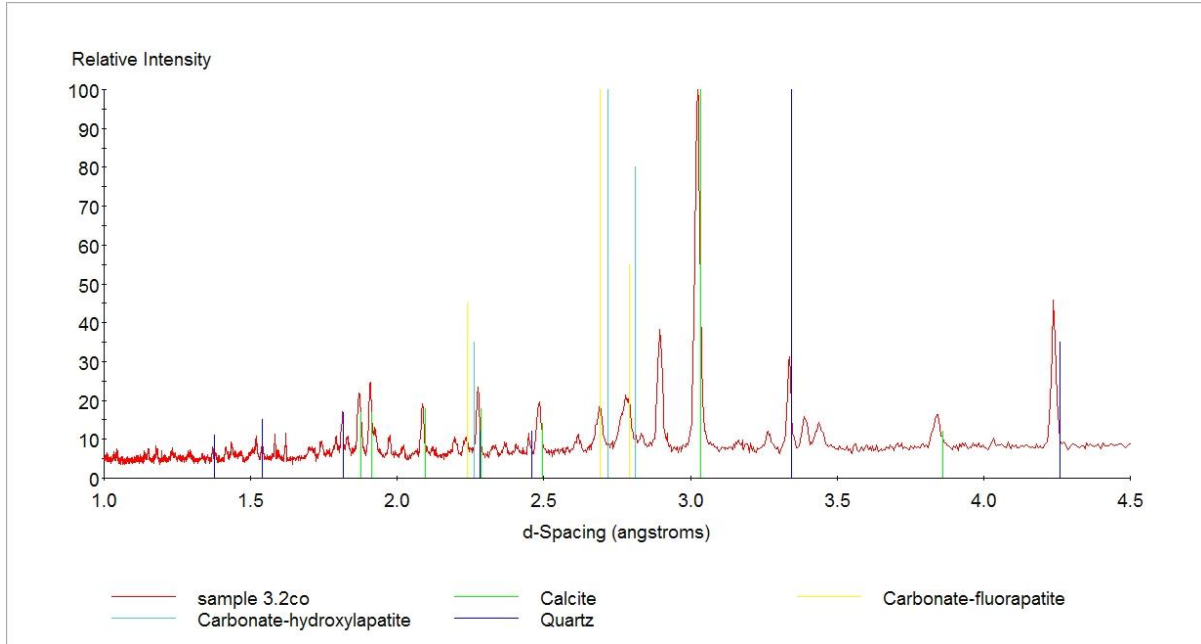


Figure G-3 XRD traces of PSP rock (Fine)

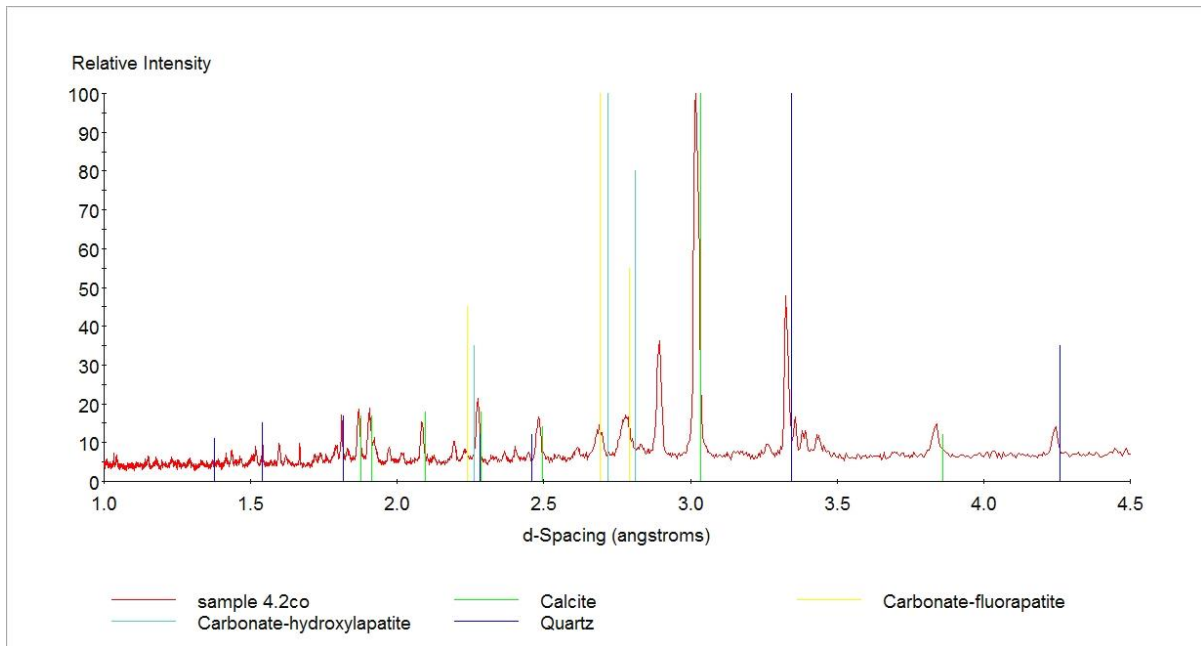


Figure G-4 XRD traces of PSP rock (Coarse)

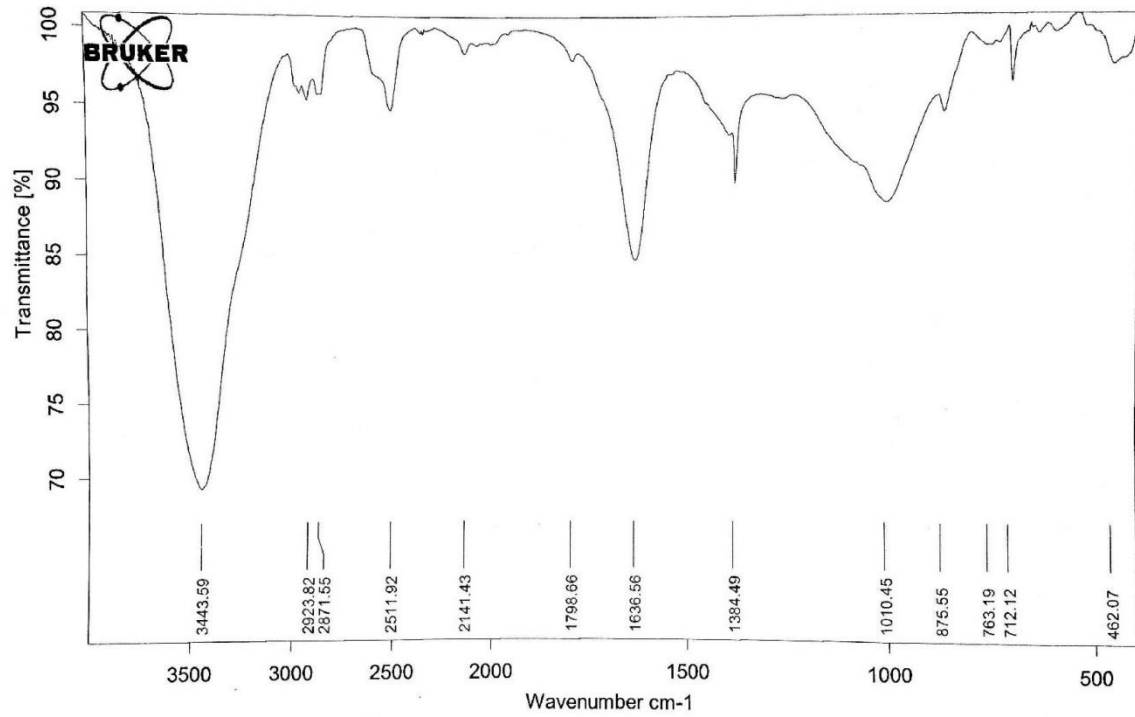


Figure G-5 FT-IR traces of Carbonatite

Table G-1 FT-IR traces analysis of Carbonatite

Peaks (cm-1)	Mineral	References
875.55, 712.12	Calcite	Reig et al., (2002)
482.07	Quartz	Ojima et al., (2003)
1636.56	Vivianite	Frost et al., (2002)

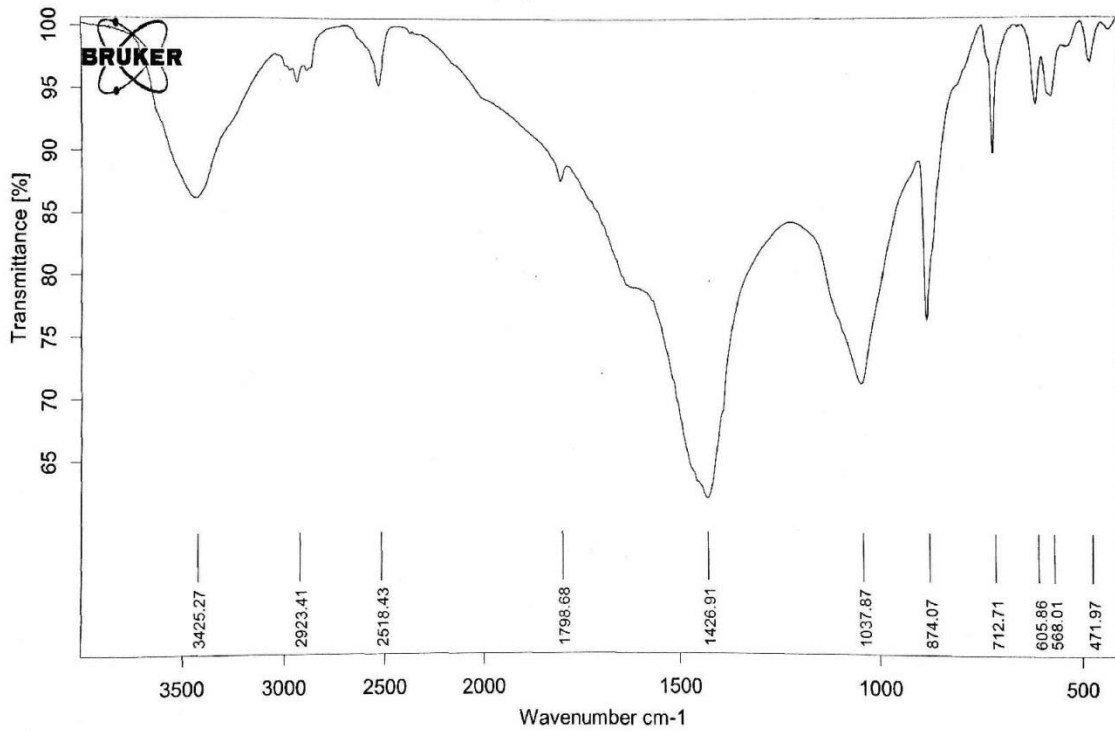


Figure G-6 FT-IR traces of Tennessee Brown

Table G-2 FT-IR traces analysis of Tennessee Brown

Peaks (cm <sup>-1</sup> )	Mineral	References
796.82, 778.61, 693.48	Quartz	Reig et al., (2002)
3425.13, 1041.91, 604.11, 569.07	Hydroxyapatite	Xianying et al., (2012)
1455.77	Dolomite	Matteson & Herron, (1993)
1431.21	Calcite	Matteson & Herron, (1993)

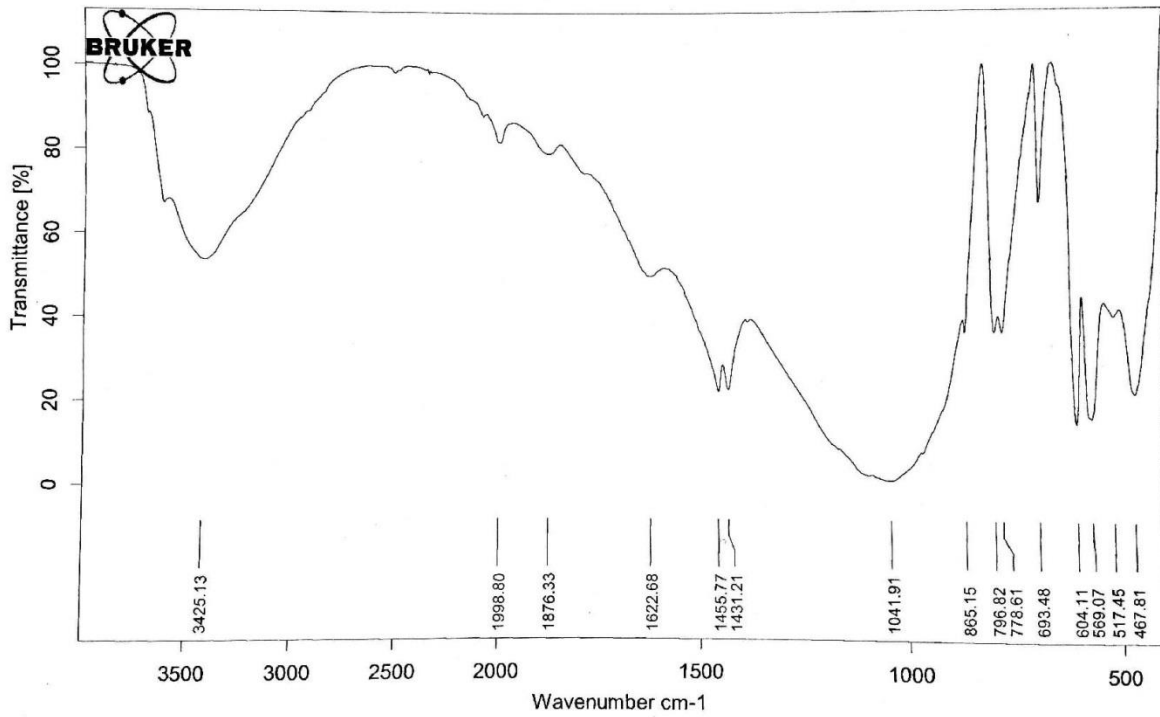


Figure G-7 FT-IR traces of PSP rock (Fine)

Table G-3 FT-IR traces analysis of PSP rock (Fine)

Peaks (cm <sup>-1</sup> )	Mineral	References
874.07, 712.71	Calcite	Reig et al., (2002)
3425.27, 1037.87, 605.86,	Hydroxyapatite	Xianying et al., (2012)

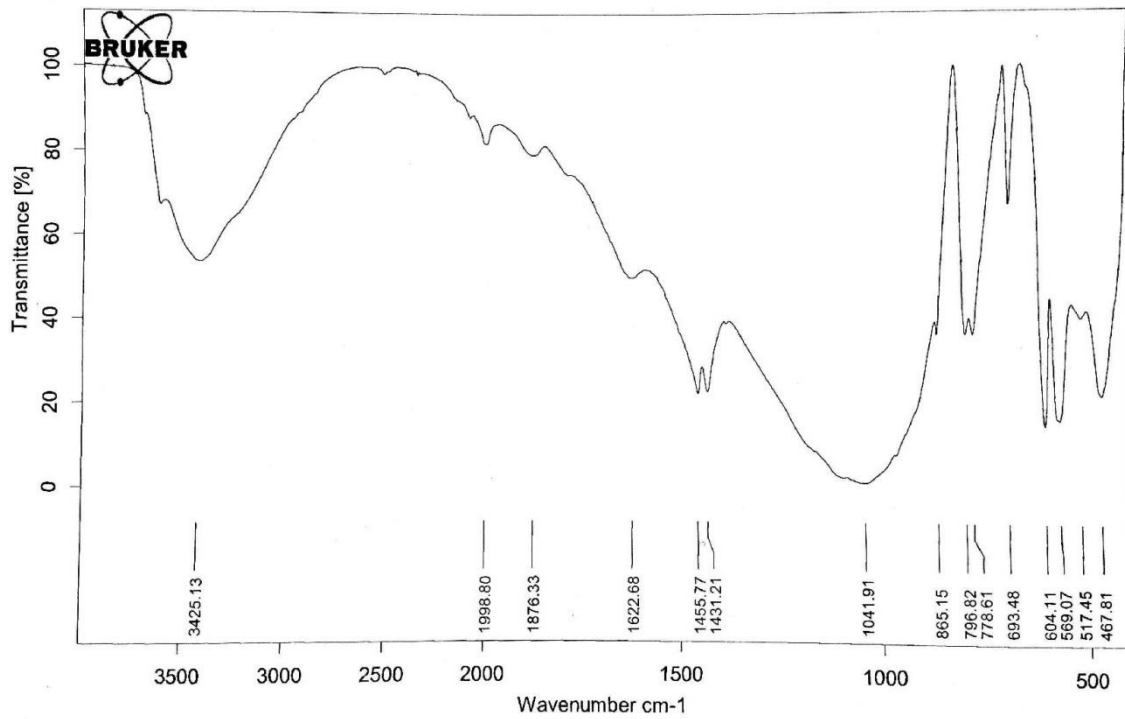


Figure G-8 FT-IR traces of PSP rock (Coarse)

Table G-4 FT-IR traces analysis of PSP rock (Coarse)

Peaks (cm <sup>-1</sup> )	Mineral	References
874.07, 712.71	Calcite	Reig et al., (2002)
3425.27, 1037.87, 605.86,	Hydroxyapatite	Xianying et al., (2012)

## Appendix H

### XRD Traces Comparisons of the Phosphate Rock Before and After Batch Test (a) and (b)

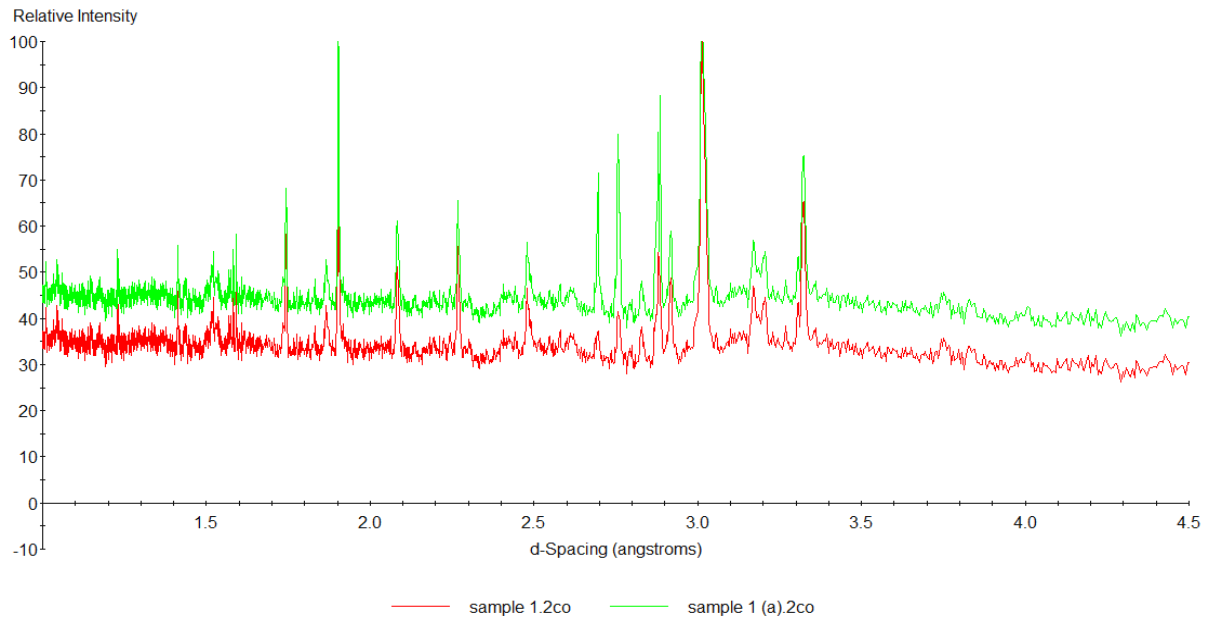


Figure H-1 XRD traces comparisons of Carbonate before and after batch test (a)

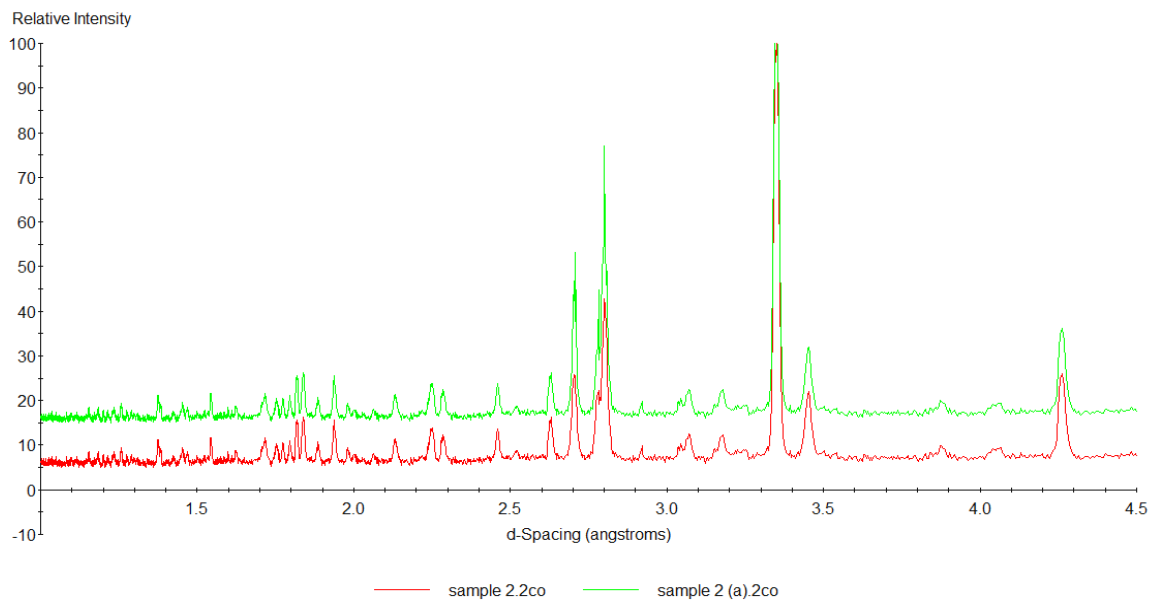


Figure H-2 XRD traces comparisons of Tennessee Brown before and after batch test (a)

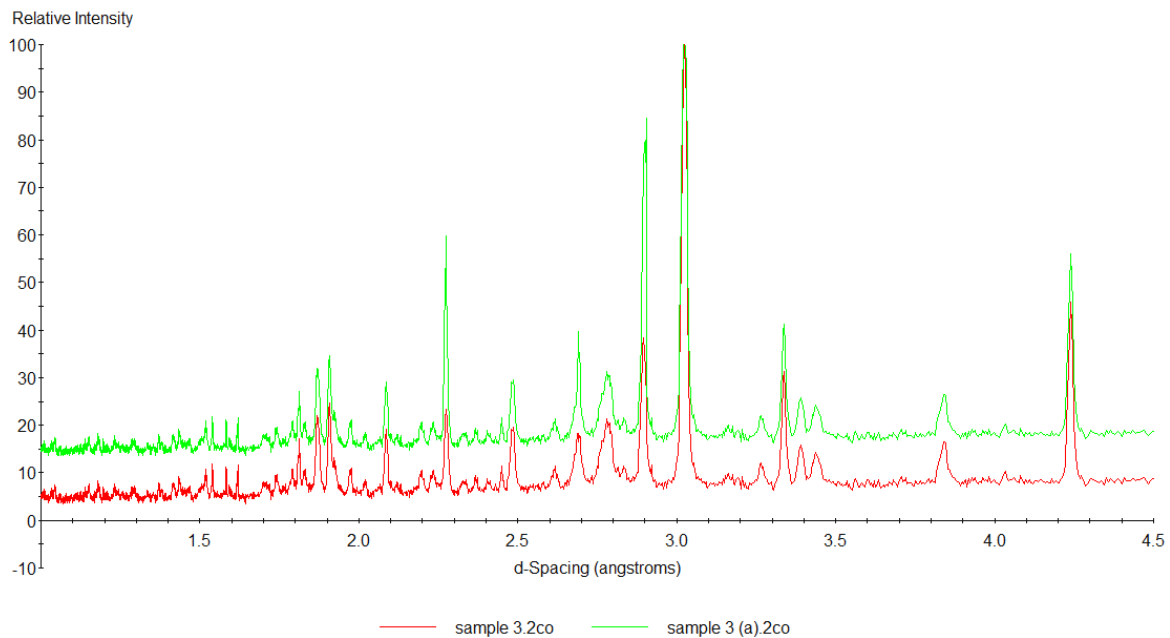


Figure H-3 XRD traces comparisons of PSP rock (fine) before and after batch test (a)

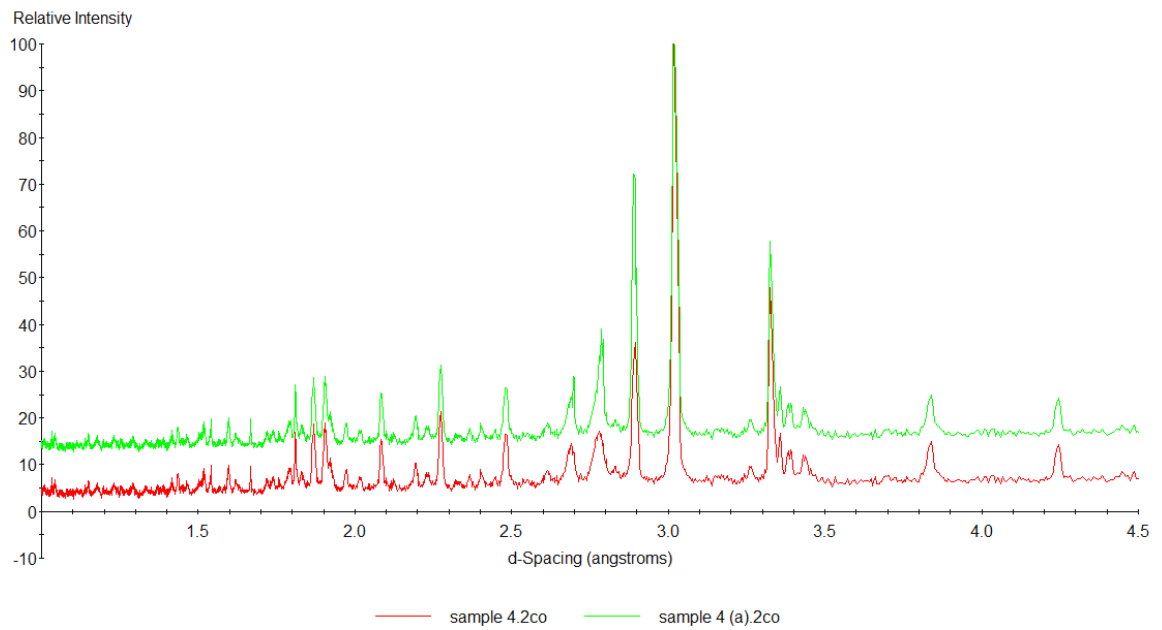


Figure H-4 XRD traces comparisons of PSP rock (coarse) before and after batch test (a)

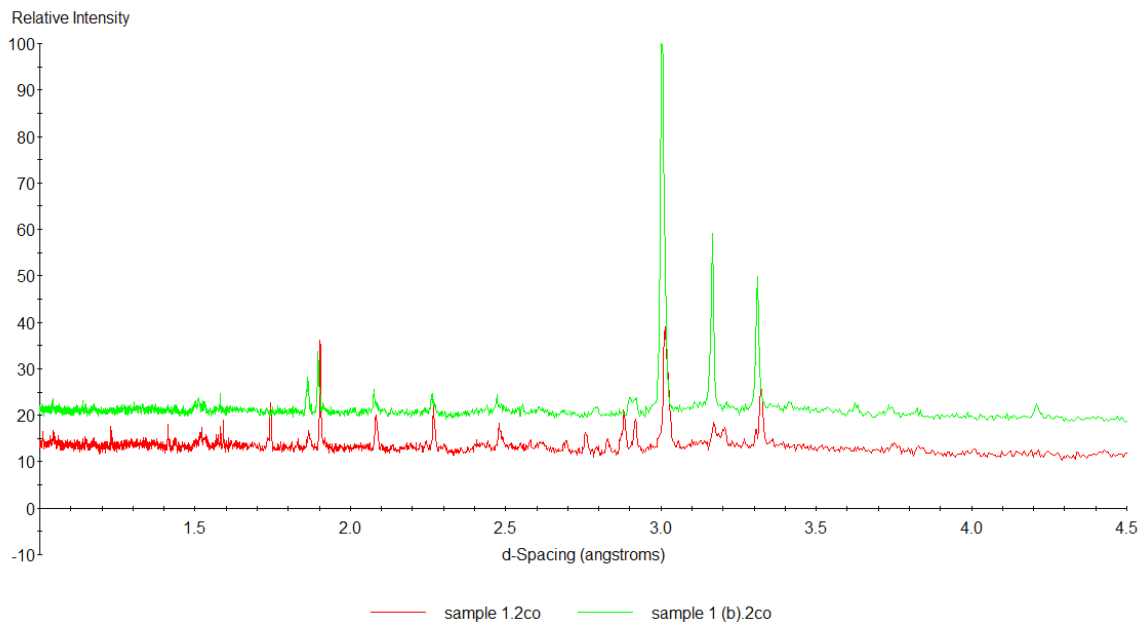


Figure H-5 XRD traces comparisons of Carbonate before and after batch test (b)

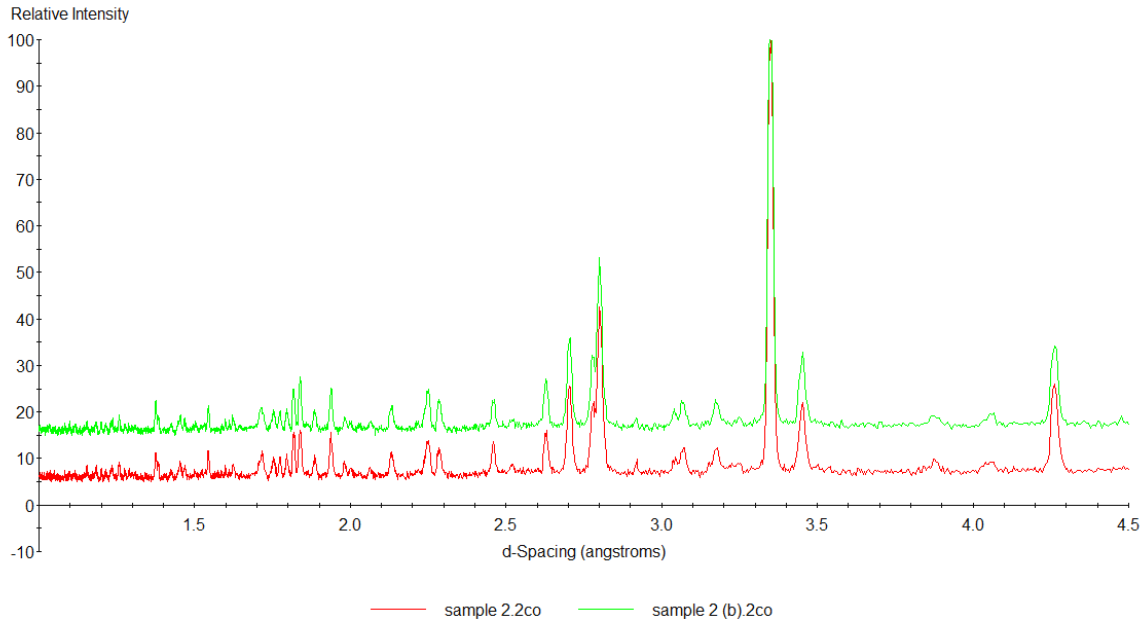


Figure H-6 XRD traces comparisons of Tennessee Brown before and after batch test (b)

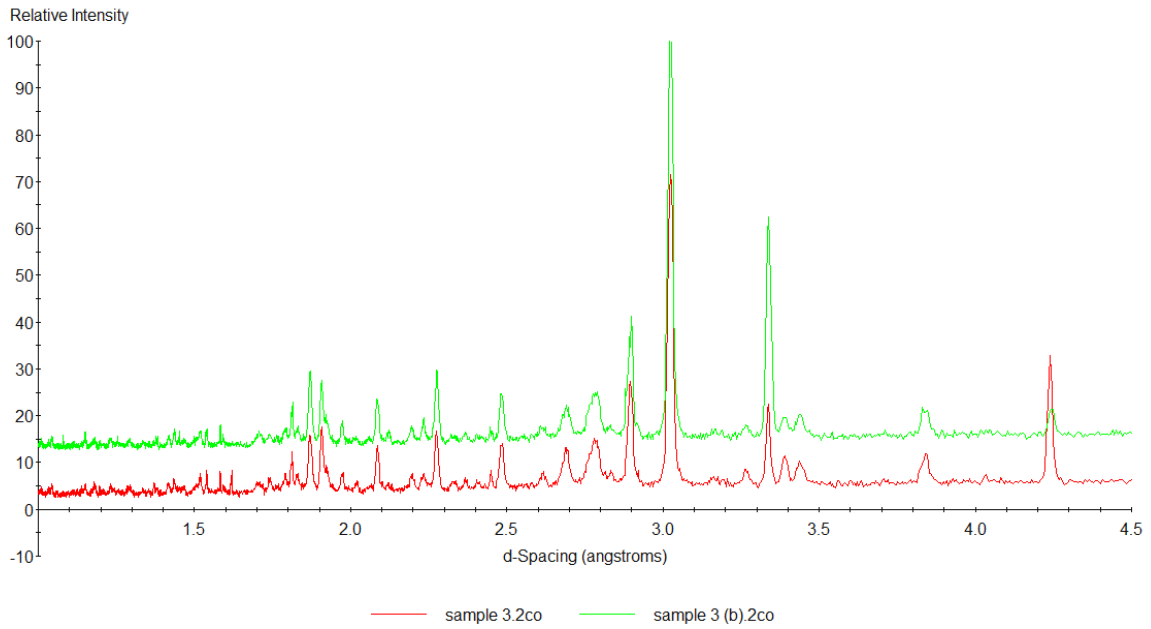


Figure H-7 XRD traces comparisons of PSP rock (fine) before and after batch test (b)

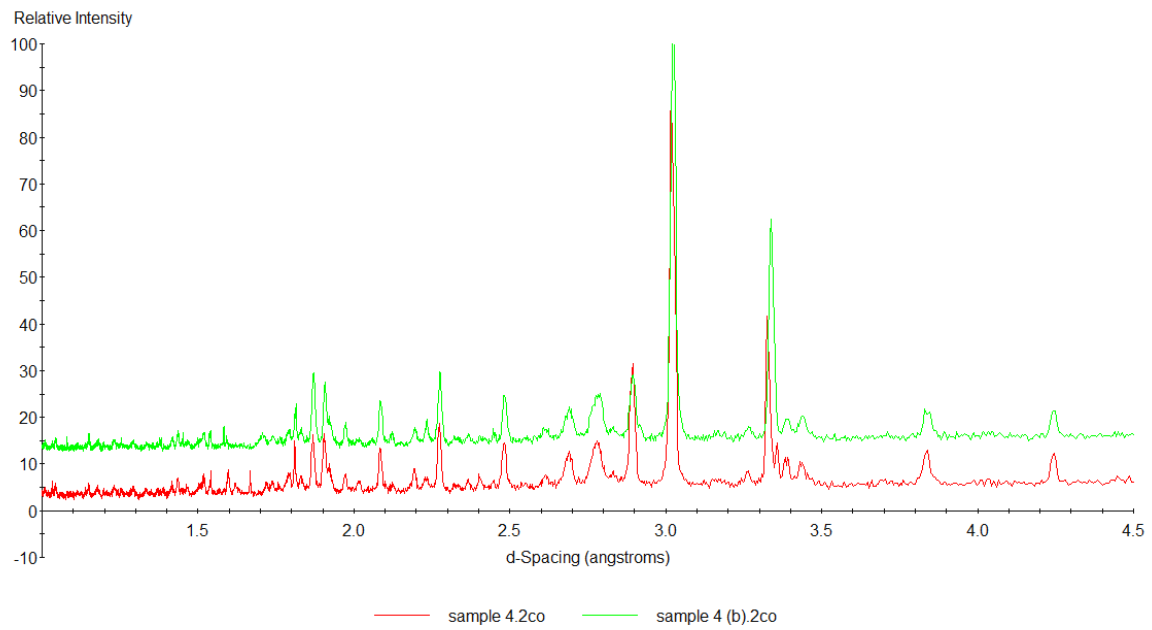


Figure H-8 XRD traces comparisons of PSP rock (coarse) before and after batch test (b)

## Bibliography

- Aitken, A., & Learmonth, M. (1996). Protein determination by UV absorption. *In the Protein Protocols Handbook* (pp. 3-6) Humana Press.
- Amor, Z., Bariou, B., Mameri, N., Taky, M., Nicolas, S., & Elmidaoui, A. (2001). Fluoride removal from brackish water by electrodialysis. *Desalination*, 133(3), 215-223.
- Ayoob, S., & Gupta, A. K. (2006). Fluoride in drinking water: A review on the status and stress effects. *Critical Reviews in Environmental Science and Technology*, 36(6), 433-487.
- Barton, C. J. (1948). Photometric analysis of phosphate rock. *Analytical Chemistry*, 20(11), 1068-1073.
- Basta, N. T., Gradwohl, R., Snethen, K. L., & Schroder, J. L. (2001). Chemical immobilization of lead, zinc, and cadmium in smelter-contaminated soils using biosolids and rock phosphate. *Journal of Environmental Quality*, 30(4), 1222.
- Berner, R. A., & Morse, J. W. (1974). Dissolution kinetics of calcium carbonate in sea water, IV. *American Journal of Science*, 274(6), 638-647.
- Bhargava, D. S., & Killedar, D. J. (1992). Fluoride adsorption on fishbone charcoal through a moving media adsorber. *Water Research*, 26(6), 781-788.
- Bhatnagar, A., Kumar, E., & Sillanpää, M. (2011). Fluoride removal from water by adsorption—a review. *Chemical Engineering Journal*, 171(3), 811-840.
- Cao, X., Du, J., Wen, F., Cao, Y., & Pang, S. (2011). Effect of nano-HAP on proliferation of hepatocellular carcinoma cells. *Bioceramics Development and Applications*, 1, 4.

- Chaturvedi, A. K., Yadava, K. P., Pathak, K. C., & Singh, V. N. (1990). Defluoridation of water by adsorption on fly ash. *Water, Air, and Soil Pollution*, 49(1), 51-61.
- Chaudhry, M. M., Irfan, N., Waheed, S., Siddique, N., & Tufail, M. (2008). Elemental analysis of phosphate rocks: For sustainable agriculture in Pakistan. *Journal of Radioanalytical and Nuclear Chemistry*, 278(1), 17-24.
- Cook, P. J., & Shergold, J. H. (1990). *Phosphate Deposits of the World: Neogene to Modern Phosphorites (vol. 156)*. Cambridge University Press.
- Crosby, N. T., Dennis, A. L., & Stevens, J. G. (1968). An evaluation of some methods for the determination of fluoride in potable waters and other aqueous solutions. *The Analyst*, 93(111), 643.
- Dissanayake, C. B. (1991). The fluoride problem in the ground water of Sri Lanka—environmental management and health. *International Journal of Environmental Studies*, 38(2-3), 137-155.
- Eaton, D. A., Clesceri, S. L., & Greenberg, E. A. (1995). *Standard Methods for the Examination of Water and Wastewater (19 th edition)*. Washington, D. C.: American Public Health Association.
- Edmunds, W. M., & Smedley, P. L. (2013). Fluoride in natural waters. *Essentials of Medical Geology*, 311-336.
- Featherstone, J. D. (1999). Prevention and reversal of dental caries: Role of low level fluoride. *Community Dentistry and Oral Epidemiology*, 27(1), 31-40.
- Frant, M., & Ross Jr, J. W. (1968). Use of a total ionic strength adjustment buffer for electrode determination of fluoride in water supplies. *Analytical Chemistry*, 40(7), 1169-1171.

- Fuchs, C., Dorn, D., Fuchs, C. A., Henning, H. V., McIntosh, C., Scheler, F., & Stennert, M. (1975). Fluoride determination in plasma by ion selective electrodes: A simplified method for the clinical laboratory. *Clinica Chimica Acta*, 60(2), 157-167.
- Gao, S., Cui, J., & Wei, Z. (2009). Study on the fluoride adsorption of various apatite materials in aqueous solution. *Journal of Fluorine Chemistry*, 130(11), 1035-1041.
- Gjerde, D. T., & Fritz, J. S. (1979). Effect of capacity on the behaviour of anion-exchange resins. *Journal of Chromatography A*, 176(2), 199-206.
- Griffin, R. A., & Jurinak, J. J. (1973). The interaction of phosphate with calcite. *Soil Science Society of America Journal*, 37(6), 847-850.
- Handa, B. K. (1975). Geochemistry and genesis of Fluoride - Containing ground waters in india. *Ground Water*, 13(3), 275-281.
- Harwood, J. E. (1969). The use of an ion-selective electrode for routine fluoride analyses on water samples. *Water Research*, 3(4), 273-280.
- Hespanhol, I., & Prost, A. (1994). WHO guidelines and national standards for reuse and water quality. *Water Research*, 28(1), 119-124.
- Ingram, B. L. (1970). Determination of fluoride in silicate rocks without separation of aluminum using a specific ion electrode. *Analytical Chemistry*, 42(14), 1825-1827.
- Jandik, P., Li, J. B., Jones, W. R., & Gjerde, D. T. (1990). New method of background eluent conductivity elimination in gradient ion chromatography. *Chromatographia*, 30(9-10), 509-517.
- Jones, W. R., & Jandik, P. (1991). Controlled changes of selectivity in the separation of ions by capillary electrophoresis. *Journal of Chromatography A*, 546, 445-458.

- Kauranen, P. (1977). The use of buffers in the determination of fluoride by an ion-selective electrode at low concentrations and in the presence of aluminum. *Analytical Letters*, 10(6), 451-465.
- Kloprogge, J. T. (2002). Raman and infrared spectroscopic study of the vivianite-group phosphates vivianite, baricite and bobierrite. *Mineralogical Magazine*, 66(6), 1063-1073.
- Krzyszowska, A. J., Vance, G. F., Blaylock, M. J., & David, M. B. (1996). Ion-chromatographic analysis of low molecular weight organic acids in spodosol forest floor solutions. *Soil Science Society of America Journal*, 60(5), 1565-1571.
- Li, Y. H., Wang, S., Zhang, X., Wei, J., Xu, C., Luan, Z., & Wu, D. (2003). Adsorption of fluoride from water by aligned carbon nanotubes. *Materials Research Bulletin*, 38(3), 469-476.
- Lounici, H., Addour, L., Belhocine, D., Grib, H., Nicolas, S., Bariou, B., & Mameri, N. (1997). Study of a new technique for fluoride removal from water. *Desalination*, 114(3), 241-251.
- Lund, K., Fogler, H. S., & McCune, C. C. (1974). Acidization—I. The dissolution of dolomite in hydrochloric acid. *Chemical Engineering Science*, 28(3), 691-IN1.
- Lund, K., Fogler, H. S., McCune, C. C., & Ault, J. W. (1975). Acidization—II. The dissolution of calcite in hydrochloric acid. *Chemical Engineering Science*, 30(8), 825-835.
- Maheshwari, R. C. (2006). Fluoride in drinking water and its removal. *Journal of Hazardous Materials*, 137(1), 456-463.
- Matteson, A., & Herron, M. M. (1993). Quantitative mineral analysis by fourier transform infrared spectroscopy. *In SCA Conference*, no.9308
- Michalski, R. (2006). Ion chromatography as a reference method for determination of inorganic ions in water and wastewater. *Critical Reviews in Analytical Chemistry*, 36(2), 107-127.

- Miretzky, P., Muñoz, C., & Carrillo-Chávez, A. (2008). Fluoride removal from aqueous solution by Ca-pretreated macrophyte biomass. *Environmental Chemistry*, 5(1), 68-72.
- Mohapatra, M., Anand, S., Mishra, B. K., Giles, D. E., & Singh, P. (2009). Review of fluoride removal from drinking water. *Journal of Environmental Management*, 91(1), 67-77.
- Nicholson, K., & Duff, E. J. (1981). Fluoride determination in water: An optimum buffer system for use with the fluoride-selective electrode. *Analytical Letters*, 14(12), 887-912.
- Nordstrom, D. K., & Jenne, E. A. (1977). Fluorite solubility equilibria in selected geothermal waters. *Geochimica et Cosmochimica Acta*, 41(2), 175-188.
- Ojima, J. (2003). Determining of crystalline silica in respirable dust samples by infrared spectrophotometry in the presence of interferences. *Journal of Occupational Health*, 45(2), 94-103.
- Okumura, M., & Kitano, Y. (1983). Incorporation of fluoride ions into calcite. Effect of organic materials and magnesium ions in a parent solution. *Geochemical Journal*, 17(5), 257-263.
- Onyango, M. S., Kojima, Y., Aoyi, O., Bernardo, E. C., & Matsuda, H. (2004). Adsorption equilibrium modeling and solution chemistry dependence of fluoride removal from water by trivalent-cation-exchanged zeolite F-9. *Journal of Colloid and Interface Science*, 279(2), 341-350.
- Pálfi, T., Wojnárovits, L., & Takács, E. (2011). Mechanism of azo dye degradation in advanced oxidation processes: Degradation of sulfanilic acid azochromotrop and its parent compounds in aqueous solution by ionizing radiation. *Radiation Physics and Chemistry*, 80(3), 462-470.
- Patnaik, P. (2003). *Handbook of Inorganic Chemicals*. New York: New York: McGraw-Hill.

- Pizzocaro, F., Torreggiani, D., & Gilardi, G. (1993). Inhibition of apple polyphenoloxidase (PPO) by ascorbic acid, citric acid and sodium chloride. *Journal of Food Processing and Preservation*, 17(1), 21-30.
- Pokorný, J. (1991). Natural antioxidants for food use. *Trends in Food Science & Technology*, 2, 223-227.
- Pokrovsky, O. S., Golubev, S. V., Schott, J., & Castillo, A. (2009). Calcite, dolomite and magnesite dissolution kinetics in aqueous solutions at acid to circumneutral pH, 25 to 150 ° C and 1 to 55 atm pCO<sub>2</sub>: New constraints on CO<sub>2</sub> sequestration in sedimentary basins. *Chemical Geology*, 265(1), 20-32.
- Reardon, E. J., & Wang, Y. (2000). A limestone reactor for fluoride removal from wastewaters. *Environmental Science & Technology*, 34(15), 3247-3253.
- Reig, F. B., Adelantado, J. V., & Moya Moreno, M. C. M. (2002). FTIR quantitative analysis of calcium carbonate ( calcite) and silica ( quartz) mixtures using the constant ratio method. Application to geological samples. *Talanta*, 58(4), 811-821.
- Rizk, M., Zakhari, N. A., Toubar, S. S., & El-Shabrawy, Y. (2005). Spectrophotometric determination of aluminum and copper ions using SPADNS. *Microchimica Acta*, 118(3), 239-247.
- Rocklin, R. D., Pohl, C. A., & Schibler, J. A. (1987). Gradient elution in ion chromatography. *Journal of Chromatography A*, 411, 107-119.
- Saha, S. (1993). Treatment of aqueous effluent for fluoride removal. *Water Research*, 27(8), 1347-1350.
- Shen, F., Chen, X., Gao, P., & Chen, G. (2003). Electrochemical removal of fluoride ions from industrial wastewater. *Chemical Engineering Science*, 58(3), 987-993.

- Small, H., Stevens, T. S., & Bauman, W. C. (1975). Novel ion exchange chromatographic method using conductimetric detection. *Analytical Chemistry*, 47(11), 1801-1809.
- Smith, R. E., & MacQuarrie, R. A. (1988). Determination of inositol phosphates and other biologically important anions by ion chromatography. *Analytical Biochemistry*, 170(2), 308-315.
- Srimurali, M., Pragathi, A., & Karthikeyan, J. (1998). A study on removal of fluorides from drinking water by adsorption onto low-cost materials. *Environmental Pollution*, 99(2), 285-289.
- Stahr, H. M., & Clardy, D. O. (1973). Selective fluoride electrode mechanism studies. *Analytical Letters*, 6(3), 211-216.
- Sujana, M. G., Thakur, R. S., & Rao, S. B. (1998). Removal of fluoride from aqueous solution by using alum sludge. *Journal of Colloid and Interface Science*, 206(1), 94-101.
- Sukanya, C., Himabindu, V., & Anjaneyulu, Y. (2005). Spectrophotometric method for determination of fluoride ion in water samples based on its bleaching effect on aluminium-SPADNS lake. *Asian Journal of Chemistry*, 17(1), 469-474.
- Svensson, U., & Dreybrodt, W. (1992). Dissolution kinetics of natural calcite minerals in CO<sub>2</sub>-water systems approaching calcite equilibrium. *Chemical Geology*, 100(1), 129-145.
- Tomar, V., & Kumar, D. (2013). A critical study on efficiency of different materials for fluoride removal from aqueous media. *Chemistry Central Journal*, 7(1), 51.
- Tripathy, S. S., Bersillon, J. L., & Gopal, K. (2006). Removal of fluoride from drinking water by adsorption onto alum-impregnated activated alumina. *Separation and Purification Technology*, 50(3), 310-317.
- Turner, B. D., Binning, P. J., & Sloan, S. W. (2010). Impact of phosphate on fluoride removal by calcite. *Environmental Engineering Science*, 27(8), 643-650.

- Turner, B. D., Binning, P., & Stipp, S. L. S. (2005). Fluoride removal by calcite: Evidence for fluorite precipitation and surface adsorption. *Environmental Science & Technology*, 39(24), 9561.
- Van-Kauwenbergh, S. J. (2010). *World Phosphate Rock Reserves and Resources*. IFDC.
- Wang, Y., & Reardon, E. J. (2001). Activation and regeneration of a soil sorbent for defluoridation of drinking water. *Applied Geochemistry*, 16(5), 531-539.
- Wasay, S. A., Haran, M., & Tokunaga, S. (1996). Adsorption of fluoride, phosphate, and arsenate ions on lanthanum-impregnated silica gel. *Water Environment Research*, 68(3), 295-300.
- Wildman, B. J., Jackson, P. E., Jones, W. R., & Alden, P. G. (1991). Analysis of anion constituents of urine by inorganic capillary electrophoresis. *Journal of Chromatography A*, 546, 459-466.
- WHO Guidelines for Drinking Water Quality* (2006). (3rd ed.). Geneva, Switzerland: World Health Organization.